https://ntrs.nasa.gov/search.jsp?R=19680017229 2018-12-20T10:48:05+00:00Z

N68-26701

NASA CONTRACTOR REPORT

NASA CR-1085

NASA CR-1085

AUTOMATIC CONTROL OF WATER COOLING IN SPACE SUITS

by Paul Webb, James F. Annis, and Samuel J. Troutman

Prepared by
WEBB ASSOCIATES, INC.
Yellow Springs, Ohio
for

NATIONAL AERONAUTICS AND SPACE ADMINISTRATION • WASHINGTON, D. C. • JUNE 1968

NASA CR-1085

AUTOMATIC CONTROL OF WATER COOLING IN SPACE SUITS

By Paul Webb, M. D., James F. Annis, and Samuel J. Troutman

Distribution of this report is provided in the interest of information exchange. Responsibility for the contents resides in the author or organization that prepared it.

Prepared under Contract No. NASw-1529 by
WEBB ASSOCIATES, INC.
Yellow Springs, Ohio

for

NATIONAL AERONAUTICS AND SPACE ADMINISTRATION

For sale by the Clearinghouse for Federal Scientific and Technical Information
Springfield, Virginia 22151 – CFSTI price $3.00

TABLE OF CONTENTS

INTRODUCTION 3
ANALYSIS 4
EQUIPMENT AND PROCEDURE 10
The MRM 12
Experimental Q Controller 13
Thermoelectric Cooling 14
Measurement of Heat Removal 14
Temperature Measurement 15
Physiological Measurements 16
Subjects 16
EXPERIMENTS 17
Initial Series 17
Validation Runs 17
RESULTS 18
Adjusting Controller Settings 18
Validation Runs 22
DISCUSSION 27
CONCLUSIONS 30
THE FINAL Q CONTROLLER 30
Calibration Procedure 40
Operational Procedure 42
APPENDIX A: SYMBOLS AND ABBREVIATIONS 45
APPENDIX B: BIO-THERMAL MODEL OF WORKING MAN IN A WATER COOLED SUIT 46
BACKGROUND 46
BASIS OF THE MODEL 47
COMPARTMENTS OF THE MODEL 51
MODEL EQUATIONS 52
DERIVATION OF VALUES 55
Heat Transfer Coefficients 57
COMPUTER SIMULATIONS 61
DISCUSSION 64
APPENDIX C: WATER COOLING GARMENT 70
APPENDIX D: THE COOLING LOOP 74
Thermoelectric Cooler 75
APPENDIX E: PHYSIOLOGICAL MEASUREMENTS 78
Skin temperatures 78
Rectal temperature and ear canal temperature 78
Heart rate 78
Change in body weight 80
Heat production rate 80
Metabolism Measurement 80
REFERENCES 82

LIST OF FIGURES

Frontispiece. Subject at rest during evaluation of experimental Q controller 2
Figure 1. Mean curves, 1966, Activity Schedule I. 5
Figure 2. Mean curves, 1966, Activity Schedule II. 6
Figure 3. Mean curves, 1966, Activity Schedule III. 7
Figure 4. Mean curves, 1966, Activity Schedule IV. 8
Figure 5. Mean curves, 1966, Activity Schedule V. 9
Figure 6. The Cooling Loop. 10
Figure 7. A diagram of the environment control and measuring system of a working man in a water cooled suit 11
Figure 8. Diagram of the MRM (Metabolic Rate Monitor) 12
Figure 9. Computer diagram of experimental Q controller 13
Figure 10. Response of experimental Q controller to a step function in MR 14
Figure 11. Cooling responses in an exploratory experiment before controller values were established 19
Figure 12. Cooling responses after Q controller values were established 19
Figure 13. A plot of the relative changes in T_{wi} and $T_{\bar{s}}$ with their associated MR's obtained with different Q controller settings 21
Figure 14. Physiological and cooling responses to two different intermittent work-rest schedules with different system τ settings . . . 23
Figure 15. Responses obtained in an automatically controlled experiment in which the activity pattern duplicated an earlier manually controlled one (Fig. 3) 25
Figure 16. Responses obtained in an automatically controlled experiment in which the activity pattern duplicated an earlier manually controlled one (Fig. 4). 26
Figure 17. Summation of voltages using an operational amplifier 32
Figure 18. The relationship of $\dot{V}_{O_2}^{0}$ to the Gain ($B_4/5$) 34
Figure 19. A schematic of the summing amplifier. 35
Figure 20. Diagram of an integrating amplifier 35
Figure 21. Schematic of the integrating amplifier. 36
Figure 22. The ideal relationship of Q controller output to T_{wi} 37
Figure 23. The schematic of the Q controller. 38
Figure 24. Photographs of the final Q controller 39
Figure 25. The controller circuit board. 40
Figure 26. Ideal curves, 1966 data, Schedule I. 48
Figure 27. Ideal curves, 1966 data, Schedule II. 49
Figure 28. Ideal curves, 1966 data, Schedule IV. 50
Figure 29. Compartments of the Model 51
Figure 30. Heat flow pathways between compartments of the model 53
Figure 31. Q_{1s} as a function of (T_1 - $T_{\bar{s}}$) 59

Figure 32. Q_r as a function of $(T_r - T_{\bar{s}})$. 59
Figure 33. Q as a function of $(T_{\bar{s}} - T_{\bar{w}})$ 60
Figure 34. T_{wi} as a function of MR. 61
Figure 35. Analog computer diagram of the biothermal model 62
Figure 36. Comparison of experimental and simulation values for equilibria at rest and at two levels of work. 63
Figure 37. Simulated versus experimental rectal temperatures 65
Figure 38. Simulated leg compartment temperatures at two work levels 66
Figure 39. Simulated versus experimental mean skin temperatures 67
Figure 40. Simulated versus experimental heat extraction rate. 68
Figure 41. Simulated versus experimental inlet water temperature 69
Figure 42. Cross-sectional appearance of the water cooling garment . . . 70
Figure 43. The flow pattern and tubing distribution of the water cooling garment. 71
Figure 44. A simplified schematic of the cooler power supply 75
Figure 45. An illustration of the thermoelectric modules 76
Figure 46. A simplified schematic of the monitor circuit. 77
Figure 47. Thermistor locations and schema for surface area weighting. . 79

AUTOMATIC CONTROL OF WATER COOLING IN SPACE SUITS

By Paul Webb, M. D., James F. Annis, and Samuel J. Troutman

SUMMARY

Accurate and timely control of the powerful cooling available in a water cooled garment (WCG) is important during periods when work varies widely, as in extravehicular activity, and with it the need for cooling. The relationship between metabolic rate (MR) and the suit inlet water temperature (T_{wi}) can be expressed as an ordinary differential equation:

$$\tau \dot{T}_{wi} = -T_{wi} + B_4(MR_0 - MR)$$

--a relationship derived from an analysis of thirty carefully controlled experiments done in 1966. The analysis led to a biothermal model of working man in a WCG which simulated experimental data with reasonable accuracy.

An experimental Q controller was used to automatically control heat removal (Q) from men wearing a new WCG while working on a treadmill. The input to the controller was a continuous oxygen consumption signal. The cooling water was recirculated through a closed loop where the man was the heat source and a controllable thermoelectric cooler was the heat sink. The new WCG had different characteristics from those of the 1966 suit, and this required adjustment of the gain of the Q controller. After initial experiments where variation in the controller gain and time constant were explored, automatic control was evaluated in two subjects doing four different patterns of work, including brief periods of intermittent work. Physiological responses were as good as in the best of the 1966 experiments, and control was smooth and accurate. Other inputs to this controller could be developed.

Advantages of an automatic controller include: (1) no manual adjustment by an otherwise busy astronaut, who is probably a poor judge of his own thermal state during work; (2) no sweating or chilling; and (3) high heat removal and efficient use of stored coolant.

A final Q controller was designed, built, and tested in the cooling loop. The steps followed in the design are described fully. Calibration and operation of the controller are given along with circuit diagrams, a component list, and specifications.

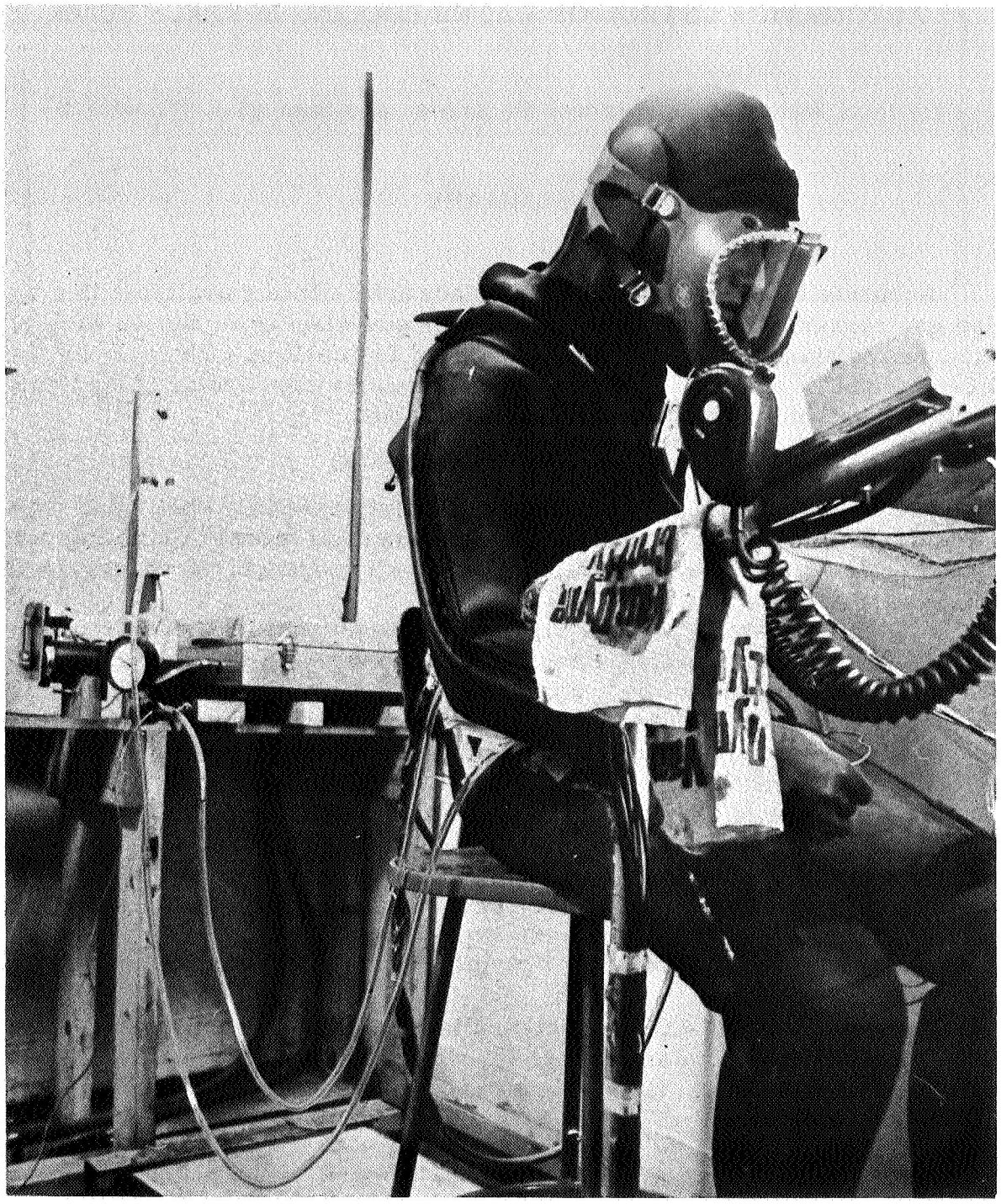

Frontispiece: A subject at rest during an evaluation of the experimental Q controller. He wears a water cooled foam rubber suit and a face mask for measuring oxygen consumption. The two loops of tubing connect the suit to a thermoelectric cooler, in the metal case, and to the water circulating pump.

INTRODUCTION

Water cooling has become the preferred means of removing body heat from an astronaut wearing a space suit outside his vehicle. Heat production is high during activity in full pressure suits (refs. 1, 2, and 3), but it is easily met by the cooling ability of water cooled suits (refs. 4, 5, and 6). In fact it is clear that a man can be overcooled even at very high rates of activity, as shown in previous reports from our laboratory (refs. 7 and 8). Overcooling is not only uncomfortable but causes vasoconstriction and possibly heat storage, while undercooling leads to sweating and storage of body heat. Clearly, there is a requirement for good control of the cooling in a water cooled garment.

What sort of control is appropriate? Manual control by the wearer has been tried in a number of laboratories (ref. 4, 6, and 9) with fair success. However, there was a tendency for the subject to overcool himself or apply cooling too quickly. Considerable adjustment was necessary in the early experiments; it was apparent that the subject was not a good judge of his own thermal state, and that he made adjustments too late to prevent sweating, or else he overcooled. A busy astronaut should not have to worry about making these adjustments, since he has a great many other things to do during his period of extravehicular activity.

Automatic control is a natural alternative, but the question is how to implement the idea. What should an automatic controller sense in order to control accurately? Our answer to this question has been to sense oxygen consumption, a primary physiological variable which changes rapidly as activity changes, and is directly proportional to a change in heat production. The automatic controller described in this report uses a continuous electrical signal which is proportional to oxygen consumption as the input to a controller which varies the temperature of the water entering the suit. The input signal comes from the Webb Associates MRM (Metabolic Rate Monitor).

We shall describe the analytical steps which led to the design of an experimental controller, and experiments which were done to verify its ability to control appropriately as subjects went through various work programs. In the last section we describe the design of the final Q controller.

ANALYSIS

The design of the controller was based on an analysis of a block of 30 experiments conducted in 1966 and reported in NASA CR-739, entitled "Biothermal Responses to Varied Work Programs in Men Kept Thermally Neutral by Water Cooled Clothing" (ref. 7). The subjects were thermally isolated in heavy impermeable clothing, which included a water cooling garment next to the skin. Cooling was constantly adjusted to that the subject did not sweat nor become chilled. The human operator monitored physiological signs including heart rate, skin temperature, rectal temperature, and sweat rate; he watched the rate of heat removal (Q) and the work rate (MR) from $\dot{V}_{O_2}$, and he listened to the subject's comments. The operator learned to control the cooling so that there was no gross sweating, the subject was not cold, and there was always the highest possible Q. If the operator overcooled, a low Q resulted from vasoconstriction in the skin, and if he undercooled a low Q resulted along with sweating, so a high Q in the experiments came to mean correct control and a thermally neutral state which was subjectively comfortable. Five different programs of activity were used, lasting from 10 minutes at a high work rate to three hours with multiple work levels. The data collected during the 1966 experiments included MR, Q, water inlet temperature (T_{wi}), and the physiological data already mentioned. We performed six experiments with four subjects for each of the five activity schedules.

To begin the analysis, we carefully reviewed the records of the 30 experiments, and derived mean values for T_{wi}, Q, MR, $T_{\bar{s}}$, and T_r from the six experiments in each activity schedule. The mean data were plotted against time as shown in Figures 1 through 5.

The important thing for our analysis was the relationship between MR and T_{wi}. Cooling power of the suit can be controlled by varying either the flow rate of water through the suit or the temperature of the water coming into the suit. We chose to control only inlet temperature and leave the flow rate fixed at 1500 ml/min. An automatic controller should convert the instantaneous value for MR into a command signal for T_{wi}.

As an analytical technique to apply to the 1966 data, we developed a biothermal model of a working man in a water cooled suit. This model is described in Appendix B. The 3-compartment model was able to predict the rectal temperature, the skin temperature, a hypothetical leg or muscle temperature, and the inlet water temperature as the subject went from rest to various levels of work.

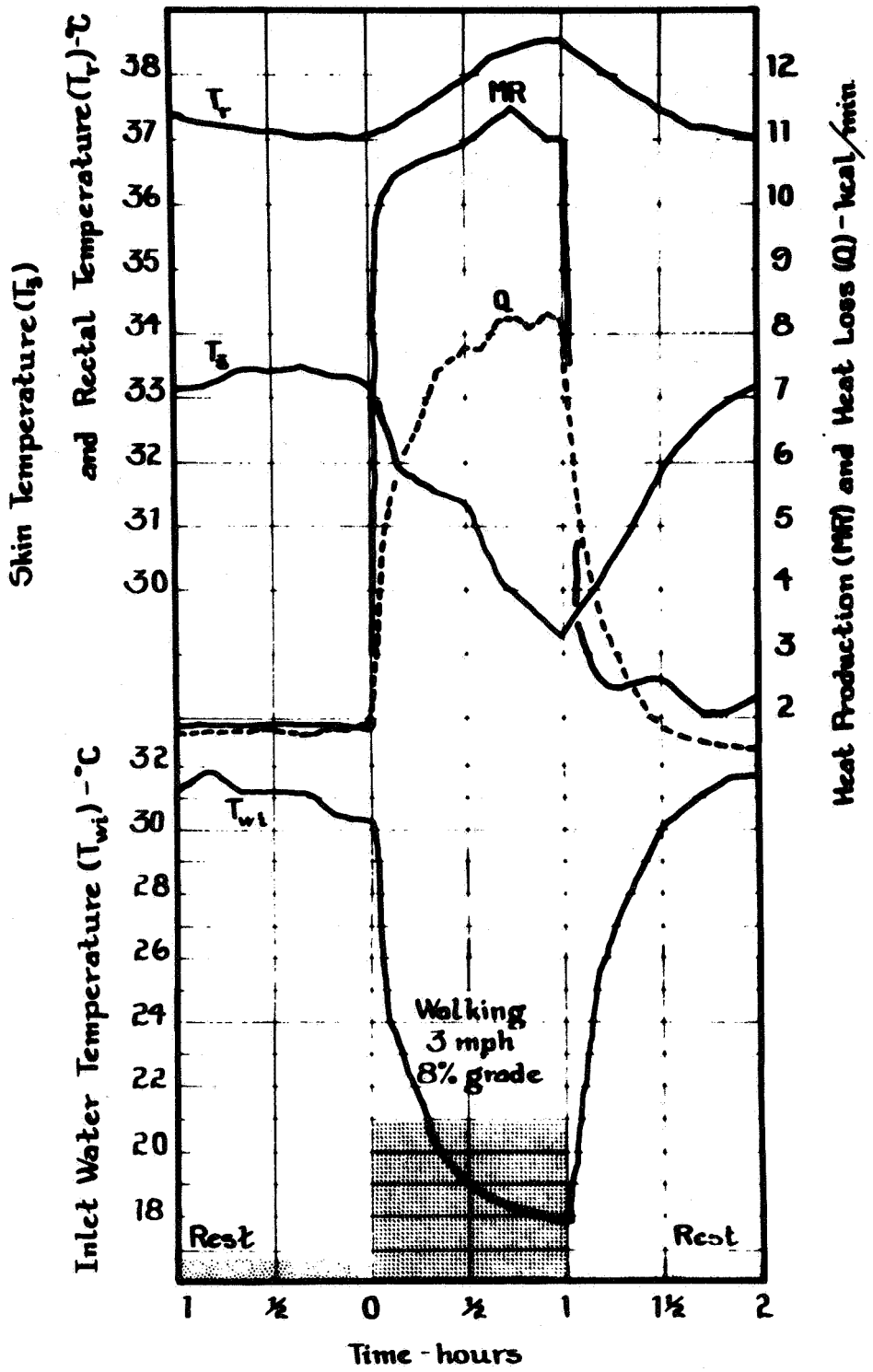

Figure 1. Mean curves, 1966, Activity Schedule I; work period shown by shaded area; manual control of T_{wi}; weight loss 83 gms/hr; Q curve includes WCG heat extraction, plus evaporative heat loss and external work.

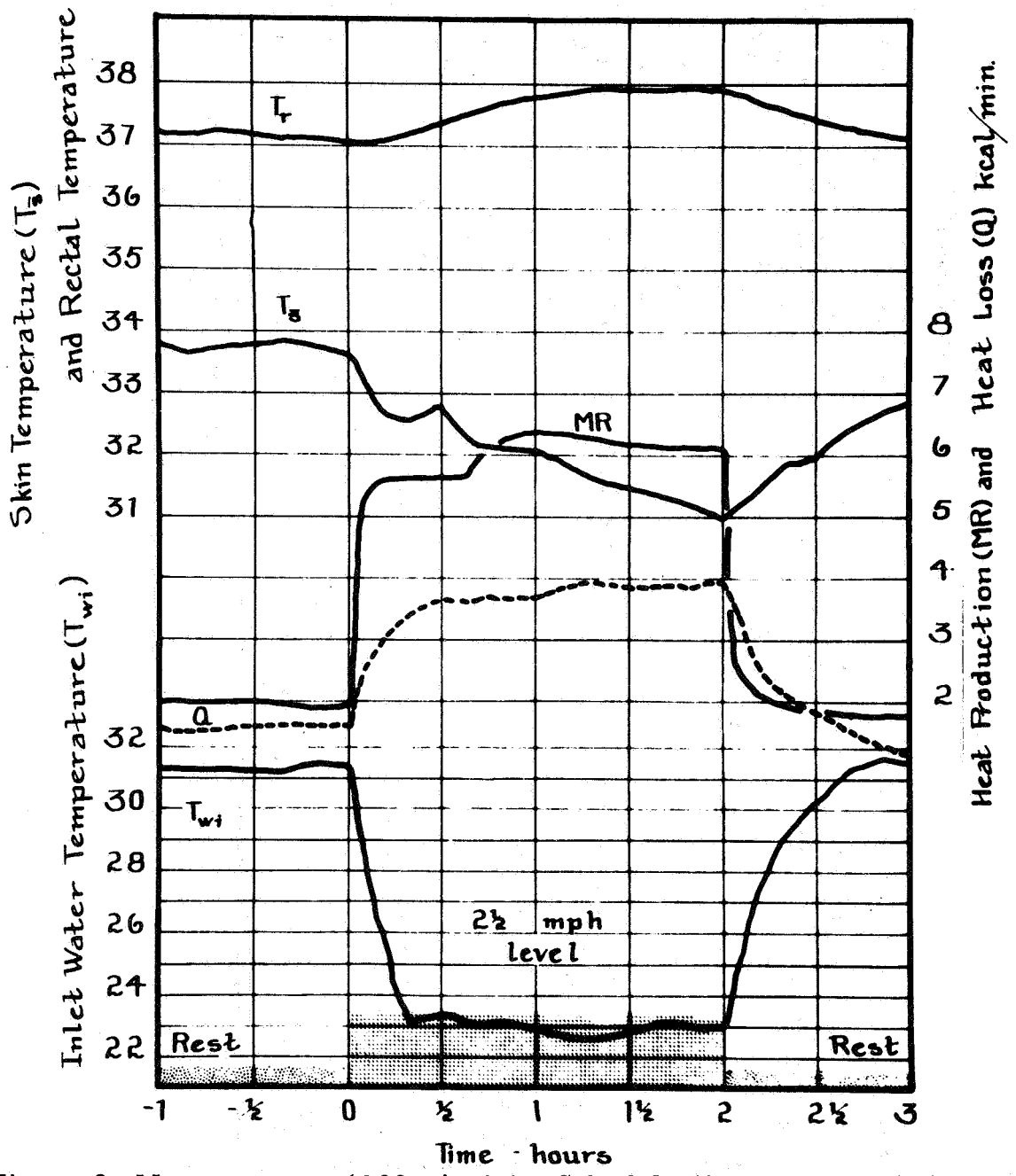

Figure 2. Mean curves, 1966, Activity Schedule II; work period shown by shaded area; manual control of T_{wi}; weight loss 69 gms/hr; Q curve includes WCG heat extraction plus evaporative heat loss.

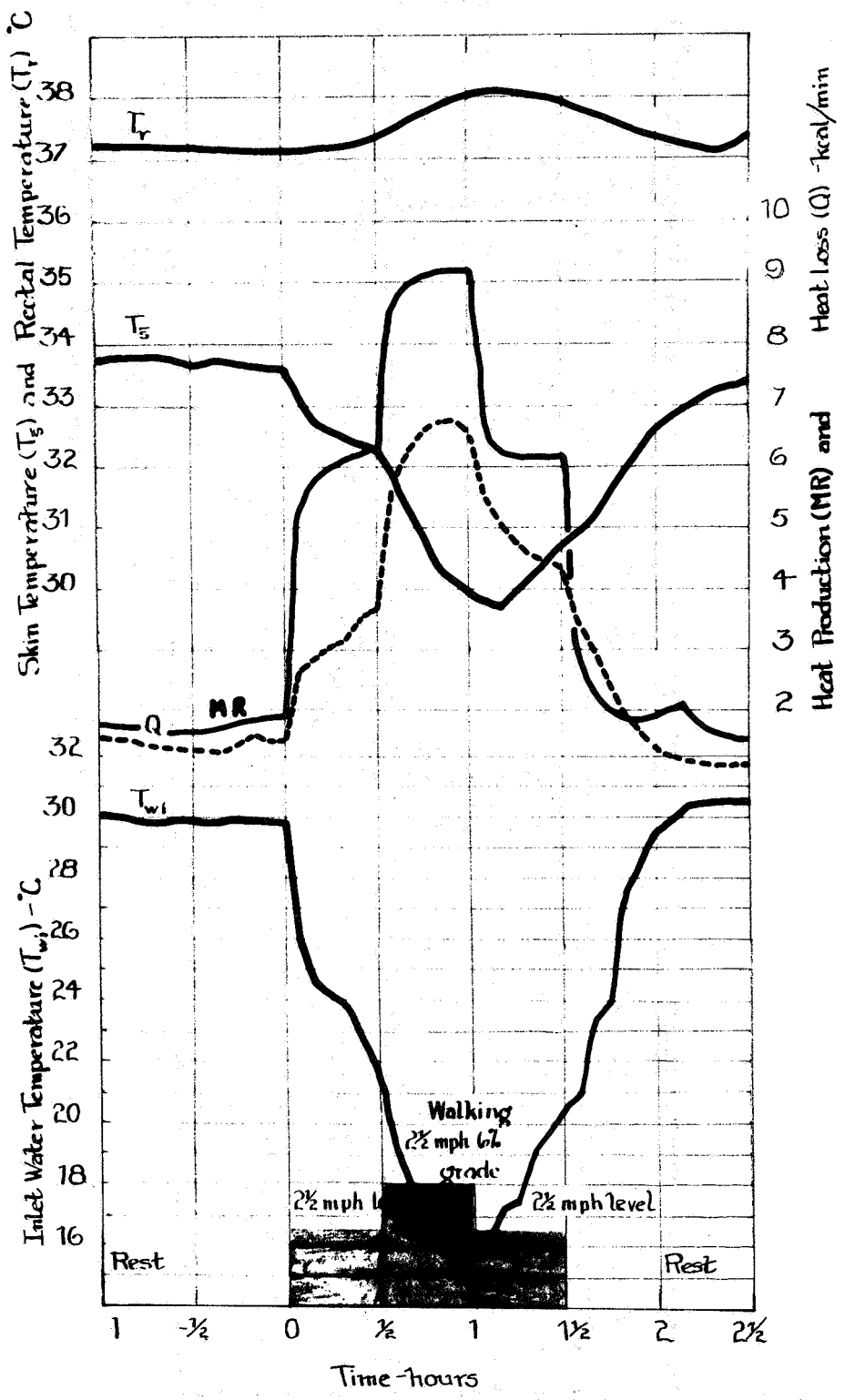

Figure 3. Mean curves, 1966, Activity Schedule III; work periods shown by shaded area; manual control of T_{wi}; weight loss 56 gms/hr; Q curve includes WCG heat extraction, evaporative heat loss, and external work when the subjects walked uphill.

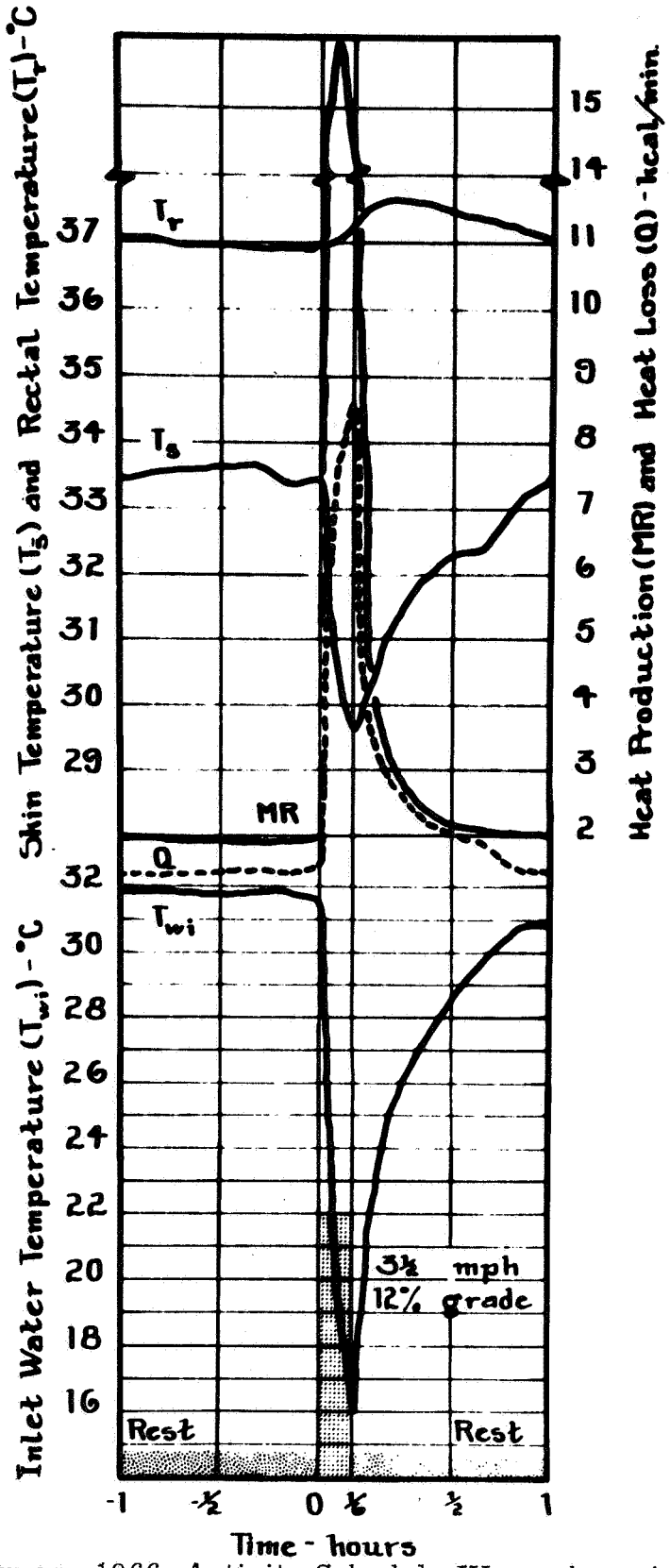

Figure 4. Mean curves, 1966, Activity Schedule IV; work period shown by shaded area; manual control of T_{wi}; weight loss 58 gms/hr; Q curve includes WCG heat extraction, plus evaporative heat loss and external work.

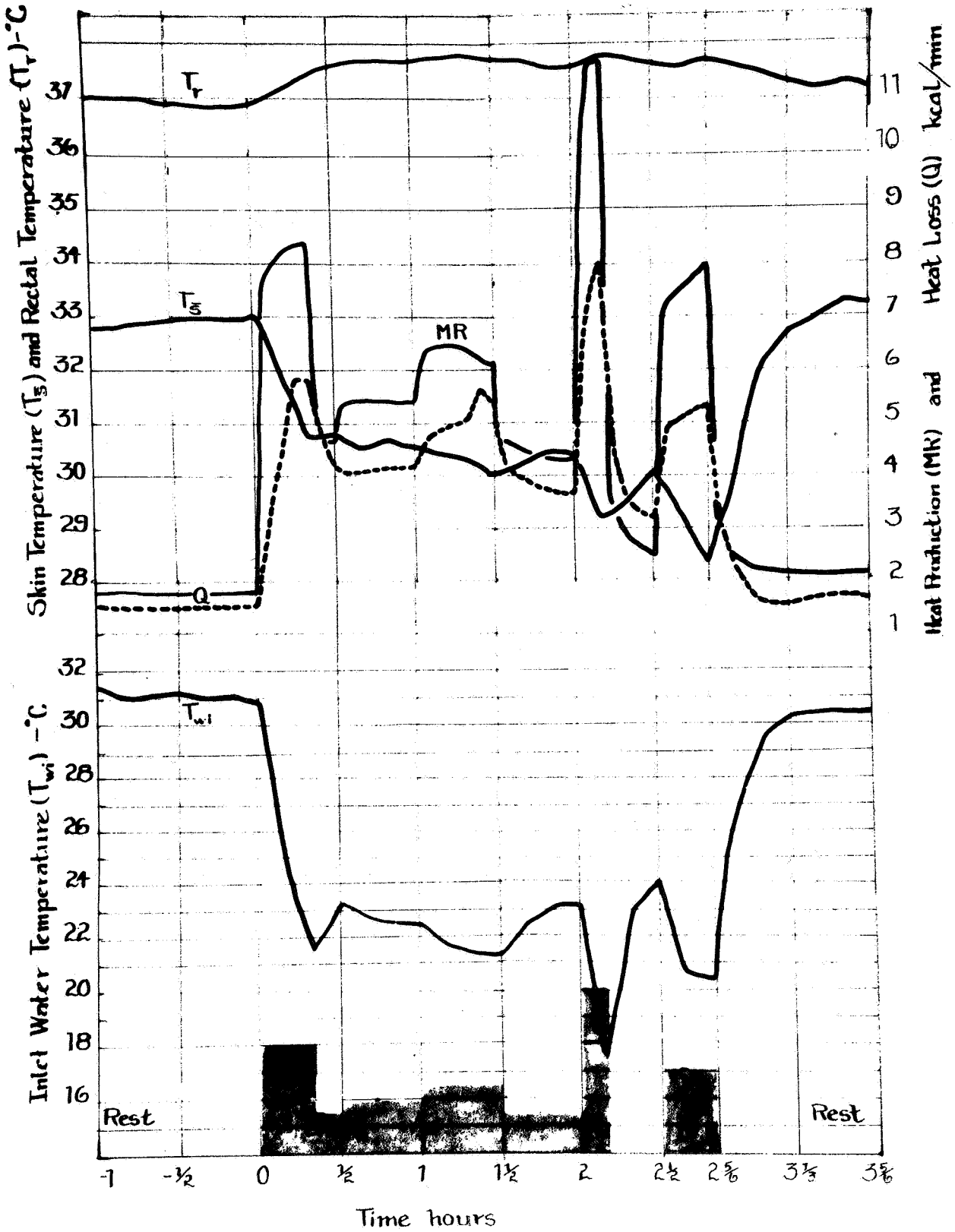

Figure 5. Mean curves, 1966, Activity Schedule V; relative levels of various work periods shown by shaded areas; manual control of T_{wi}; weight loss 63/ gms/hr; Q curve included WCG heat extraction, evaporative heat loss, and external work when the subjects walked uphill.

The model was verified by mechanizing it on an analog computer and doing simulation runs in which the compartment temperatures were generated over time and the records compared with the actual temperatures logged during experiments.

We thus had a verified mathematical model of the system we were concerned with, and an equation to describe the behavior of an automatic controller. We proceeded to make an experimental Q controller, and to show by experiment that it controlled correctly during various patterns of work.

EQUIPMENT AND PROCEDURE

To carry out experimental validation of the experimental Q controller, we designed a new water cooled garment (WCG) which was convenient to use, and we put together a laboratory arrangement which was similar in purpose to that of the earlier 30 experiments but with improved components. Cooling of the water circulated through the suit was done thermoelectrically, and the water was circulated around a closed loop where the man was the heat source and the thermoelectric cooler the heat sink (Figure 6). The WCG is described in Appendix C and the components of the cooling loop are described in Appendix D.

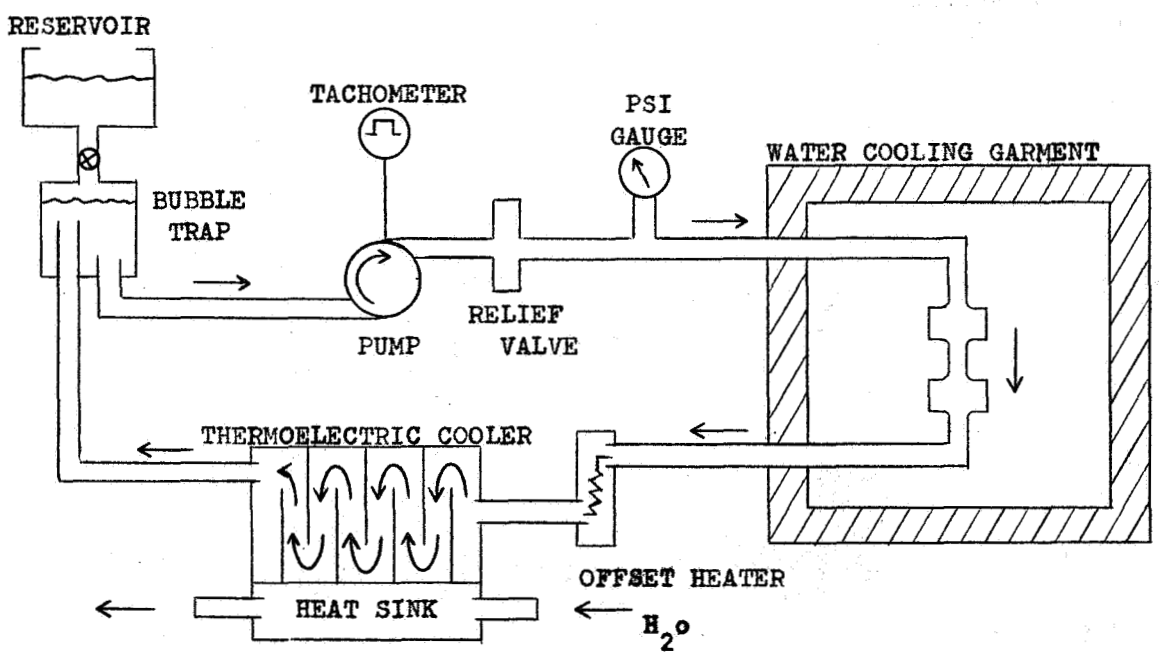

Figure 6. The Cooling Loop

Control and measuring equipment used in the experiments was related to the subject as shown in Figure 7. The following paragraphs deal with the various elements individually.

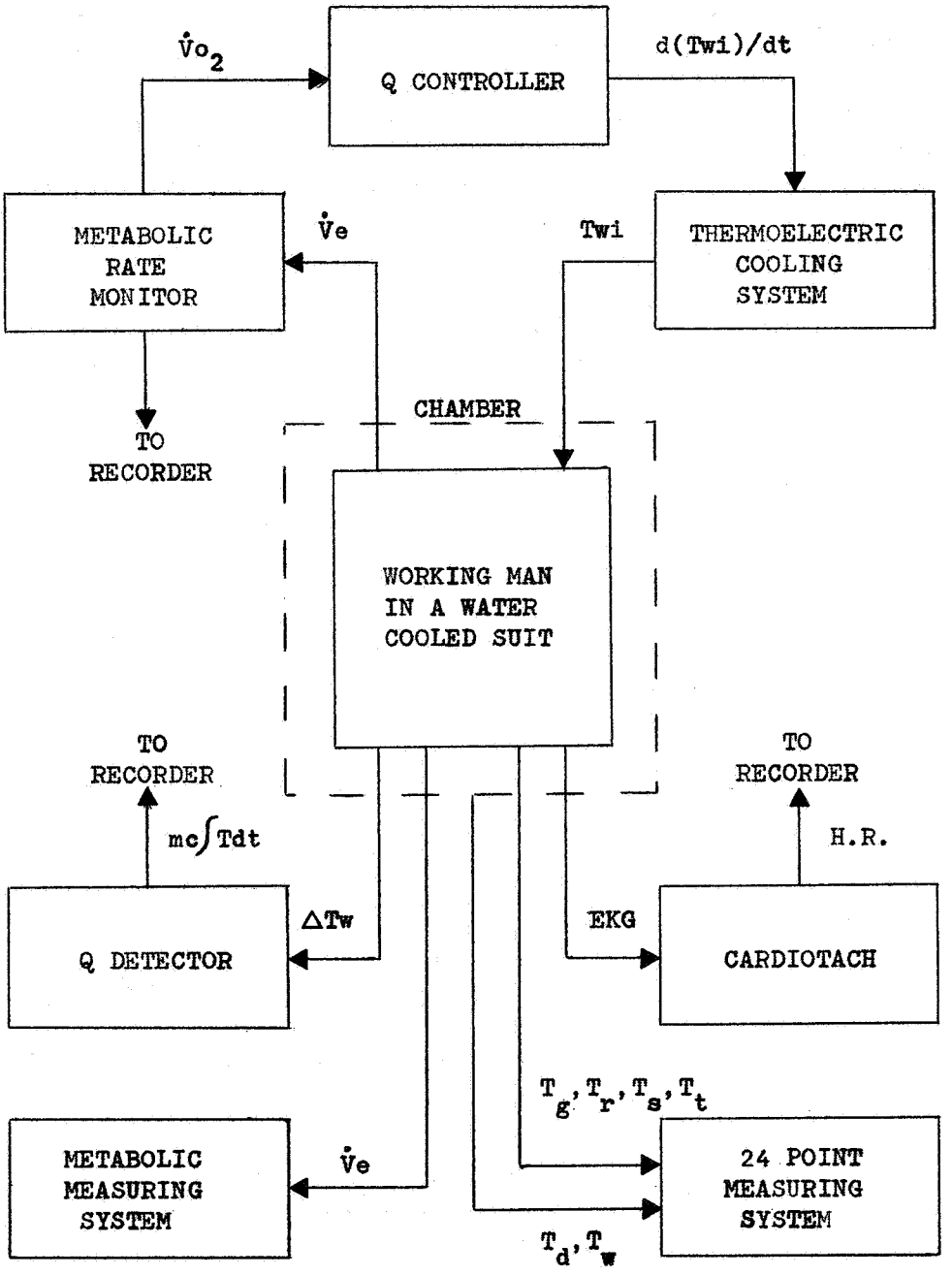

Figure 7. A diagram of the environment control and measuring system of a working man in a water cooled suit.

The MRM

Oxygen consumption was continuously monitored with a Webb Associates MRM, Figure 8. The principle of operation is that of a closed loop servo system. A motor-blower drawing ambient air through the system is servo controlled by sensing the partial pressure of oxygen in the air stream by a polarographic cell located downstream from the man. As the downstream oxygen content decreases the blower speeds up, increasing the volume flow and thereby returning the downstream oxygen content toward that of ambient air. The blower speed, or its excitation voltage, is proportional to the volume flow and oxygen consumption. A continuous analog voltage (0 to 5 VDC) is provided which is equal to oxygen consumption, based on 1 volt per liter of oxygen consumed/min. The accuracy is similar to that obtained by collection of expired air in a Douglas bag, with gas analysis. Our standardized technique for measurement of metabolism is described in Appendix E.

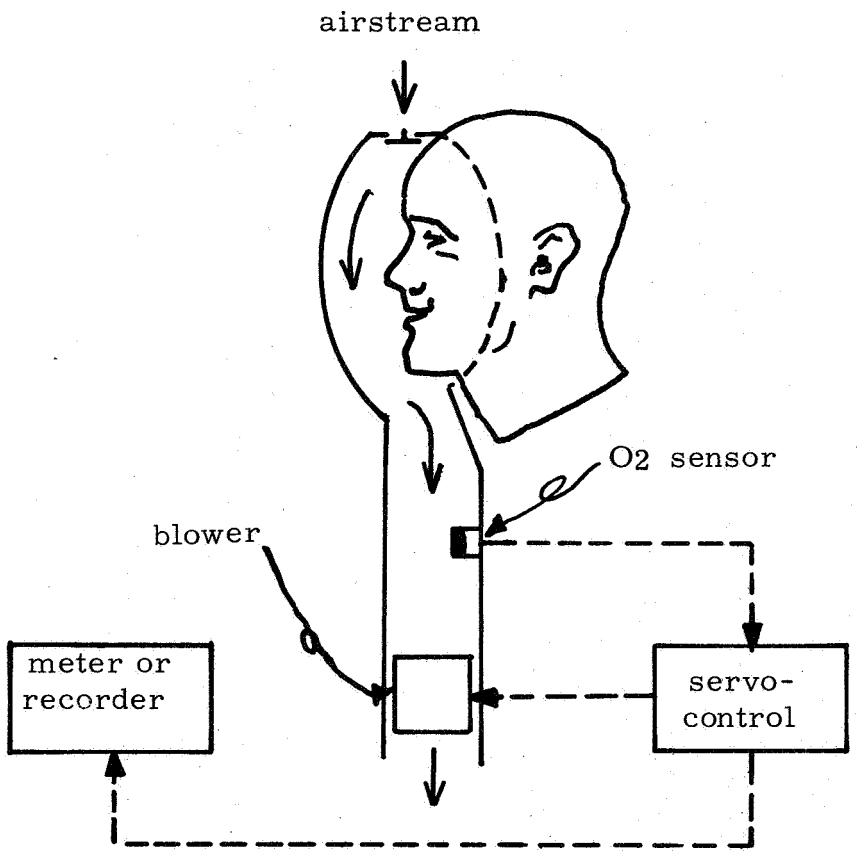

Figure 8. Diagram of the MRM (Metabolic Rate Monitor)

Experimental Q Controller

An analog computer (TR-20, Electronic Associates, Inc., Princeton, N. J.) was used as the experimental Q controller, and it provided the electronic interface between the MRM and the thermoelectric cooler controller. Its operating parameters were based on the following equation, which was established in the mathematical model (Appendix B):

$$\tau \dot{T}_{wi} = -T_{wi} + B_4(MR_0 - MR) \tag{1}$$

where: T_{wi} = the instantaneous inlet water temperature

MR_0 = the oxygen consumption in lpm requiring an inlet water temperature of 0°C

τ = the time constant (1/e) of the response of T_{wi}

B_4 = the degrees change in T_{wi} per liter of oxygen consumed per minute

Equation 1 was scaled with respect to time and magnitude to obtain Equation 2:

$$\tau \frac{\dot{T}_{wi}}{5} = -\frac{T_{wi}}{300} + \frac{B_4}{300}(MR_0 - MR) \tag{2}$$

Equation 2 was implemented as shown in the computer diagram, Figure 9:

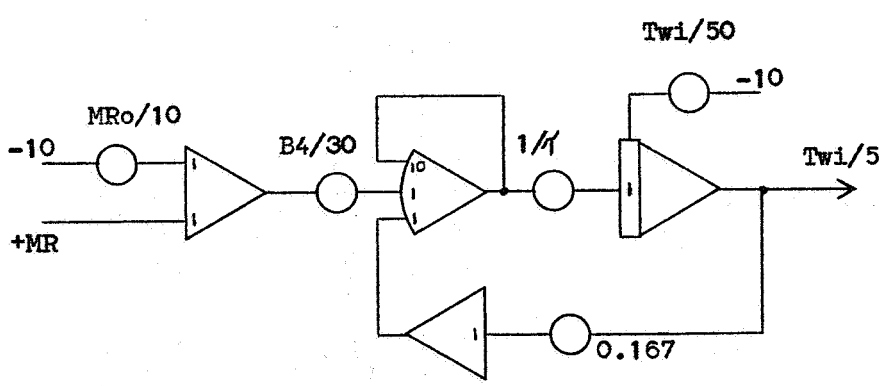

Figure 9. Computer diagram of experimental Q controller

The experimental Q controller responded to an increase in the MR signal by generating a decaying exponential output with a time constant, τ. The analog input varied over a range of 0.0 to +3.11 VDC depending upon the level of oxygen consumption, whereas the exponential response had a range of +5.2 to 0.0 VDC. This exponential response provided the driving voltage for the resistance bridge in the thermoelectric cooler controller. A typical response of the Q controller to a step function in MR is shown in Figure 10:

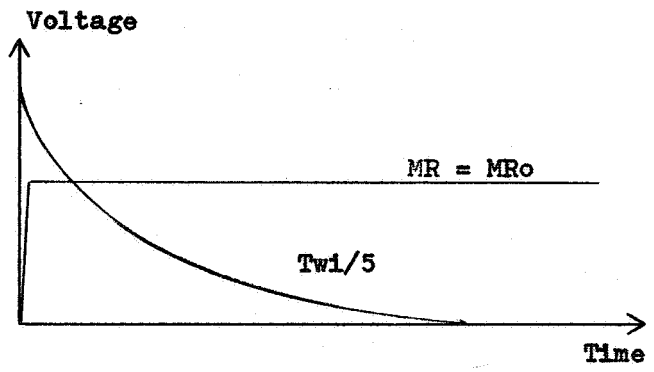

Figure 10. Response of experimental Q controller to a step function in MR

Thermoelectric Cooling

Accurate control of the inlet water temperature was achieved by thermoelectric cooling. Control was accurate to ±0.2°C, and the maximum cooling power was 3900 Btu/hr. The cooler could lower T_{wi} by 6°C/min, which was faster than needed. The cooler is described in Appendix D.

Measurement of Heat Removal

The heat removed was monitored continuously by a Q detector, which provided an analog voltage which represented $\dot{m}c\ (\Delta T_w)$. The analog signal was scaled to obtain discrete increments per kcal of heat removed and provided the input to one channel of a dual channel recorder (Model RDC-100, Dohrman Instruments, Mountain View, California).

The water temperatures at the inlet and outlet of the WCG were detected by thermistor probes (Model 423, Yellow Springs Instrument Co., Yellow Springs, Ohio) located in their respective manifolds. To reduce the error from thermal conduction along the probe leads, the probes were inserted 2-1/2 in. into the manifolds. The probes were elements in each leg of a modified Wheatstone bridge circuit, the output of which was the analog of ΔT_w.

Instrumentation circuitry consisted of a regulated constant voltage supply and Wheatstone bridge. The bridge was modified to allow the response of the inlet probe to be averaged by integration, thus preventing a transient response in inlet temperature from appearing in the output of the instrument. The time constant of integration was equal to the purge time of the water cooled garment; therefore the analog output was equal to the instantaneous average of the heat being removed in the water coolant. The error in the system was governed by the matched response of the sensing probes which was ±0.1°C maximum.

Temperature Measurement

Subject, chamber environment, and the cooling system temperatures were monitored on a 24-point potentiometric recorder (Honeywell-Brown Electronik). The instrument had a range of from 0°C to 50°C and printed an individual temperature every 5 seconds, hence a cycle time of 2 minutes. The recorder was modified with a Wheatstone resistance bridge which allowed the use of Yellow Springs Instrument Co. series 400 thermistor probes as the temperature sensing elements. The inputs consisted of 22 such probes. The remaining two positions were used for an internal fixed resistor calibration standard and for the mean skin temperature ($T_{\bar{s}}$). The $T_{\bar{s}}$ resulted from a parallel resistive equivalent of the 16 skin thermistors. The recorder point assignment was as follows:

Points #1-16: individual skin temperatures
Point #17: calibration standard, set at 39.99°C
Point #18: mean skin temperature ($T_{\bar{s}}$)
Point #19: suit inlet water temperature (T_{wi})
Point #20: suit outlet water temperature (T_{wo})
Point #21: rectal temperature (T_r)
Point #22: chamber dry-bulb temperature (T_d)
Point #23: chamber wet-bulb temperature (T_w)
Point #24: suit surface temperature (T_g), or tympanic membrane temperature (T_t)

Magnetic switching between the Honeywell-Brown recorder and a digital thermometer (Digitec Model 501, United Systems, Dayton, Ohio) permitted "at will" observations of temperatures recorded on points 19 through 24. Generally the T_t was observed continuously in this manner. Accuracy for the total system was set by the thermistor probes at ±0.1°C. All thermistors were calibrated in water against a National Bureau of Standards certified mercury thermometer before installation.

Physiological Measurements

The physiological measurements made during experimental evaluation of automatic cooling were the following:

a. skin temperature (T_s) and mean skin temperature ($T_{\bar{s}}$)

b. rectal temperature (T_r)

c. ear canal temperature (T_t)

d. heart rate (HR)

e. metabolic rate (MR)

f. weight loss

g. heat extraction rate (Q)

Each of these measurements is described in Appendix E.

Subjects

Two healthy male subjects (RT and JA) were used in the experiments. Both subjects were experienced participants in physiological tests; subject JA had participated in the 1966 experiments. The two subjects were similar in physical type, size, and physical condition. Personal and anthropometric data are given below:

Subj.	Age yrs.	Height in.	Height cm.	Nude Weight lb.	Nude Weight kg.	Surface Area m^2	Ht/Wt ratio
RT	29	74	188	165	75	2.0	.448
JA	35	72	183	152	69	1.9	.474

EXPERIMENTS

Two kinds of experiments were carried out: an initial series of tests to establish the correct settings for the experimental Q controller, and a second series of validation runs using both familiar and untried work patterns.

A total of 15 experiments was completed. Each of these was done under complete automatic control; no changes in controller settings were made after a given experiment began. The experimental Q controller set the rates of change and levels of T_{wi} on the basis of the MRM input signal.

Initial Series

We chose a simple experiment schedule for the initial trials of the experimental Q controller. The subject rested for 1 to 2 hours, went to work at a rate in which the $\dot{V}_{O_2}$ was equivalent to approximately 9 kcal/min for 1 hour, and then he returned to rest. In these experiments we were able to establish the correct T_{wi} for rest, to estimate the $\dot{V}_{O_2}$ which would call for a T_{wi} of 0°C, and to calculate the required gain of the controller. At the same time we varied the time constant, τ, from 20 minutes (twice the apparent τ in the 1966 data) to 5 minutes (1/2 the apparent τ from the 1966 data). When the correct controller settings for this activity schedule had been found, we also tried an intermittent work pattern where the subject worked for 5 minutes and rested for 5 minutes. This caused a further adjustment in the time constant.

Validation Runs

With the experimental Q controller adjusted properly, we obtained data with the following work schedules:

a. work level constant at 9 kcal/min for 1 hour (similar to activity schedule I, 1966, as shown in Figure 1, p. 5).
b. a work schedule where the subject worked at approximately 5 kcal/min for half an hour, then 8 kcal/min for half an hour, then 5 kcal/min for half an hour again (similar to activity schedule III, 1966, as shown in Figure 3, p. 7).
c. near maximal work for 10 minutes (similar to activity schedule IV, 1966, as shown in Figure 4, p. 8).
d. an intermittent work period in which the subject worked near-maximally for 1 minute, followed by a 1 minute rest period, and the cycle repeated for 20 minutes.

These four types of activity were considered sufficient to show how well the experimental Q controller could handle different patterns of work.

RESULTS

Adjusting Controller Settings

All of the values in the controller equation (1), p. 13, turned out to be somewhat different from those calculated from the analysis of the 1966 data. First, the inlet water temperature at rest in the new WCG was 26°C, as compared to 31.25°C in the 1966 suit. This was established during observations of the subject at rest in which higher water temperatures caused gradually increasing skin temperatures and mild sweating, while lower temperatures caused a fall in skin temperature and gradual chilling. For long periods of rest, e. g. two or three hours, as little as 1 degree above or below the 26° set point caused a significant change. The value of 26°C for T_{wi} held for both subjects. It appeared to be a specific characteristic of the suit.

As experiments were conducted, it became apparent that not only was the resting value for T_{wi} lower this year, but the final temperatures at work were also lower. This caused a recalculation of the estimated $\dot{V}_{O_2}$, which would require a T_{wi} of 0°C, the value for MR_0 in equation (1). In the 1966 data this value came out at 4.5 lpm. This year the number was estimated to be 3.11 lpm. Thus the range of T_{wi} from rest to a work level calling for 0°C was smaller with this year's suit. This meant that the gain, B_4, had to be higher than that estimated from the 1966 data. From a calculated 7.5°C change in T_{wi} per liter of oxygen consumed per minute in the 1966 experiments, the value became 9.4°C per lpm.

The new values for resting T_{wi}, MR_0, and B_4 show how this year's WCG differs from the WCG used in 1966. This year's suit was less efficient in removing heat. It had 150 feet of cooling tubes, while the 1966 suit had 356 feet of cooling tubes. The new WCG had larger tubing, hence wider areas of contact with the skin, but it did not fit as snugly, or conform to moving parts as closely as the diamond pattern of the 1966 suit. Both suits were able to handle the heat removal task, but the apparent efficiency of heat removal for this year's suit had to be matched by appropriate controller settings.

To illustrate the effect of these adjustments in the experimental Q controller, physiological effects for two experiments are shown side by side in Figures 11 and 12. In Figure 11, on the left, the time constant was too long at 20 minutes and the gain was too low. The result was that as the subject went to work at approximately 9 kcal/min, his skin temperature rose slowly and he sweated enough to cause a weight loss of 177 gms/hr during the 60 minutes of work. The fall in T_{wi} was too little and too slow.

In Figure 12, T_{wi} changes more rapidly and it reaches a correct level of about 13°C. In this experiment τ was 8 minutes and B_4 correctly adjusted

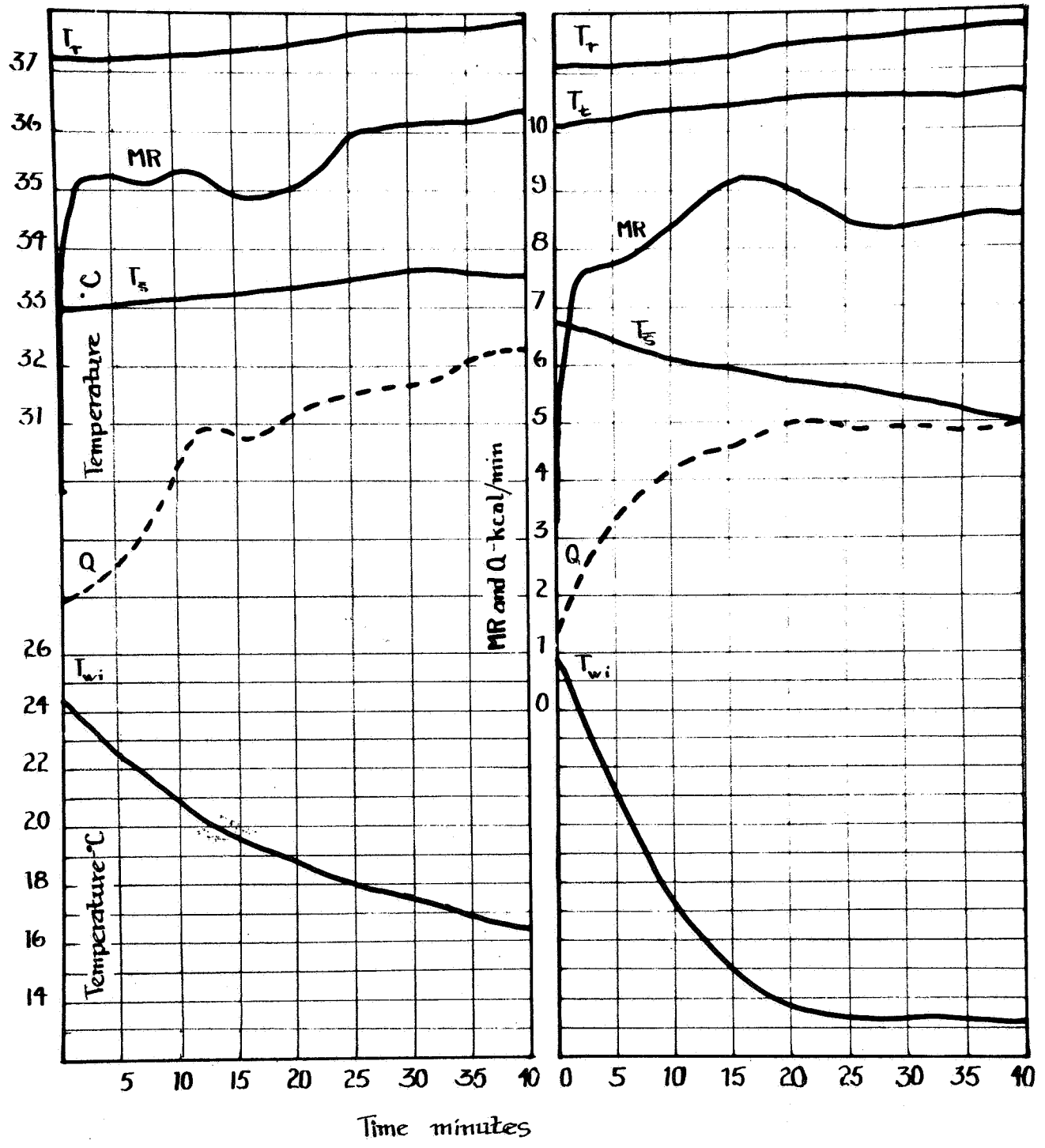

Figure 11 (left) shows cooling responses in an exploratory experiment before Q controller values were established, and Figure 12 (right) shows cooling responses after the values were established.

at 9.42°C per liter of oxygen consumed per minute. Skin temperatures fell throughout the hour of work and the sweat rate was close to 100 gms/hr, a criterion of correct control in our laboratory. The physiological responses in Figure 12 we consider to be appropriate to the work level, while the responses in Figure 11 show definite undercooling. Notice that in both experiments the rectal temperature approached equilibrium at 38°C (reached between 50 and 60 minutes into work). In Figure 12 one of the better records of the temperature of the external ear canal, T_t, shows that the cranial blood temperature, which this measurement is supposed to represent, rose steadily from the onset of work, while the rectal temperature showed its usual plateau for the first 10 minutes. The fact that T_t is lower than T_r is thought to be due to cooling of the ear canal from the cooling tubes in the WCG helmet.

Notice also that in both experiments the heat extraction rate, Q, is approximately 60% of the MR.

Actually the two experiments illustrated in Figures 11 and 12 were separated by several intermediate experiments in which the controller settings were being adjusted to their final values. The effects of the various adjustments are shown in Figure 13, where four experiments at the 9 kcal/min work level (upper curves) are plotted together to show the response of mean skin temperature (middle curves) and of T_{wi} (lower curves). In these four experiments with nearly equal metabolic rates, four different T_{wi} curves were produced with different controller settings, and four different skin temperature responses appeared. The principal controller setting being varied was τ, which ranged from 5 to 20 minutes. With the short τ of 5 minutes and a correct gain, the T_{wi} fell rapidly to the correct low value for the indicated MR, but because it went too quickly the subject complained of being cold and he shivered after 20 minutes. Notice that the skin temperature change for the same experiment was rather abrupt. At the other extreme, the experiment with a τ of 20 minutes was coupled with a low gain. Here T_{wi} fell slowly and not far enough. The effect was to allow a rise in skin temperature and sweating. In another experiment, τ was 10 minutes but the gain was low. Here the rate of change of T_{wi} was appropriate but the final value was too high and skin temperature fell slightly to begin with and then rose past the initial value. This subject also sweated. The fourth curve is identified with a τ of 8 minutes and the correct gain. Here the T_{wi} fell over the appropriate time course to the correct final level. Skin temperature fell properly and the subject was neither sweating nor chilled.

We observed again, as we had during the 1966 experiments, that the skin temperature must not be allowed to rise; it must fall during work. The harder the work the lower the final skin temperature. The skin temperature should fall at a rate approximately half as great as the water temperature. In other words, the time constant for skin temperature in a good experiment

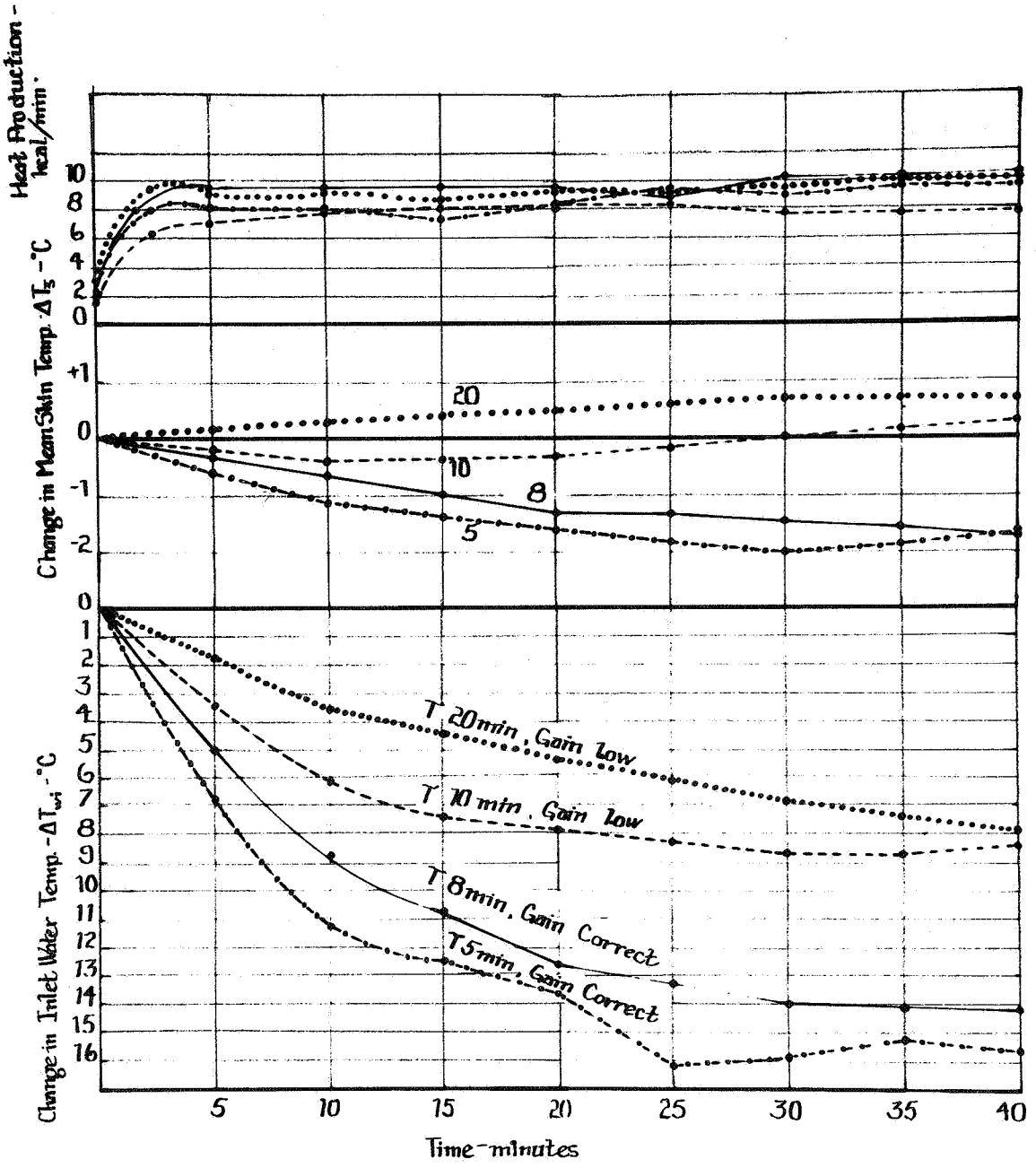

Figure 13. A plot of the relative changes in T_{wi} and $T_{\bar{s}}$ with their associated MR's obtained with different Q controller settings.

seems to be approximately twice that of the time constant for T_{wi}. Conversely the skin temperature cannot be made to fall too rapidly, as occurred in the experiment with the 5 minute time constant, because shivering occurred about 20 minutes into work. This was overcooling, although the final value for T_{wi} was nearly correct. The subject stayed cold for nearly the full hour of work.

Experiments with τ = 10 minutes, and gain correct, were reasonably good in this initial series, until we tried intermittent work. In these experiments 10 minutes was a bit too long, and the final value for τ became 8 minutes. Figure 14 illustrates this.

In the lower half of Figure 14 is data from an experiment in which the subject, for a period of half an hour, alternately worked for 5 minutes at 12 kcal/min and rested for 5 minutes. Notice that the MR and heart rate respond immediately to a work episode, and these two curves are essentially in phase with the work periods. The Q curve is slightly out of phase, with the peak of heat removal appearing just after each work period is finished. T_{wi} generated from the MR signal with a τ of 10 minutes is approximately 180° out of phase with the work periods. This allowed the skin temperature to remain essentially unchanged on the average and the subject sweated slightly. His weight loss rate for the half hour was 147 gms/hr. Because the response time of T_{wi} was too long, T_{wi} did not have time to get to the correct low point of 13°C; it reached 16°C.

These results, plus those which were illustrated in Figure 13, led to the selection of 8 minutes as being the appropriate value for τ. This 8 minute τ in the controller produced changes in actual values for T_{wi} with 10 minute time constants. The slightly shorter τ in the controller was needed to compensate for lags in the TE cooler and for the fact that $\dot{V}_{O_2}$ does not change as a square wave, but rather as an exponent with a short time constant (perhaps 30 seconds).

Validation Runs

One of the validation runs is shown in the upper half of Figure 14. Here the subject was asked to do intermittent work for a period of 20 minutes, with one minute of work followed by one minute of rest. The work level was high, 14 kcal/min, and the short cycle time was considered to be a severe test of the experimental Q controller. With this short cycle time, the heart rate was slightly out of phase with work, and the MR curve a little more out of phase; their peaks came after the work periods were finished. Q appeared to be out of phase but quite similar in timing to the MR curve. Notice that in this experiment skin temperature fell progressively from the outset, and the subject did not sweat. His weight loss rate was 87 gms/hr. T_{wi} also fell progressively, reaching a low value of 8°C, which was appropriate to the

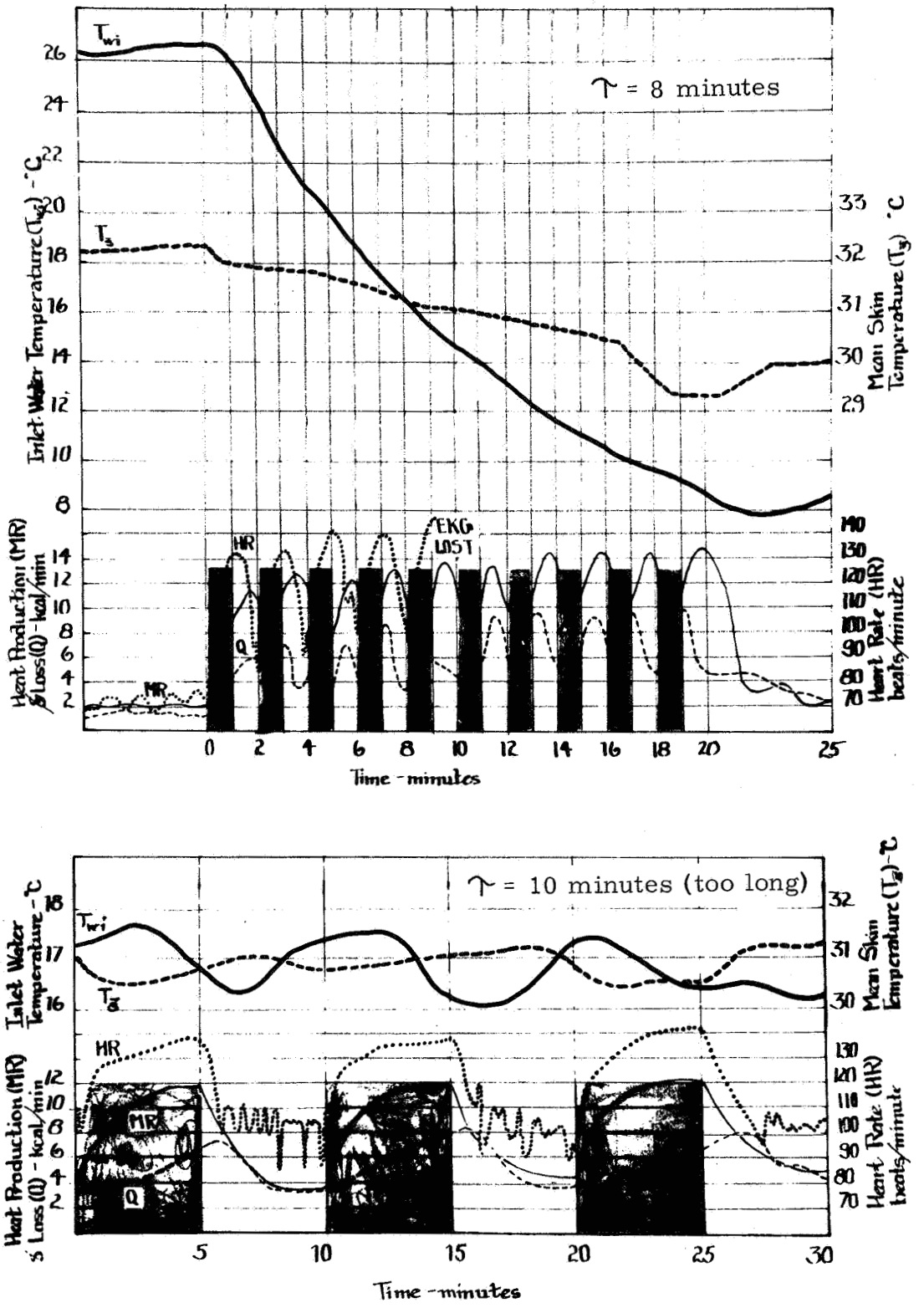

Figure 14. Physiological and cooling responses to two different intermittent work-rest schedules with different system τ settings.

average work level of 11 kcal/min. Incidentally, there may have been cycling in both T_s and T_{wi}, but these were not observed since the recorder printed these temperatures only once every two minutes. The control was entirely satisfactory.

We proceeded to further validate the controller settings by running experiments on the second subject, who had also been a subject during the 1966 experiments. Three of the earlier work schedules were repeated. Physiological responses to one hour of work at a nominal value of 8 kcal/min were essentially the same as those for the first subject, and very similar to the average response in the 1966 experiments shown in Figure 1. This was no surprise, although it was interesting to confirm that the resting and work values for T_{wi} were the same for both subjects, and that the gain and time constant settings held for both subjects. These values seemed to be determined more by the nature of the water cooled suit than by the characteristics of different subjects.

A more interesting test of the automatic controller was a repeat of activity schedules III and IV from the 1966 series. These experiments are shown in Figures 15 and 16.

Figure 15 shows the physiological responses and T_{wi} for the work schedule where the subject worked at a 5 kcal/min level for 20 minutes, followed immediately by 30 minutes at 8 kcal/min, and again for 30 minutes at 5 kcal/min. The data are quite similar to the averaged data from the 1966 experiments shown in Figure 3. The subject was well controlled in that he was not chilled, felt subjectively comfortable, and his weight loss rate was only 45 gms/hr. Notice that despite the rather irregular shape of the MR curve the T_{wi} signal generated by the controller was smooth and correct.

Figure 16 shows the data from near maximal work lasting for 10 minutes. These responses can be compared to the mean data from 1966 shown in Figure 4. The automatic controller produced an appropriate change in T_{wi}, and again the subject sweated at a rate of only 45 gms/hr.

These experiments validated our approach to automatic control. The values for the controller settings had been established for a particular WCG. We found that automatic control using $\dot{V}_{O_2}$ as an input met our basic criterion for good control, minimal sweating without chilling. The experienced subject compared automatic control in these experiments with the best manual control achieved in the 1966 series; he stated that the automatic control was smoother and subjectively preferable.

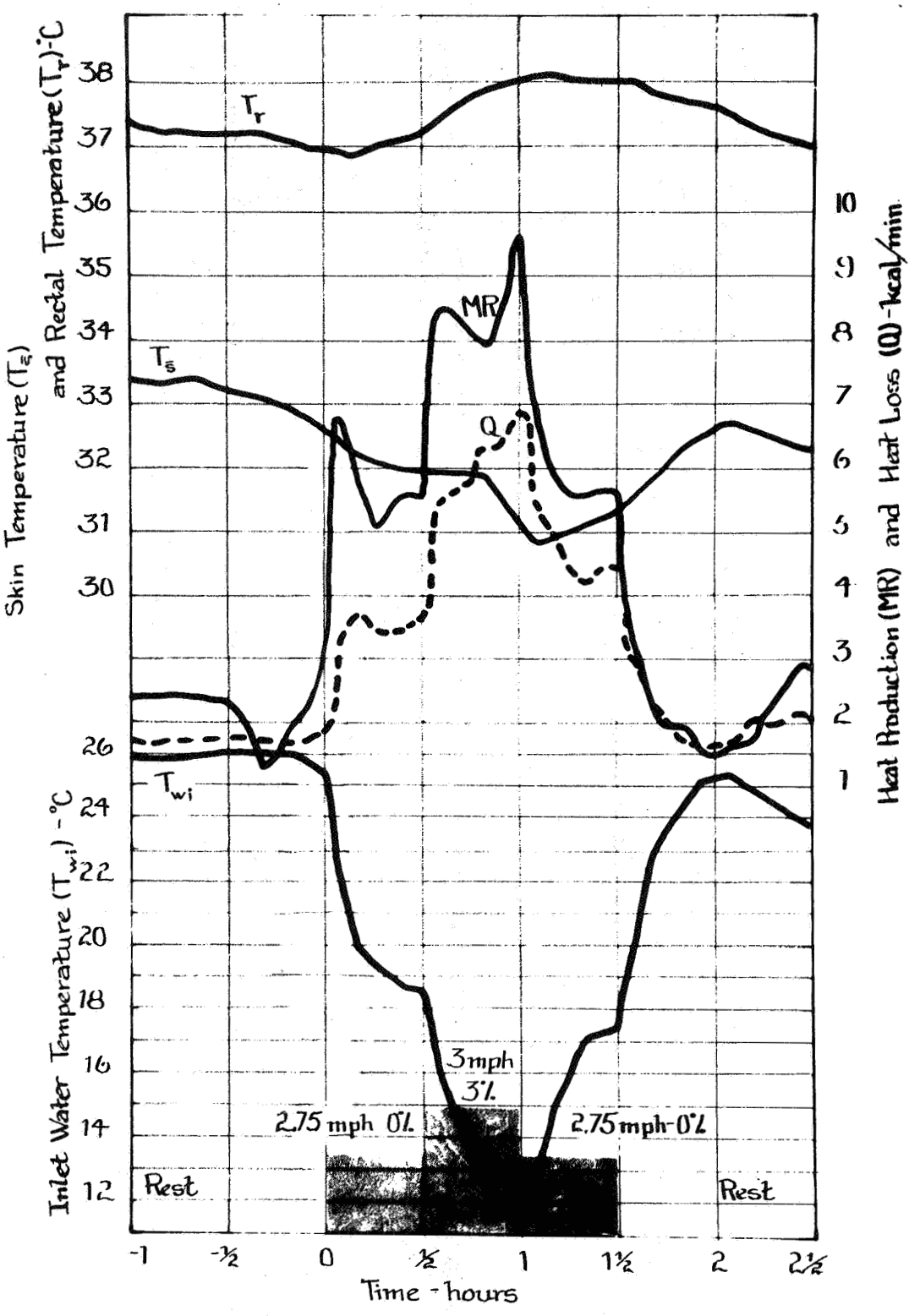

Figure 15. Responses obtained in an automatically controlled experiment in which the activity pattern duplicated an earlier manually controlled one (Fig.3).

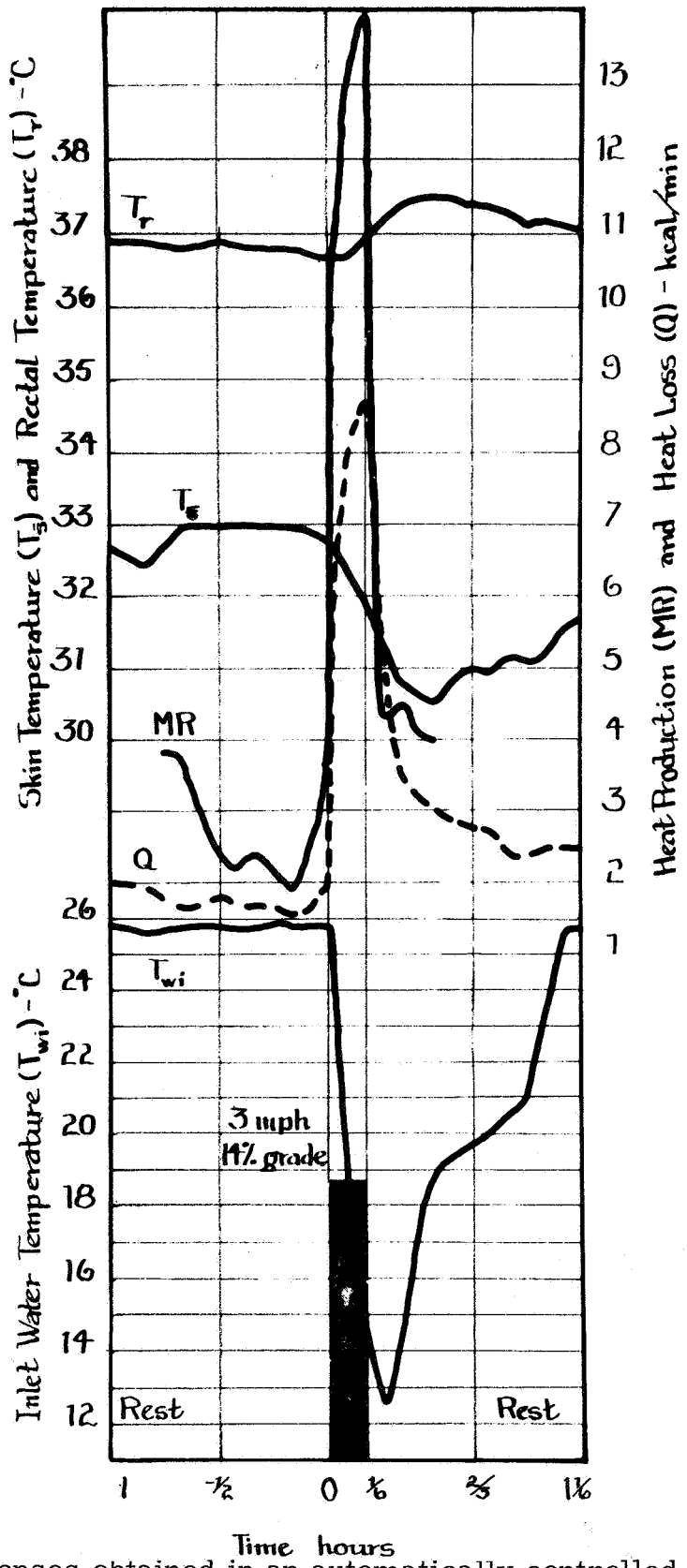

Figure 16. Responses obtained in an automatically controlled experiment in which the activity pattern duplicated an earlier manually controlled one (Fig. 4).

DISCUSSION

The work reported here is specific to the automatic control of a particular WCG used in a particular environment. However, the adjustments available in the final Q controller, described in the following section, permit it to be used with other WCG's--for example, our own suit used in the 1966 experiments--and with other cooling devices which are controllable by varying a DC voltage.

Our automatic control system worked despite a number of simplifications in modeling the complex physiological adjustments in man. In constructing the model we linearized heat transfer coefficients and used mean values rather than ranges of values. The gain of the controller (B_4) was a constant, although we suspect it should be a nonlinear function proportional to the $\dot{V}_{O2}$ signal. A number of refinements have been thought of which would add to the complexity of the controller, but our present device worked with satisfactory accuracy.

We have not explored a number of human variables such as diurnal variation of temperature and metabolic rate, variations between individuals, and variations from day to day in the same individual. These are real phenomena, and we do not know at this time how important they are for operational use of an automatic controller.

The present Q controller has not been tried for long periods of quiet activity. We suspect that slight undercooling or overcooling extended over a period of many hours would lead to undesirable cumulative effects. Prolonged slight overcooling at rest would lead eventually to low skin temperature, loss of body heat, and shivering. The shivering would cause an increase in oxygen uptake and hence a stronger cooling signal. Our experiments were focused primarily on the use of the controller in a working man for periods ranging from one or two minutes up to several hours. We feel that in its present form it is sufficiently accurate for this purpose.

To improve the present controller, it would be important to add some kind of feedback. For example, the measurement of skin temperature when used to correct the controller during long periods of quiet activity should be able to prevent drift or accumulated error.

Critical adjustments of the present controller must be made after the determination of the proper T_{wi} for rest in a given WCG, since the analog of this temperature must be defined. As explained in the description of the final Q controller, there is a definite relationship between this analog (IC), the gain (B_4), and the offset voltage ($\dot{V}_{O_2}^0$). A WCG with better heat removal

capability than our present suit--for example, the suit used in the 1966 experiments--will call for a higher resting T_{wi}, e. g. 31 or 32°C. When this setting is made, then the correct (higher) water temperatures during work will result.

Our controller uses as an input a voltage which is proportional to $\dot{V}_{O_2}$. This signal may not be readily available during space operations, so other inputs must be considered. At first look, the heart rate would be a suitable input, if it were possible to filter out those changes in heart rate which are not related to a change in heat production. Certainly it would be possible to remove transients which occur from momentary excitement, and a smoothed averaged heart rate ought to look very much like the $\dot{V}_{O_2}$ curve which we generate with our MRM. Whether or not the heart rate can be sustained for a long period without a sustained increase in MR is not clear physiologically. There may also be other usable inputs. The essential characteristics for any input are: it must be directly related to heat production, and it should have a response time as short as $\dot{V}_{O_2}$ or heart rate.

There is one puzzling aspect of the data collected this year which was also in the data of the 1966 experiments. This is the mismatch between Q and MR. Even at the end of a two hour period of work, the heat loss did not equal the heat production. (External work and evaporative cooling are included in the Q curves.) Storage of heat in the body, which is difficult to measure, especially with as few sampling points as we used, may be a large part of the explanation. It is also possible that the absolute values for metabolic rate taken by our MRM are in error. We calibrate the MRM signal against the values obtained by collection of expired air and gas analysis, and there may be a mismatch between the two procedures. There may also be losses of energy from our system which were not measured and which were larger than we estimated. The resolution of this problem will have to await a careful calorimetric study.

We are often asked, why bother with automatic control; isn't a simple manual adjustment adequate? On the basis of our experience to date, and making no effort to disguise our bias in favor of automatic control, we offer the following arguments for and against:

Pro:

1. The subject is a poor judge of his own thermal state, often reacting too late to sensations of cold or warmth. By this time the damage has been done.

2. Automatic control relieves a busy astronaut of one more thing to think about.

3. Automatic control is smooth and accurate; there are no rude surprises, no overshoot or undershoot with sudden chilling or sweating.

4. Automatic control leads to a high rate of heat extraction, i. e. maximum Q.

5. Automatic control and the minimization of sweating during work prevents overloading of the cooling device in the portable life support system (PLSS), which may cause wetting in the suit, fogging of the helmet face plate, and distressing subjective symptoms.

6. Correct automatic control should provide the most efficient use of the stored coolant in the PLSS.

7. An automatic controller can be adjusted to match individual requirements and to match the heat removal capability of particular WCG's.

Con:

1. The present controller requires the measurement of $\dot{V}_{O_2}$ continuously, which may not be feasible operationally, and alternate inputs have not yet been explored.

2. The present automatic controller does not operate as a closed loop system, hence neither drift or accumulated error is corrected. If the device inadvertently overcools, the subject may begin to shiver, causing an increase in MR and a lowering of T_{wi}. This type of controller is probably not suitable for long periods of quiet activity, or for continuous use inside the spacecraft.

3. It is necessary to adjust and to calibrate the controller for each man and each suit, and possibly for each kind of mission.

4. The gain of the system probably should be generated from the $\dot{V}_{O_2}$ signal and not be a constant as used in the present design. Other refinements of the present Q controller would make it more accurate, more stable, and more flexible.

5. Any addition of equipment, even something as basically simple as this automatic controller, has its effect on the reliability of the total PLSS.

The important fact to us is that an open loop automatic controller works, and its performance is equal to and in some ways better than our best continuous manual control.

CONCLUSIONS

1. Automatic control of heat removal in a water cooled suit worn by men going through various patterns of work is feasible and has been experimentally validated.

2. The present automatic controller produced smooth temperature control, good heat extraction, a comfortable subject, and no sweating or chilling.

3. T_{wi} is related to changes in metabolic rate by an ordinary differential equation:

$$\tau \dot{T}_{wi} = -T_{wi} + B_4(MR_0 - MR)$$

4. The τ for T_{wi} was 10 minutes in both our present and earlier series of experiments. (The 8-minute time constant used this year in the experimental controller compensated for cooler lags, but T_{wi} changed with a τ of 10 minutes.)

5. It is likely that other physiological variables which are proportional to metabolic rate would serve as inputs to automatic controllers.

6. A closed-loop, self-correcting control system is theoretically possible. The advantages of stability and long term accuracy in such a controller recommend its development.

THE FINAL Q CONTROLLER

In the preceding sections we have described the evolution of an experimental Q controller from analysis through design, adjustment, and validation. The experimental Q controller satisfactorily controlled the heat removal from subjects following various patterns of work. Armed with these results, we were then able to design and construct a final Q controller to be delivered as an end item of the study. In this section we discuss the design procedure followed, show circuit diagrams, list components used, and discuss the calibration of the device. From this discussion one should be able to duplicate the final Q controller, and know how it is adjusted and calibrated for use.

The purpose of the Q controller is to control inlet water temperatures from an analog signal which is proportional to oxygen consumption. The first requisite in the specification of the design parameters was the mathematical statement of the Q controller function.

Equation (1), page 13, is:

$$\tau \dot{T}_{wi} = -T_{wi} + B_4(MR_0 - MR) \qquad (1)$$

The performance of the hypothetical controller in the biothermal model (Appendix B) and the operation of the experimental Q controller defined the design parameters related to the initial inlet water temperature (T_{wi_0}); the time constant (τ) of the cooling command ($\dot{T}_{wi}$); the metabolic rate (MR_0) which would require a water temperature of 0°C; and the gain of the system (B_4). A second form of Equation (1) which relates oxygen consumption to inlet water temperature where $\dot{V}_{O_2}^0$ and $\dot{V}_{O_2}$ are the oxygen consumption equivalents of MR_0 and MR respectively is expressed in Equation (3):

$$\tau \dot{T}_{wi} = -T_{wi} + B_4(\dot{V}_{O_2}^0 + \dot{V}_{O_2}) \qquad (3)$$

The design parameters that resulted from the analysis of the experimental controller performance were:

$$T_{wi_0} = 26.0 \pm 0.5°C$$

$$\tau = 8 \text{ minutes}$$

$$\dot{V}_{O_2}^0 = 3.11 \text{ liters } O_2/\text{min}$$

$$B_4 = 9.42°C/\text{liters } O_2/\text{min}$$

Conversion of these parameters into their electrical equivalents required time and magnitude scaling. Equation(4) is the relationship between metabolic rate and oxygen consumption, assuming a constant RQ:

$$MR = k\dot{V}_{O_2} \qquad (4)$$

where: MR = the metabolic rate in kcal/min
k = the standard conversion constant of 4.825 kcal/liter O_2
$\dot{V}_{O_2}$ = the oxygen consumption in liters O_2/min

The range and magnitude of the controller inputs and outputs were scaled to be compatible with the analog requirements of the thermoelectric cooler controller and the MRM. The cooler controller required input signal levels ranging from +6.25 VDC to 0.0 VDC; therefore the analog of the inlet water temperature was determined from Equation (5):

$$\begin{aligned} \text{VDC (analog)} &= T_{wi}/5 \\ &= 26.0°C/5 = 5.2 \text{ VDC (initial)} \\ &= 0.0°C/5 = 0.0 \text{ VDC (minimum)} \end{aligned} \qquad (5)$$

The analog output of the MRM was based on 1.0 VDC being equivalent to 1.0 liter of oxygen consumed and did not require scaling, as long as oxygen consumption would not exceed 3.11 liters/min during use. The gain of the

system (B_4) was scaled by a factor of 5, thus maintaining a uniform scaling constant; it is stated in Equation (6):

$$\begin{aligned} \text{Gain} &= B_4/5 \\ &= 9.42/5 \text{ (initial)} \end{aligned} \tag{6}$$

The time constant of the cooling command (τ) was multiplied by 60, thus converting 8 minutes into 480 seconds. The scaled mathematical expression for the controller is stated in Equation (7).

$$\tau \frac{\dot{T}_{wi}}{5} = -\frac{T_{wi}}{5} + \frac{B_4}{5}(\dot{V}_{O_2}^{0} - \dot{V}_{O_2}) \tag{7}$$

The relationship of oxygen consumption to inlet water temperature provides an exponential output response to $\dot{V}_{O_2}$ inputs.

Analysis of the experimental Q controller performance determined that the design of the final controller could be considered in two stages: (1) the summation and amplification of the inputs ($\dot{V}_{O_2}^{0}$ and $\dot{V}_{O_2}$); and (2) the generation of the exponential analog command signal. The discrete components of the circuit were selected for their temperature characteristics, reliability, size, and compatibility with the circuit design.

Summation and amplification of the inputs was accomplished by a DC operational amplifier (Model 3007/15C, Burr-Brown Research Corp., Tucson, Arizona) used in connection with a resistive summing and feedback network, as shown in Figure 17:

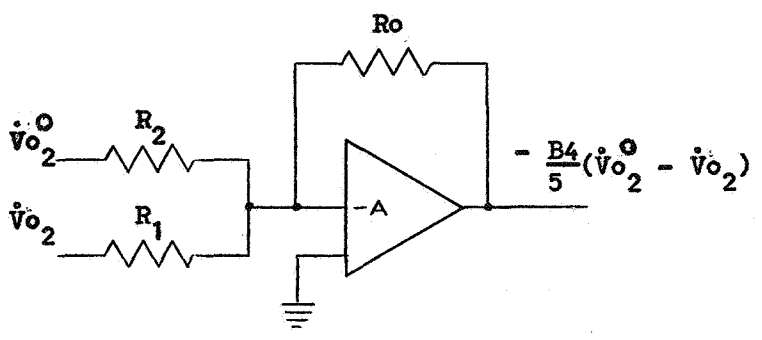

Figure 17. Summation of voltages using an operational amplifier.

Since the open loop gain of the operational amplifier (A) is of the order of 10^5, the output voltage is related to the inputs by Equation (8):

$$\frac{B_4}{5}(\dot{V}_{O_2}^0 - \dot{V}_{O_2}) = -\dot{V}_{O_2}^0 \frac{R_0}{R_2} - (-\dot{V}_{O_2}) \frac{R_0}{R_1} \tag{8}$$

but:

$$\frac{R_0}{R_1} = \frac{R_0}{R_2}$$

$$\therefore \quad \frac{B_4}{5}(\dot{V}_{O_2}^0 - \dot{V}_{O_2}) = -\frac{R_0}{R_1}(\dot{V}_{O_2}^0 - \dot{V}_{O_2}) \tag{9}$$

It is clear from Equation (9) that $B_4/5$, or $[R_0/R_1]$ is the amplification factor or gain of the input stage. The principal sources of error considered were: voltage drift, resistive values of the input and feedback components, and amplifier gain. In the error analysis the amplifier gain was neglected because of its magnitude. The feedback component was selected to be variable, thus allowing calibration of the amplification factor and reducing the probable error to the relative error in the summing components and the voltage drift. The relative errors Δe_1 (resistive) and Δe_2 (drift) and their probable effect on performance are related by Equation (10):

$$(\Delta e) \text{ probable} \cong \frac{\sqrt{2(\Delta e_1)^2 + (\Delta e_2)^2 + (\Delta_{12})(\Delta e_1)(\Delta e_2)}}{4} \tag{10}$$

$$\cong 0.0218$$

This probable error (Δe) was further reduced by providing a variable $\dot{V}_{O_2}^0$, thus allowing the relative error of the input components to be offset by this voltage adjustment. The initial gain of this stage, determined earlier in the analysis, and the provision for its calibration are important, since variations in the $\dot{V}_{O_2}^0$ offset voltage and the initial condition (IC) or analog of the resting inlet water temperature of the second stage require additional flexibility in the gain adjustment. The relationship of these parameters is illustrated in Figure 18, where the four curves shown represent the family of initial conditions. The component values are shown in Figure 19, and are given in detail in Table I, p. 43.

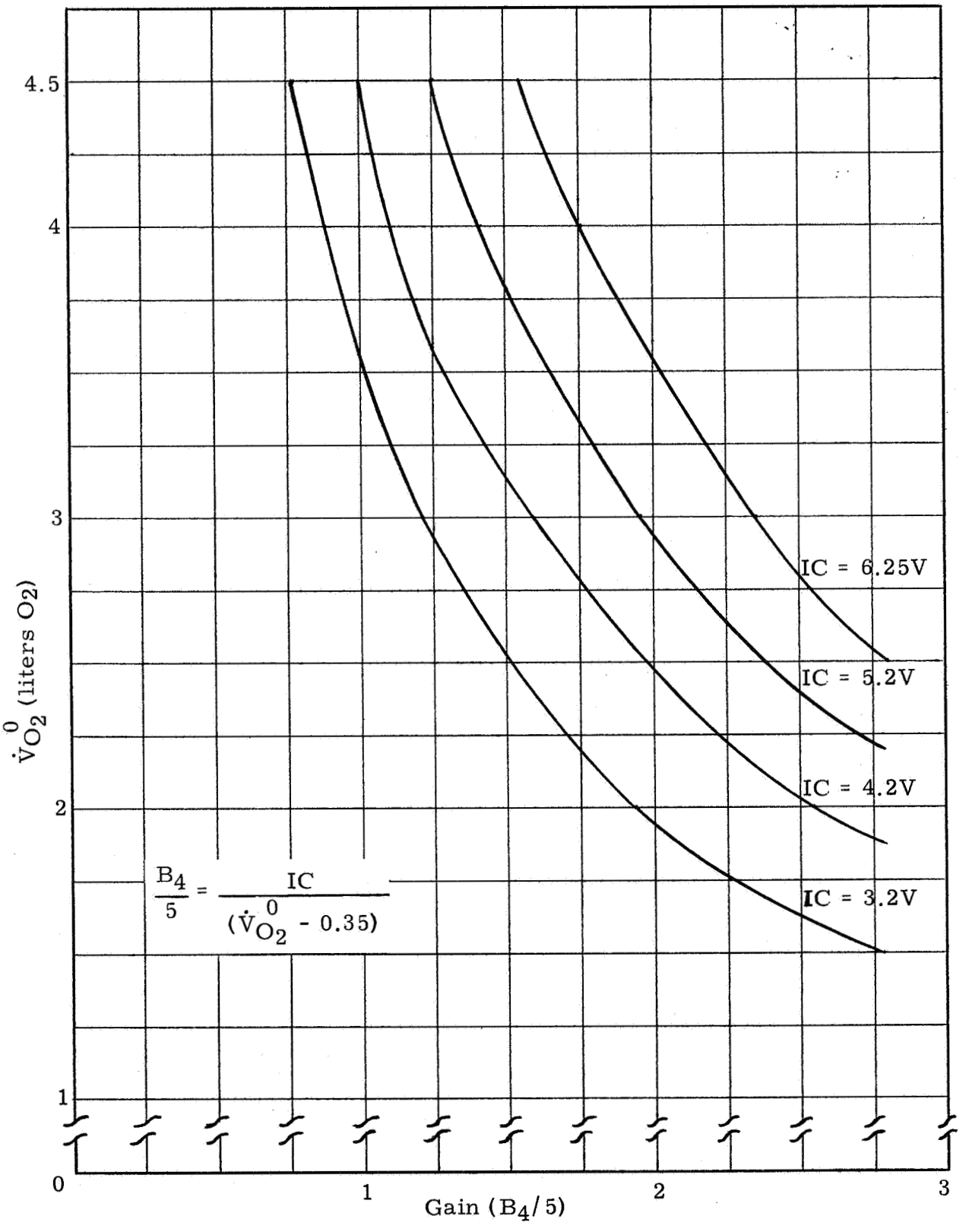

Figure 18. The relationship of $\dot{V}^0_{O_2}$ to the Gain (B_4/5).

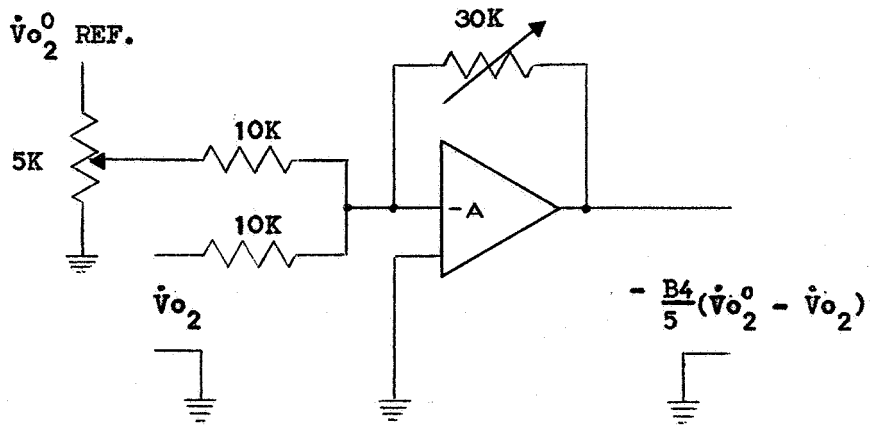

Figure 19. A schematic of the summing amplifier

Generation of the analog output was performed with a chopper stabilized DC operational amplifier (Model 3012/25 Burr-Brown) used as an integrating amplifier, as shown in Figure 20:

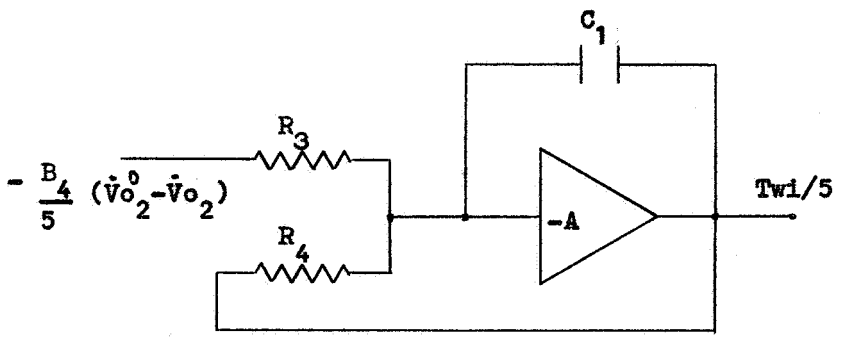

Figure 20. Diagram of an integrating amplifier

Once again the amplifier gain may be neglected because of its magnitude (10^6); therefore the relationship of the output to the inputs is given in Equation (11).

$$\frac{T_{wi}}{5} = \frac{1}{R_4C_1}\int_{t_0}^{t_1} -\frac{T_{wi}}{5}\,dt + \frac{1}{R_3C_1}\int_{t_0}^{t_1} \frac{B_4}{5}(\dot{V}_{O_2}^{0} - \dot{V}_{O_2})\,dt + IC \qquad (11)$$

Since the rate of integration or time constant is dependent on the inverse magnitude of R_nC_1, the requirement that $R_3C_1 = R_4C_1$ must be satisfied. The low frequency time constant τ is equal to $R_nC_1/2$. Equation (12) states these relationships:

$$\frac{T_{wi}}{5} = \frac{0.1}{R_n C_1}\left[\int_{t_0}^{t_1} - T_{wi}\,dt + B_4 \int_{t_0}^{t_1} (\dot{V}_{O_2}^{0} - \dot{V}_{O_2})\,dt\right] + IC \qquad (12)$$

The probable sources of error considered were: voltage drift, resistive and capacitive values of the input and feedback components, leakage resistance, and amplifier gain (A). As in the preceding analysis, the amplifier gain may be neglected because of its magnitude. The relative errors of e_1 (drift), e_2 (resistive and capacitive), and e_3 (capacitive leakage) and their probable effect are related by Equation (13), which does not exceed the performance requirements of the controller.

$$\Delta e_{probable} \cong \frac{\sqrt{(\Delta e_1)2 + (\Delta e_2)^2 + (\Delta e_3)^2 + \Delta_{12}\Delta e_1 \Delta e_2 + \Delta_{13}\Delta e_1 \Delta e_3 + \Delta_{23}\Delta e_2 \Delta e_3}}{4}$$

$$\cong 0.033 \qquad (13)$$

Reduction of this error is obtained by (1) matching the input component values; (2) the incorporation of a variable resistor in series with the integrator input components. The second method of reduction provided the capability to offset the capacitive tolerance and adjust the time constant within a limited range, as shown in Figure 21. The component values shown in Figure 21 are given in detail in Table I, p. 43.

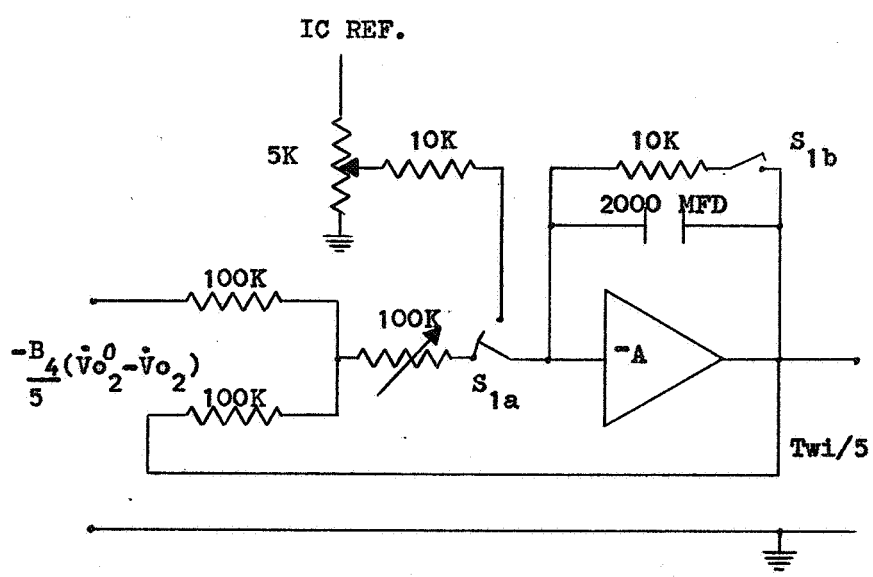

Figure 21. Schematic of the integrating amplifier.

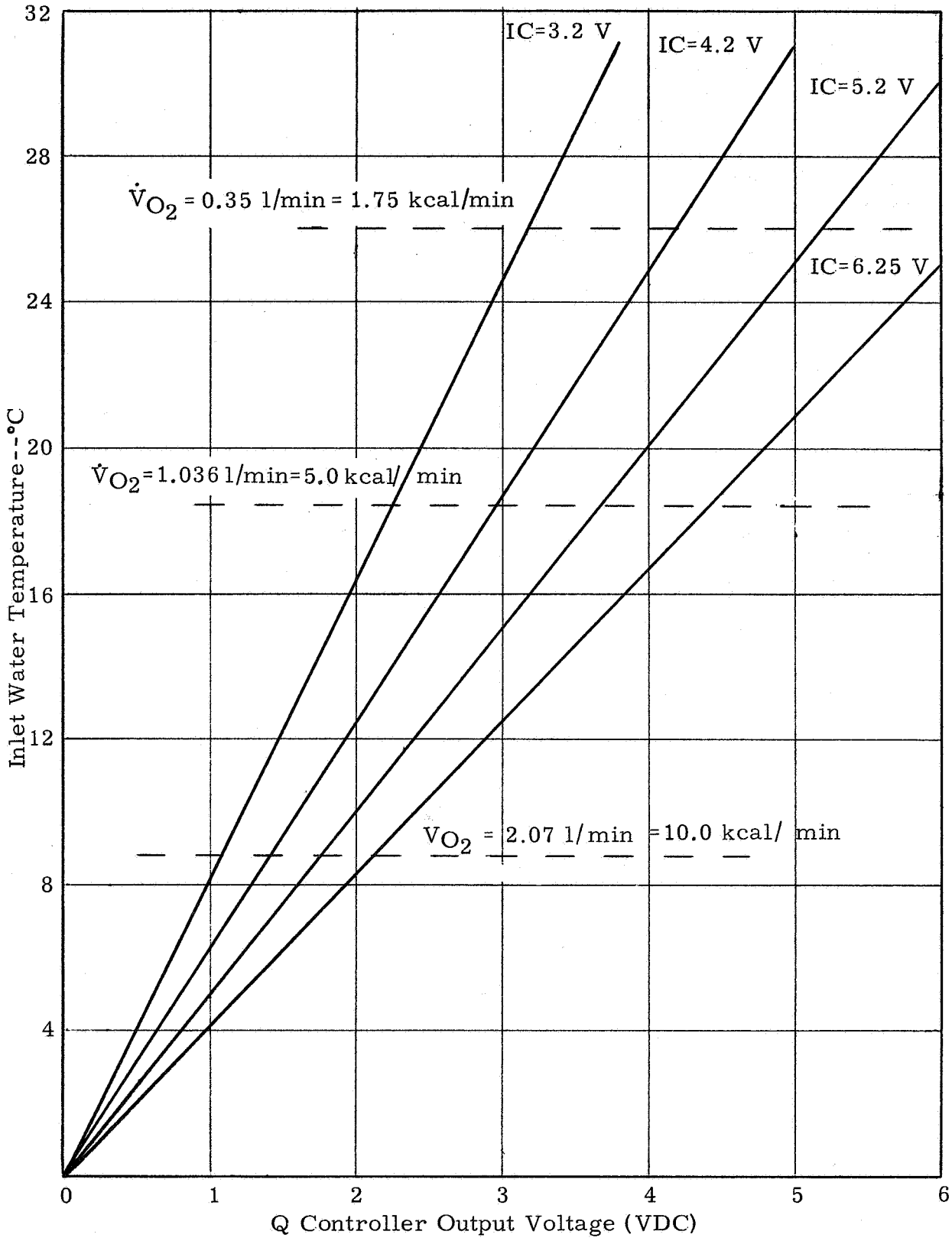

Figure 22. The ideal relationship of Q controller output to T_{wi}.

It was assumed that steady state output levels were obtained in five time constants, and Figure 22 illustrates the relationship between these output levels and the inlet water temperature.

The performance of the final Q controller was verified by testing it in the water cooling system, where $\dot{V}_{O_2}$ analog inputs were converted to T_{wi} analog signals that correctly controlled the thermoelectric cooler and T_{wi}, based on the criteria represented in Figure 22 and Table II, page 44. The complete schematic of the Q controller is shown in Figure 23:

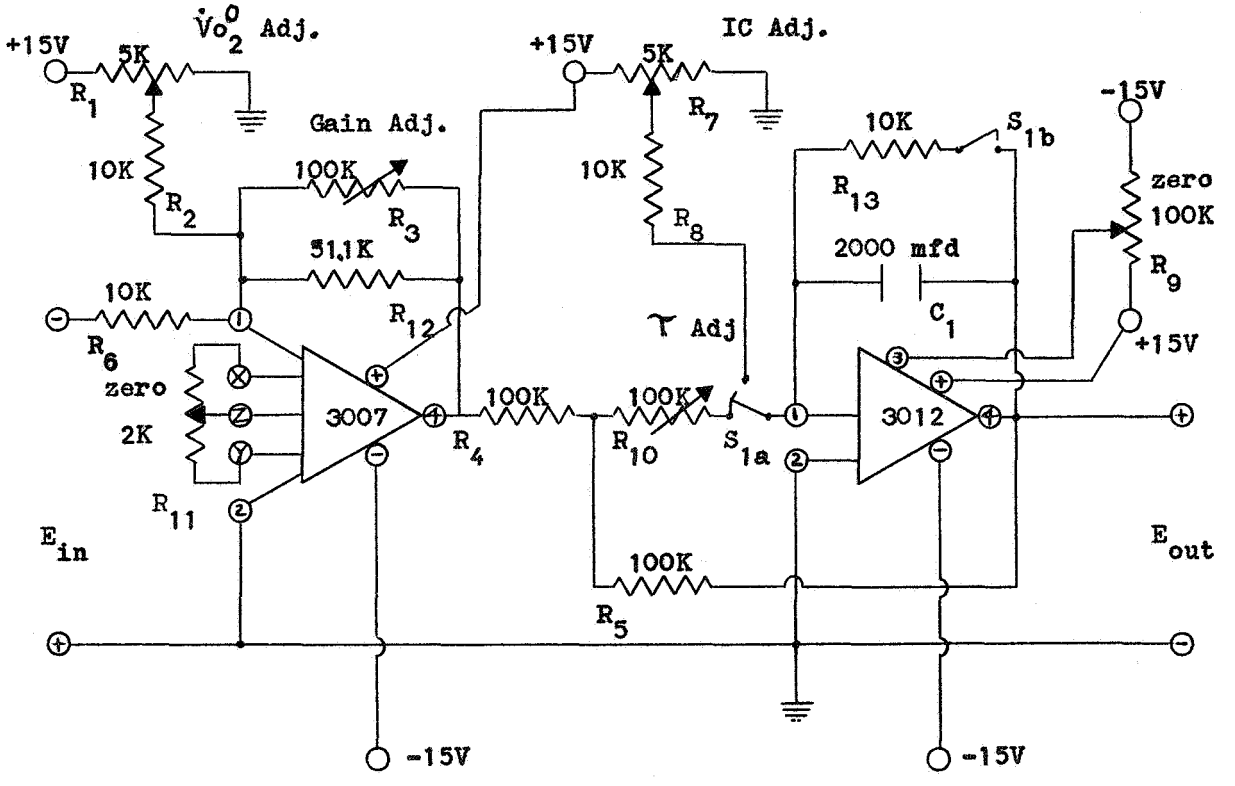

Figure 23. The schematic of the Q controller.

Figures 24 and 25 are photographs of the final Q controller and the circuit components, respectively. The variable parameters of the controller are: $\dot{V}_{O_2}^0$ (0-5 VDC); gain, or $B_4/5$ (0-3); and the time constant τ (8-20 min), which allow the adaptation of the controller to other water cooled garments and to other metabolic rates.

The initial calibration of the controller based on the design parameters and requirements specified in the preceding analysis may be obtained by following the Calibration Procedure. It is characteristic of the operational amplifiers to swing to a saturation level for several seconds prior to obtaining a stable level; therefore, one should allow the controller to stabilize before calibrating.

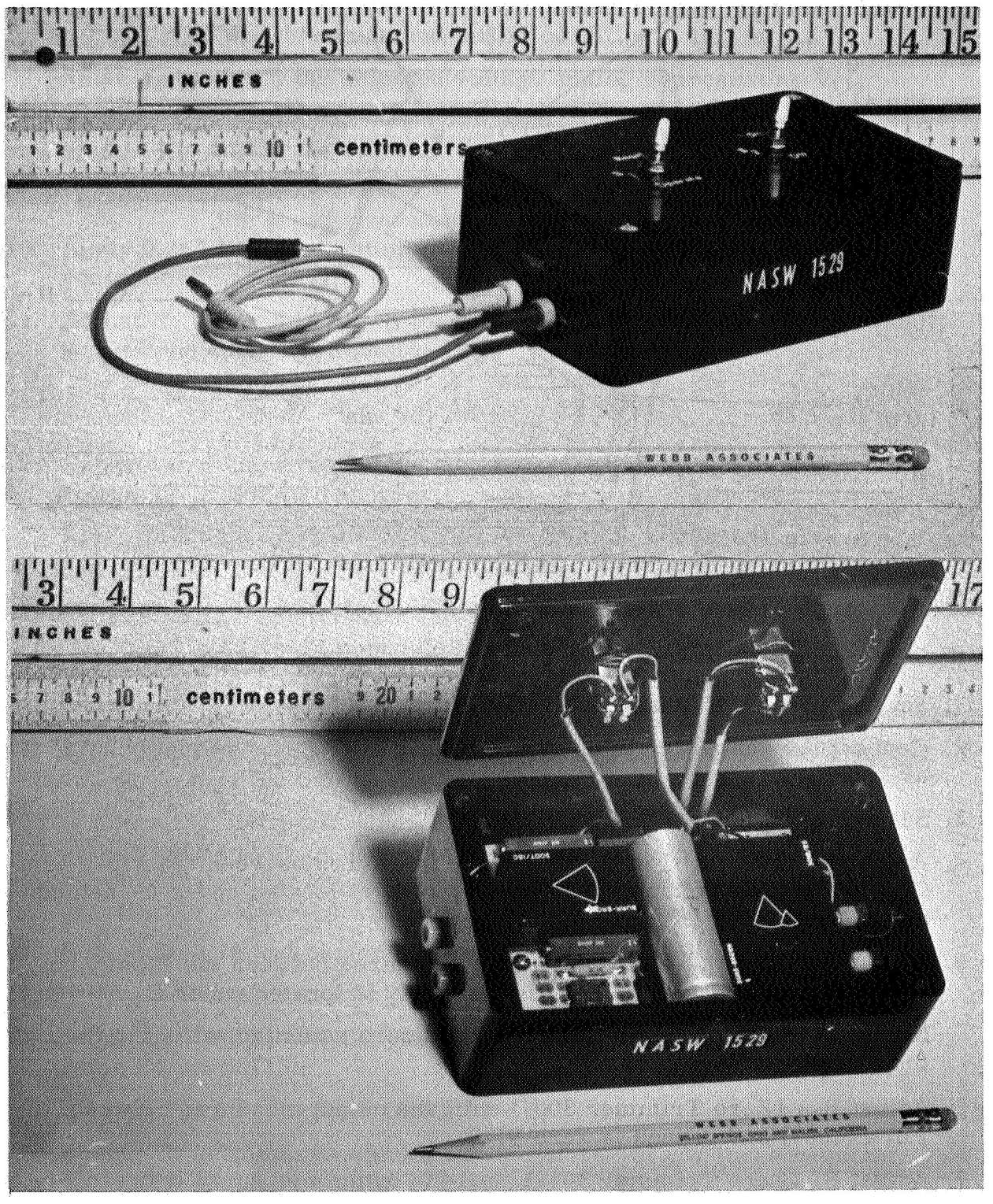

Figure 24. Photographs of the final Q controller.

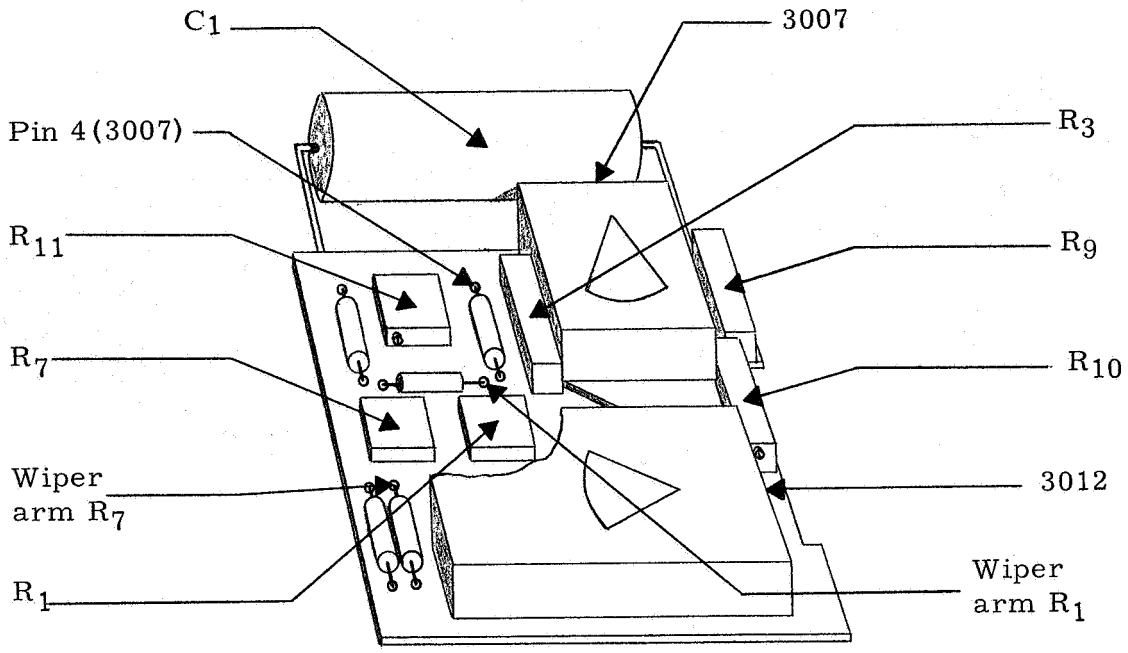

Figure 25. The controller circuit board.

Calibration Procedure (Reference Figs. 23 & 25)

1. Set switches S_1 to Reset and S_2 to Off.
2. Connect the controller to an appropriate ± 15 VDC power supply, as specified in Table II.
3. Set switch S_2 to On.
4. Adjust R_1 ($\dot{V}_{O_2}^0$ Adj.) until the voltage measured between the wiper arm (R_1) and ground is zero VDC. Resistor R_1 is located under C_1 behind amplifier (3007).
5. Adjust R_7 (IC Adj.) until the voltage measured between the wiper arm (R_7) and ground is zero VDC. Resistor R_7 is located under C_1 next to R_1.

   Note: the inputs of the amplifiers are at zero potential, allowing their inputs to be balanced.
6. Adjust R_{11} (Zero Trimmer 3007) until the output measured between Pin 4 (3007) and ground is zero VDC.
7. Adjust R_9 (Zero Trimmer 3012) until the output measured between Pin 4 (3007) and ground is zero VDC.

Note: the controller amplifiers are now balanced and ready for the application of the reference and initial condition voltages.

8. Adjust R_1 to obtain the selected voltage analog representing $\dot{V}_{O_2}^0$ measured between the wiper arm (R_1) and the ground.

9. Adjust R_7 to obtain the selected voltage analog representing the resting inlet water temperature measured between Pin 4 (3012) and ground (E_{out}).

10. Apply 0.35 VDC (the resting oxygen consumption analog) to the controller input (E_{in}).

11. Adjust R_3 (Gain Adj.) until the voltage measured between Pin 4 (3007) and ground satisfies Equation (14):

$$E_{pin\ 4} = -E_{out} \tag{14}$$

12. Connect the output terminals (E_{out}) to a suitable high impedance voltmeter or analog recorder.

    Note: the stability of the controller at resting conditions may now be observed.

13. Set switch S_1 to Operate and observe the stability of the output voltage (E_{out}).

    Note: negative drift indicates the gain of amplifier is low where the converse is true for positive drift.

14. Adjust R_3 (Gain Adj.) until the output (E_{out}) is stable at the selected analog voltage for the resting inlet water temperature.

15. Measure the voltage between Pin 4 (3007) and the ground. If this voltage exceeds or is less than the selected analog voltage for the resting inlet water temperature, reduce or increase the voltage between the wiper arm (R_1) and ground by the same percent deviation.

16. Repeat Step 14 and perform Step 17.

17. Set S_1 to Reset.

18. Set R_{10} (τ Adj.) to FCCW and adjust to the desired time constant using Equation (15):

$$N \cong (2.80)(\tau - 8) \tag{15}$$

    where: τ is in minutes and N is the number of CW turns required.
    τ shall not exceed 20 minutes.

19. Apply a voltage to the input (E_{in}) equal in magnitude to the selected $\dot{V}_{O_2}$ analog voltage.

20. Set S_1 to Operate and observe the exponential response for its time constant and magnitude over a time period equal to 5τ.

    Note: the output should obtain the minimum desired level in a time period equal to 5τ. An analog recorder is recommended for this measurement due to the long time constants involved.

21. Make adjustments to τ as required until the desired time response is obtained by repeating steps 15, 17, and 18.

22. Set S_1 in Reset and S_2 to Off.

Operational Procedure

1. Set S_1 to Reset and S_2 (power switch) to Off.

2. Connect controller to ± 15 VDC regulated power supply.

3. Connect output of controller to the appropriate interface for cooling circuit.

4. Connect input of the controller to the oxygen consumption analog generator (where 1 liter of O_2 consumed = 1 VDC).

5. Set S_2 to On and allow 5 minutes for establishing the IC voltage level.

6. Set S_1 to Operate for the desired period of control.

7. At the conclusion of the control period set S_1 to Reset and S_2 to Off.

The controller will operate as designed when the appropriate inputs and power supply connections have been made as stated in the performance specifications. See Table II.

Webb Associates, Inc.
Yellow Springs, Ohio
February 5, 1968

Table I. COMPONENT DESCRIPTION

Item	Description	amount required
R_1, R_7	5 K ohm ±5% subminiature trimmer, Amphenol series 2900 wire-wound, RT22C2P502, 1 watt	1 ea.
R_2, R_6, R_8, R_{13}	10 K ohm ±1% deposited carbon resistor, type DCC, IRC MIL-RN20X, 1/2 watt	1 ea.
R_3, R_9, R_{10}	100 K ohm ±5% high temperature trimmer, Amphenol series 2850 wire-wound 2850 P-104, 1 watt	1 ea.
R_4, R_5	100 K ohm ±1% coated metal film resistor type CEC, IRC MIL-RN60, 1/2 watt	1 ea.
R_{11}	2 K ohm ±5% subminiature trimmer, Amphenol series 2900 wire-wound, RT22C2P502, 1 watt	1 ea.
R_{12}	51.1 K ohm ±1% coated metal film resistor type CEC, IRC MIL-RN60, 1/2 watt	1 ea.
C_1	2000 MFD/10VDC DC electrolyte computer grade capacitor, CDE type BWH 2000-10	1 ea.
A_1	DC operational amplifier, Burr-Brown 3007/15C	1 ea.
A_2	DC operational amplifier, Burr-Brown chopper stabilized 3012/25	1 ea.
H_1	Plastic enclosure, HD type 6-1/4 x 3-3/4 x 1-7/8, black with cover	1 ea.
BJ	Banana jack, E. F. Johnson series 108-900, nylon insulated	7 ea.
S_1, S_2	Switch, subminiature toggle, Arrow-Hart & Hegeman DDDT type PM-6	1 ea.
P C_1	Universal printed circuit card Triad type 13510 modified	1 ea.

Table II. PERFORMANCE SPECIFICATIONS

SPECIFICATIONS -- Performance at 25° C with rated supply

	Min.	Typ.	Max.	Units
Input Impedance	50			MΩ
Gain Stability vs. Temperature		0.1		db/°C
vs. Supply		0.2		db/°C
Output Impedance		5		KΩ
Rated Output -- Voltage	±10			V
-- Current	±20			ma
Slewing Rate		2		V/μs
Output Current Limits		±40		ma
Equivalent Input Noise--DC to 10 kc			15	μV, rms
Input Voltage Drift vs. Temperature		±2	±5	μV/°C
vs. Supply		±30		μV/%
vs. Time		±50		μV/24h
Input Voltage Signal Level			±10	V
Temperature Range				
Specification	-25		+85	°C
Operating	-40		+85	°C
Storage	-40		+85	°C
Power Supply Requirements				
Rated Supply Voltage		±15		Vdc
Voltage Range	±12		±18	Vdc
Supply Drain--Quiescent			±15	ma
--Rated Output		±38		ma
Supply Regulation			1	%
Noise and Ripple			1	mV/rms

APPENDIX A

SYMBOLS AND ABBREVIATIONS

A	amplifier gain
B_3	a constant
B_4	controller gain, based on $-\Delta T_{wi}/\Delta \dot{V}_{O_2}$
c	heat capacity, kcal/°C
C	m times c, kcal/kg°C
E_o	output voltage
E_{in}	input voltage
EKG	electrocardiogram
e	error
Δe	probable error
f	fractional value
HR	heart rate, beats/min
H	heat content, kcal
h	height, cm
IC	initial conditions
K	coefficient of heat transfer, kcal/min/°C
k	calorific equivalent of oxygen, kcal/liter
L	heat loss, kcal/min
LR	inductive-resistive
lpm	liters per minute
MR	metabolic rate, kcal/min
MR_0	MR when T_{wi} is 0°C
m	mass, kg
$\dot{m}$	mass flow, kg/min
Q	quantity of heat transferred, kcal/min
R	resistance or resistor, ohms
RMR	resting metabolic rate, kcal/min
RQ	respiratory quotient
SCR	silicon controlled rectifier
T	temperature, °C
$\dot{V}$	volume flow rate, lpm
v	velocity
W	work, kcal/min
WCG	water cooling garment
ρ	density, grams/cm^3
τ	time constant, 1/e

Subscripts:

b	blood
d	dry bulb
e	expired air
g	garment
l	leg
r	rectal
s	skin
$\bar{s}$	skin, mean (temperature)
w	water, or wet bulb
wi	WCG inlet water
wo	WCG outlet water

APPENDIX B

BIO-THERMAL MODEL OF WORKING MAN IN A WATER COOLED SUIT

This section concerns a mathematical model describing the changing thermal states and the heat flows in men working in clothing containing water cooling tubes next to the skin. The model was mechanized on an analog computer, simulation runs made, and the results compared with results from laboratory experiments. The verified model was used in the design of the experimental Q controller.

A special note of thanks is due our consultant, Mr. A. Ben Clymer, of Columbus, Ohio, who played a major role in constructing the model, and who taught us some of the values of analog simulation.

BACKGROUND

Previously described biothermal models have dealt with human physiological responses to thermal stress, usually with a resting man. Stolwijk and Hardy (ref. 10) developed an elegant model of human thermoregulation, accounting for heat transfer internally via the blood, for skin to environment transfer of heat, and for regulatory responses of vasoconstriction, shivering, vasodilation, and sweating. This model supersedes an earlier one reported by Crosbie, Hardy, and Fessenden (ref. 11) which dealt with body temperatures, and with physiological responses in steady state and transient conditions. Wissler (ref. 12) developed a mathematical model which predicted temperatures in several body compartments under various environmental states, for resting and working men. Brown (refs. 13 and 14) constructed a model of resting man who exchanges heat with his environment and who responds to cold stress, e. g. water immersion, by vasoconstriction and an increase in metabolic rate. In his second report his model is expanded and its predictions of changing body temperatures under cyclic heat and cold stress are compared with experimental data. The main concern was with changes in core temperature and the accompanying physiological responses.

Woodcock et al (ref. 15) developed a passive electrical circuit analog for soldiers in various climates and clothing assemblies; it predicted heat loss and skin temperature in transient states. The analog computer model developed by Smith and James (ref. 16) dealt with both transients and steady states, and predicted heart rate response for men working under mild heat stress. The model's ability to predict dynamic heart rate responses to intermittent work in heat was impressive; predictions matched actual experience nicely.

None of these previous models dealt with men who were cooled when they worked. A man in a water cooled suit is in a special environment. If cooling is properly controlled, major physiological responses to regulate heat loss, sweating, and shivering are not seen. The active control of cooling matches changes in heat production. This is the biothermal system we are concerned with.

Man's biothermal responses during work with water cooling were studied in the laboratory and the results reported by Webb and Annis (ref. 7). Our subjects were thermally isolated and cooling was continuously controlled by hand as the work rates were varied. Data from these experiments are shown in Figures 1-5, pp. 5-9.

BASIS OF THE MODEL

The model was based upon the data from 18 experiments in which four subjects did three simple step changes from rest to work and back to rest. The nominal work rates were: 5 kcal/min (1200 Btu/hr) for 2 hours; 10 kcal/min (2400 Btu/hr) for 1 hour; and 15 kcal/min (3600 Btu/hr) for 1/6 hour. Figures 26, 27, and 28 show the "ideal" curves for these three work levels.

The term "ideal" is used because we normalized and smoothed the mean data in several ways. For example, the initial resting values for metabolic rate were standardized at 1.75 kcal/min, the rectal temperature at 37.08°C, and the mean skin at 33.3°C. The mean skin temperature curves are smoothed representations of mean data adjusted for unusual individual responses, e. g. one subject who started with a high skin temperature and stayed high until we overcooled him in the experiment. Similarly, the inlet water temperatures were averaged and smoothed data, and only those data used when there was no undercooling or overcooling. The curves for metabolic rate are constructions based on two or more expired air samples taken during each rest and work period. On the basis of other data in our laboratory, and particularly those from MRM records, the shapes of the MR curves were derived. Also for these ideal curves the MR stays flat during the work period, although in the actual experiments it tended to rise toward the end of the first hour, and rose further during the second hour when the experiment ran that long. The final value of Q in each experiment lasting an hour or more was about 80% of the indicated MR.

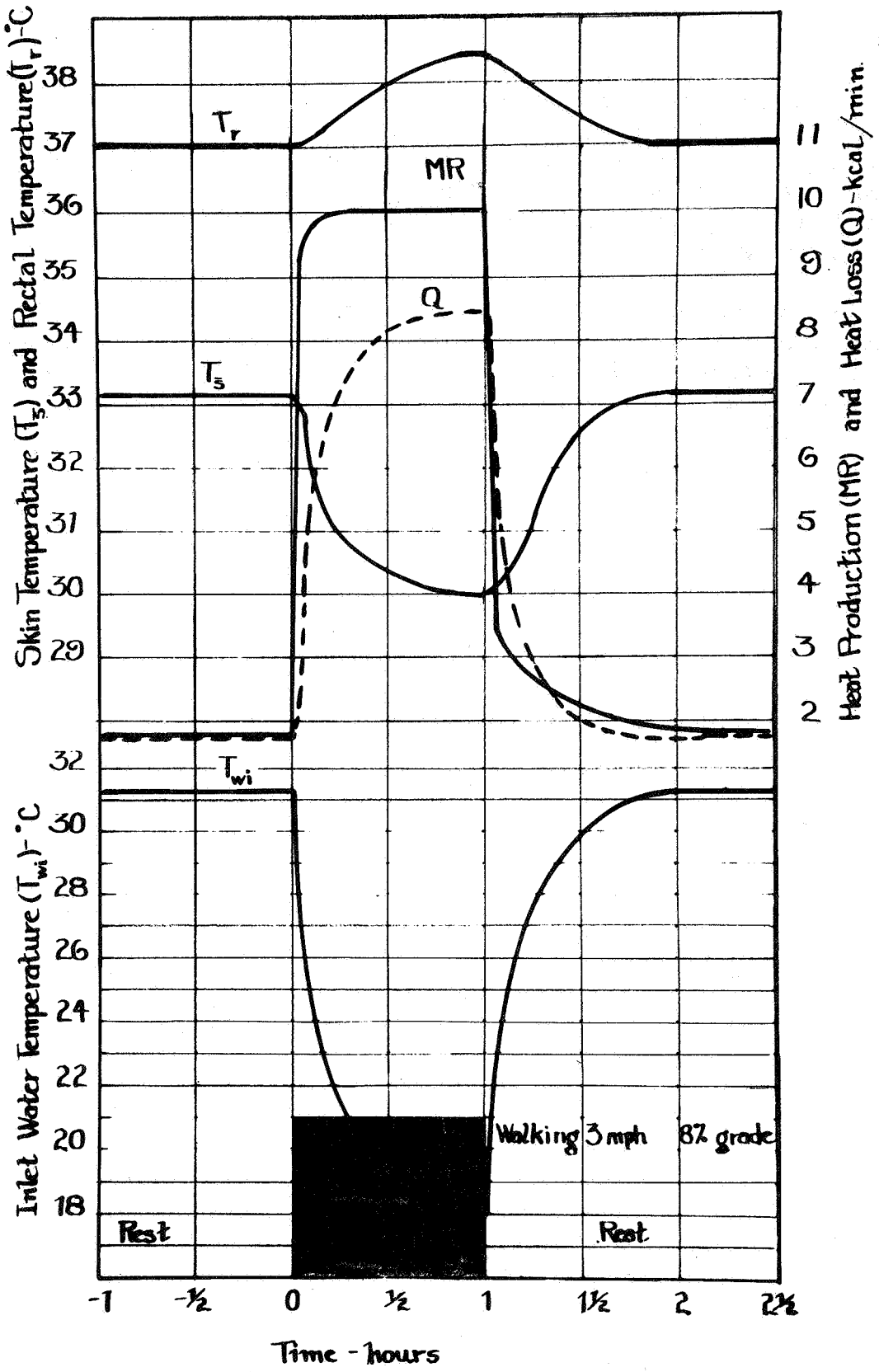

Figure 26. Ideal curves, 1966 data, Schedule I (10 kcal/min for 1 hour).

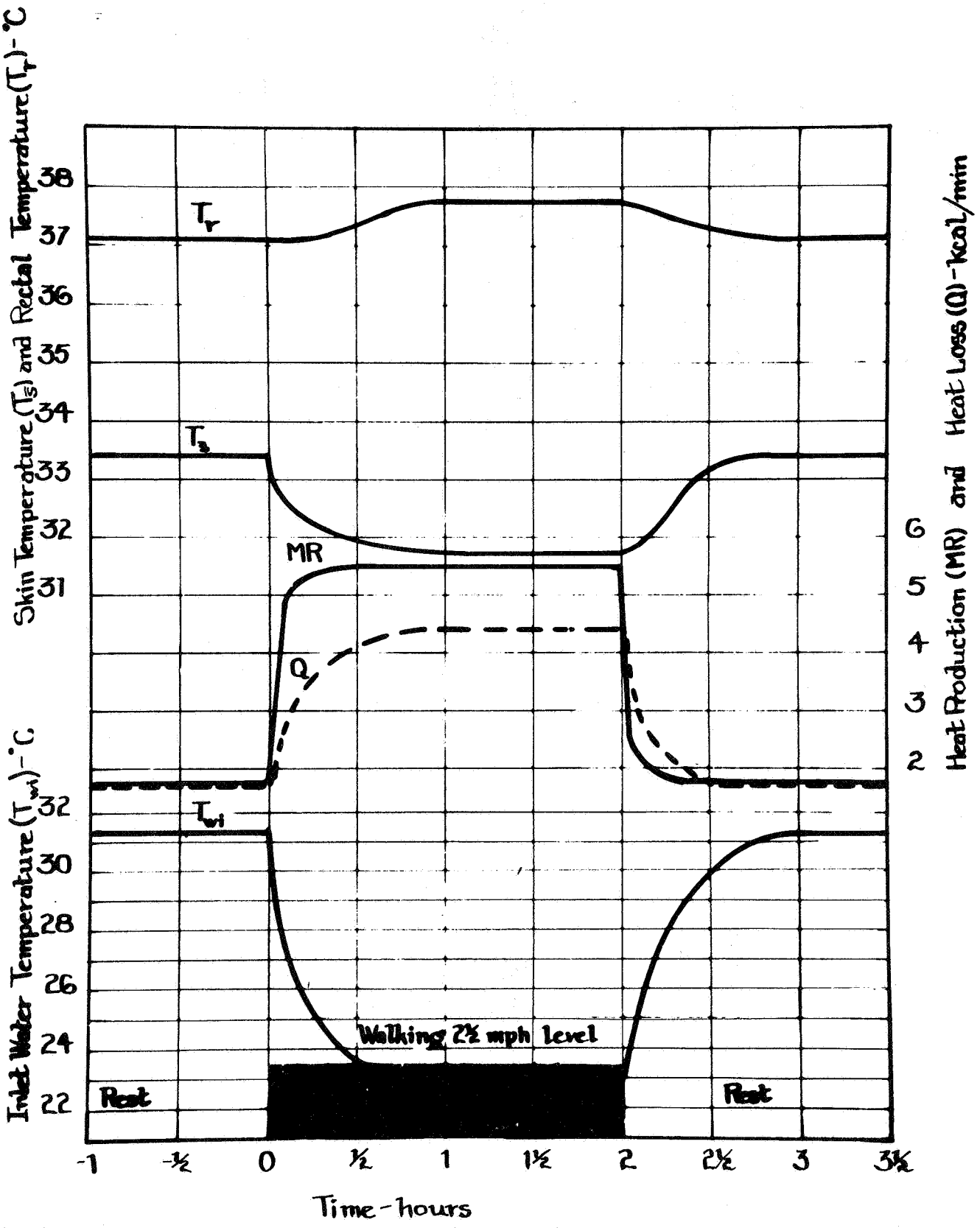

Figure 27. Ideal curves, 1966 data, Schedule II (5 kcal/min for 2 hours).

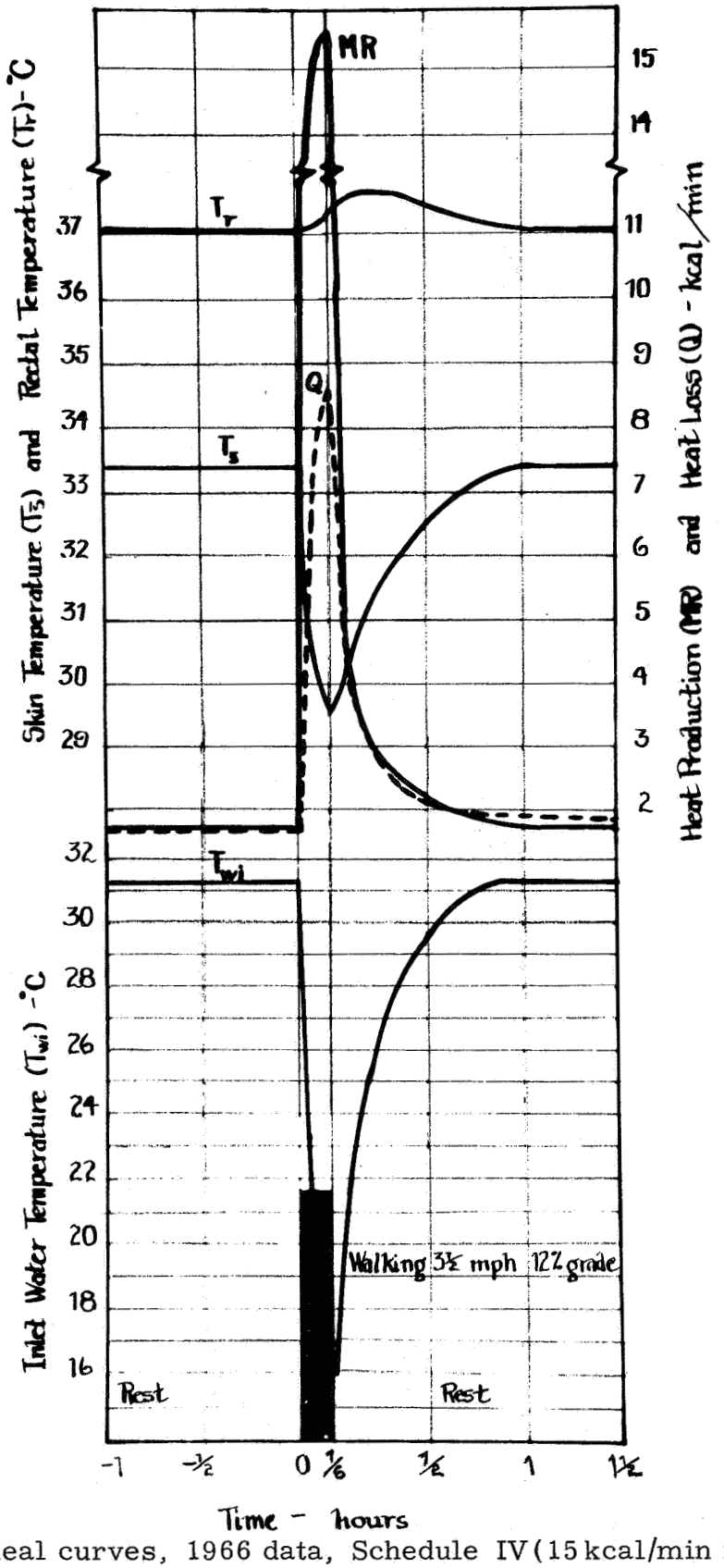

Figure 28. Ideal curves, 1966 data, Schedule IV (15 kcal/min for 1/6 hour).

COMPARTMENTS OF THE MODEL

The clothed man can be analyzed conveniently by considering that he is made up of the compartments shown on the diagram in Figure 29. The core or RECTAL compartment is assumed to have a constant resting heat production (RMR_r) of 0.7 RMR with a standard initial temperature of 37.08°C and a mass of 48 kg for a 73.6 kg man (the mean weight of our four subjects). The remaining mass of the man, excluding the skin, is labeled the LEG or muscle compartment; it has, at rest, a heat production (RMR_l) of 0.23 RMR, and a mass of 22 kg. The leg compartment is defined functionally as that part of the body mass which changes heat production during work. The increase in metabolic rate (ΔMR) over RMR during work takes place in the leg. The SKIN compartment has a constant heat production (RMR_s) of .06 RMR, a mass of 4 kg. It functions as one side of the interface between the man and the water cooled suit. The water cooled suit is assumed to have no mass and a mean temperature which lies half way between the measured inlet and outlet temperature of the water.

Initial temperatures for each compartment are shown in the figure, and the range of temperature observed in each compartment is also given. Notice that all three compartments produce heat.

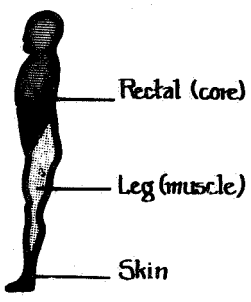

	mass	heat production		temperature	
		rest	work	rest	work
	kg	kcal/min		°C	
rectal	48.1	1.25	1.25	37	39
leg	21.7	.4	8.7	35	40
skin	3.8	.1	.1	33	28
totals	73.6	1.75	10.		

Figure 29. Compartments of the Model

Important reasons for including the leg compartment are that its temperature swings from below the core temperature to above the core temperature shortly after work begins, and it represents a sizable part of the body mass. It plays a key role in the changing body heat content during work. Lumping the muscle mass into the core made a model which would not behave. At rest heat moves both from core to skin and from core to leg, then to the skin. At work heat moves from the leg to the core and to the skin at the same time. In the laboratory T_r curves at the start of work do not change for approximately 10 minutes, or may go down. It is during this 10 minutes that the leg compartment temperature rises to and passes the temperature of the rectal compartment and the direction of heat flow reverses. Since we had made no measurements of muscle temperature, we estimated the changing temperatures of the leg compartment from studies by Robinson (ref. 17), Carlson et al (ref. 18), Saltin and Hermansen (ref. 19), and Äikäs et al (ref. 20).

MODEL EQUATIONS

At equilibrium during rest, compartment temperatures do not change, and heat production equals heat loss:

$$MR = RMR = RMR_r + RMR_l + RMR_s = Q + L \tag{15}$$

where Q is heat removed by the WCG and L represents losses of heat elsewhere than to the suit.

Some time after the man starts to work, a new equilibrium is reached with new steady state values for compartment temperatures:

$$MR = \Delta MR + RMR_r + RMR_l + RMR_s = Q + L + W \tag{16}$$

where ΔMR is the added heat production from working and W is external work done.

The instantaneous heat content, H, of each body compartment may be written as:

$$H_l = m_l c_l T_l \tag{17}$$

$$H_r = m_r c_r T_r \tag{18}$$

$$H_s = m_s c_s T_s \tag{19}$$

where m is mass, c is specific heat, and T is absolute temperature.

During the transition from rest to work, and from work to rest, compartment temperatures change according to the general equation for change in heat content:

$$\Delta H(t) = Q(t) = mc \int_{t_1}^{t_2} T(t)\,dt \tag{20}$$

Heat flow pathways between compartments, and heat inputs and losses, are shown diagrammatically in Figure 30:

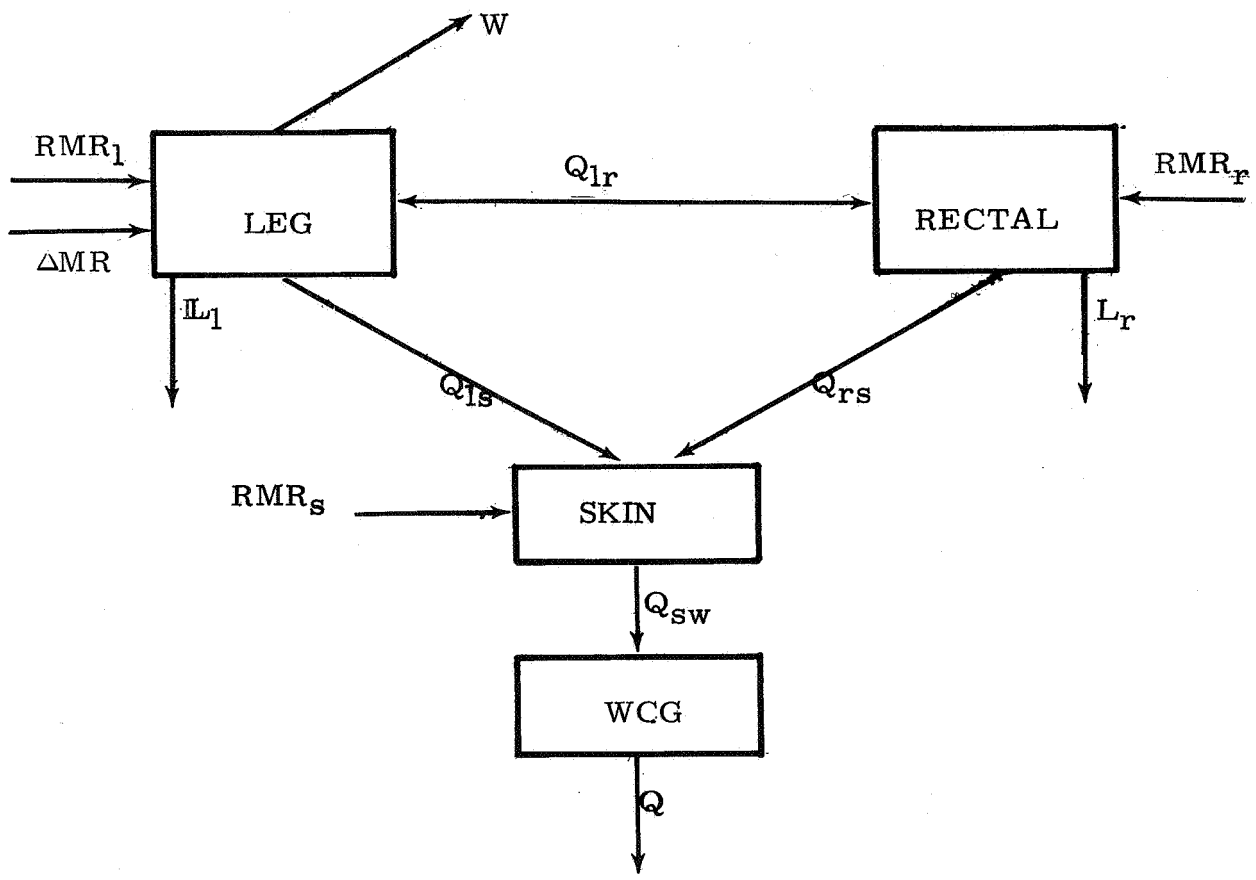

Figure 30. Heat flow pathways between compartments of the model.

Heat flow (Q) between two compartments is defined by:

$$Q = K(T_2 - T_1) \tag{21}$$

where K is a heat transfer coefficient.

We may now write an expression for temperature changes in the leg compartment:

$$C_l\dot{T}_l = \Delta MR + RMR_l - W - K_{lr}(T_l - T_r) - K_{ls}(T_l - T_{\bar{s}}) - L_l \tag{22}$$

where: $C_l\dot{T}_l = m_l c_l \int_{T_1}^{T_2} dT$

Similarly, in the rectal compartment:

$$C_r\dot{T}_r = RMR_r + K_{lr}(T_l - T_r) - K_{rs}(T_r - T_{\bar{s}}) - L_r \tag{23}$$

and in the skin compartment:

$$C_s\dot{T}_s = RMR_s + K_{ls}(T_l - T_{\bar{s}}) + K_{rs}(T_r - T_s) - K_{sw}(T_{\bar{s}} - T_{wi}) \tag{24}$$

No loss term is shown for the skin since we assumed all heat from the skin went into the WCG. Respiratory heat loss and the small evaporative water loss were assigned to L_r.

Heat flow from the skin to the WCG is determined by a transfer coefficient, K_{sw}, and the temperature gradient:

$$Q_{sw} = K_{sw}(T_{\bar{s}} - T_{wi}) \tag{25}$$

We treated the suit as having no mass and no losses, hence $Q_{sw} = Q$, and Q was measured by the Q detector experimentally from $\dot{m}c(\Delta T_w)$.

Finally, the model included an equation for generating T_{wi} from MR. Inspection of the 1966 data had shown that for step increases in MR* the manually controlled T_{wi} had changed exponentially, with a new level being achieved in about 50 minutes. We could also see that T_{wi} was proportional to MR.

We can write:

$$\Delta T_{wi} = T_{wi}(0) - T_{wi}(t) \tag{26}$$

where $T_{wi}(0)$ is an initial inlet temperature, and $T_{wi}(t)$ is the inlet temperature at time t.

---

*Actually, work changes were step functions, but $\dot{V}_{O_2}$ changed exponentially, with a short time constant--approximately 30 seconds. This was so rapid compared to the time constants of T_{wi}, T_r, $T_{\bar{s}}$, etc., that it may be considered instantaneous change.

The exponential change in T_{wi} can be written as:

$$T_{wi}(t) = T_{wi}(0)e^{-\frac{t}{\tau}} \tag{27}$$

Using the observed proportionality between MR and T_{wi}:

$$({}_1MR_2) \approx T_{wi} + \tau \dot{T}_{wi} \tag{28}$$

Defining $({}_1MR_2)$ as:

$$({}_1MR_2) = MR_0 - MR \tag{29}$$

where MR_0 is a reference level of MR,

and adding a proportionality constant, B_4, then from (28) and (29):

$$B_4(MR_0 - MR) = T_{wi} + \tau \dot{T}_{wi} \tag{30}$$

or, rearranging terms:

$$\tau \dot{T}_{wi} = -T_{wi} + B_4(MR_0 - MR) \tag{31}$$

Equation (31) is the equation defining the function of a Q controller, the development of which was the central purpose of our project. It appears in the body of the report on pages 13 and 31 as Equation (1).

DERIVATION OF VALUES

The terms used in the model equations (22), (23), (24), and (31), and in the analog diagram, Figure 35 (page 62), are defined in Table III:

Table III. -- Model Terms

Symbol	Units	Program Value	Source
	Heat Transfer Coefficients:		
K_{1r}	kcal/min/°C	5.0	$\rho_b C_b(\overline{V}_{1r})$
K_{1s}	"	0.3	Figure 31
K_{sw}	"	0.5	Figure 33
K_{rs}	"	generated	input to multiplier
$\overline{K}_{rs}$	"	0.11	estimated from $Q_r/T_r - T_s$

Table IV. (continued)

Symbol	Unit	Program Value	Source
		Constants:	
B_3	kcal/min/°C^2	- 0.099	$K_{s_{T_{\bar{s}_1}}} - K_{s_{T_{\bar{s}_2}}} / T_{\bar{s}_1} - T_{\bar{s}_2}$ where $K_s = \Delta Q_s / \Delta T_{\bar{s}}$
B_4	°C/kcal/min	1.6	Figure 34
C_r	kcal/°C	40.0	$m \times c \times f_r$, where c = 0.83 kcal/kg/°C; m = 73.6 kg; & f_r = 0.654
C_l	"	18.0	$m \times c \times f_l$, where f_l = 0.295
C_s	"	3.1	$m \times c \times f_s$, where f_s = 0.051
MR_0	kcal/min	20	that MR when T_{wi} = 0°C
RMR	"	1.75	mean of experimental data
RMR_r	"	1.25	RMR × .714
RMR_l	"	0.40	RMR × .229
RMR_s	"	0.10	RMR × .057
		Accessory Terms:	
τ	mins	10 (for T_{wi})	estimated from experimental data curves
L_r	kcal/min	0.150 0.220	at MR = 5, estimated at MR = 10, estimated
L_l	"	0.071	estimated
Q_{rs}	"	generated	from multiplier
Q	"	1.75 - 9	$\dot{m}c(T_{wo} - T_{wi})$, from experiments
T_{r_0}	°C	37.08	mean resting T_r from experiments
$T_{\bar{s}_0}$	°C	33.3	mean resting $T_{\bar{s}}$ from experiments
$T_{\bar{w}}$	°C	14-32	$1/2(T_{wo} + T_{wi})$
T_{wi_0}	°C	31.25	mean resting T_{wi} from experiments
T_{l_0}	°C	35.5	$1/2(T_{l_{max}} + T_{l_{min}})$
W	kcal/min	0.0 1.5	at MR = 5, when treadmill flat at MR = 10, treadmill grade 8%, speed 3 mph

From the 1966 experiments we took initial and final working values for compartment temperatures and for Q as summarized in Table IV:

Table IV. Equilibrium Values and Ranges

	Initial	5 kcal/min	10 kcal/min	Range
T_r	37.08°C	37.75°C	38.45°C	37.0-38.5°C
$T_{\bar{s}}$	33.30°C	31.70°C	30.05°C	30.0-33.5°C
T_l(est)	35.50°C	38.50°C	39.50°C	35.0-40.0°C
T_{wi}	31.25°C	23.00°C	17.00°C	17.0-31.5°C
Q	1.18 kcal/min	3.35 kcal/min	5.82 kcal/min	1.1-6.0 kcal/min

In this table the values for leg temperatures were estimated from the previously cited literature (Refs. 17, 18, 19, and 20). The values for Q were uncorrected values, i. e. they are the recorded values from the Q detector and do not include the additional losses from evaporative heat loss and external work. (We customarily add these losses to the Q curves when showing an experiment, as in Figures 1-5.)

Heat Transfer Coefficients

K_{lr}. --The coefficient of transfer from leg to rectal compartment was defined from:

$$Q_{lr} = K_{lr}(T_l - T_r) \tag{32}$$

It was assumed that all thermal transfer between these compartments was via the muscle blood flow, and further that net blood inflow and outflow were equal, i. e. no pooling occurred, and that the blood reached the temperature of each compartment. Then the thermal flux is: $\rho_b C_b \dot{V}_{lr}(T_l - T_r)$, and from (32):

$$K_{lr} = \rho_b C_b \dot{V}_{lr} \tag{33}$$

where ρ is blood density (1.058 gm/cc, ref. 21); C_b is specific heat of blood (.89 kcal/liter, ref. 22); and $\dot{V}_{lr}$ is blood flow from leg to rectal compartment.

Experimental data on change in muscle blood flow during exercise were found in the reports of Barcroft (ref. 23), Barcroft and Millen (ref. 24), and Elsner and Carlson (ref. 25). The major flow is via deep veins from muscle to core, but apparently some of the blood from the muscle travels radially toward the skin surface, where it is cooled before it returns to the rectal compartment (ref. 26). From resting state to working state, the muscle blood flow changes up to tenfold, depending on the severity of work. Calculating the values for K_{1r} for blood flows from 50/cc min (rest) to 5500 cc/min (work at 10 kcal/min) gave 0.5 to 5.2 kcal/min°C. We found that a single value of 5.0 was best; this corresponds to a blood flow of 4350 ml/min.

K_{1s}. -- Heat goes directly from hot muscle to cool skin, probably both by conduction and by convection via radial blood flow. Our 1966 data yielded values for mean temperature of the skin of the thighs ($T_{\overline{s1}}$) from the individual records of the four thermocouples mounted there. Internal leg compartment temperatures were estimated, as shown in Table V. We assumed that the heat removed by the WCG directly from the leg surface (Q_{1s}) was 1/2 (fm_1) Q, where fm_1 is the fraction: leg mass/body mass. Table V shows these values.

Table V. Values used in calculating K_{1s}

MR kcal/min	$T_{\overline{s1}}$ °C	T_1 °C	$T_1 - T_{\overline{s1}}$ °C	Q_{1s} kcal/min
1.75	33.0	35.0	2.0	.174
5	31.5	37.5	6.0	.494
10	32.0	39.0	7.0	.858
15	32.0	40.0	8.0	1.475

Heat flow from leg to skin was graphed as a function of the temperature difference ($T_1 - T_{\overline{s1}}$), as shown in Figure 31. The slope of that line is approximately 0.3, the value used in simulation. Notice that the line is determined only by the work values. This choice was similar to the choice of a high (working) muscle blood flow in the determination of K_{1r}.

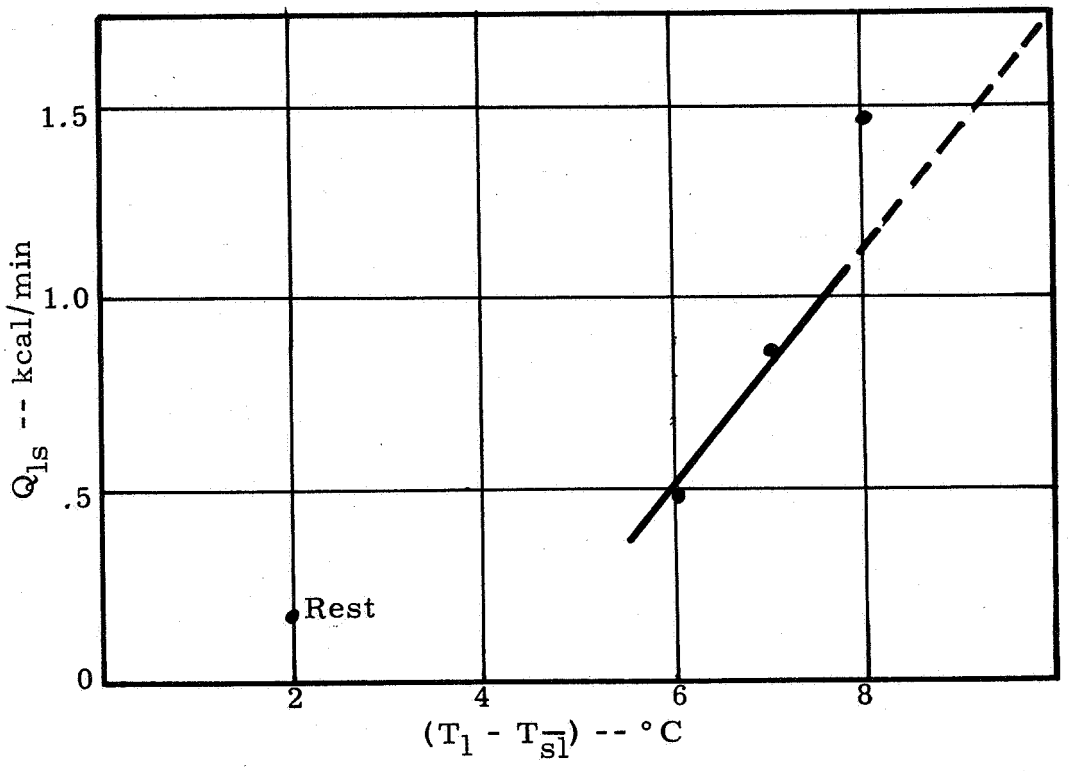

Figure 31. Q_{ls} as a function of $(T_l - T_{\bar{s}})$. The slope of the line is K_{ls}.

K_{rs}. -- This coefficient was derived originally from the experimental data from the relationship:

$$Q_{rs} = K_{rs}(T_r - T_{\bar{s}}) \tag{34}$$

which is shown in Figure 32.

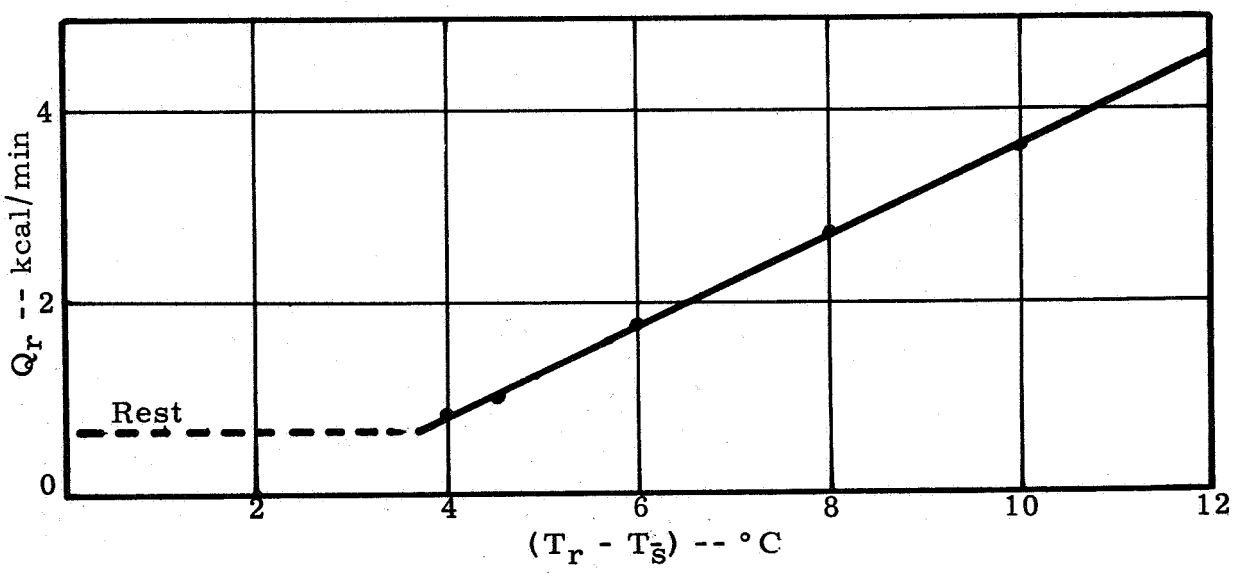

Figure 32. Q_r as a function of $(T_r - T_{\bar{s}})$. The slope of the line is K_{rs}.

The slope, K_{rs}, was 0.42. However, since Q_{rs} is a complex quantity influenced by the varying heat input from the leg and since T_r and $T_{\bar{s}}$ change during work, K_{rs} was generated from $T_{\bar{s}}$ and from the expression $\overline{K}_{rs} - B_3(T_{\bar{s}_0} - 30)$ as shown on the analog diagram, Figure 35. $\overline{K}_{rs}$ is a chosen fixed value of 0.11. Other K's could have been generated in similar fashion, but K_{rs} is the coefficient for the major heat flow, hence it was important to generate it at least.

K_{sw}. -- This coefficient was derived from the experimental data from the relationship:

$$Q_{sw} = K_{sw}(T_{\bar{s}} - T_{\overline{w}}) \tag{35}$$

where $T_{\overline{w}}$ was the mean of T_{wi} and T_{wo}.

Again assuming linearity, the slope of the line in Figure 33 is 0.5, which is the value used for K_{sw}.

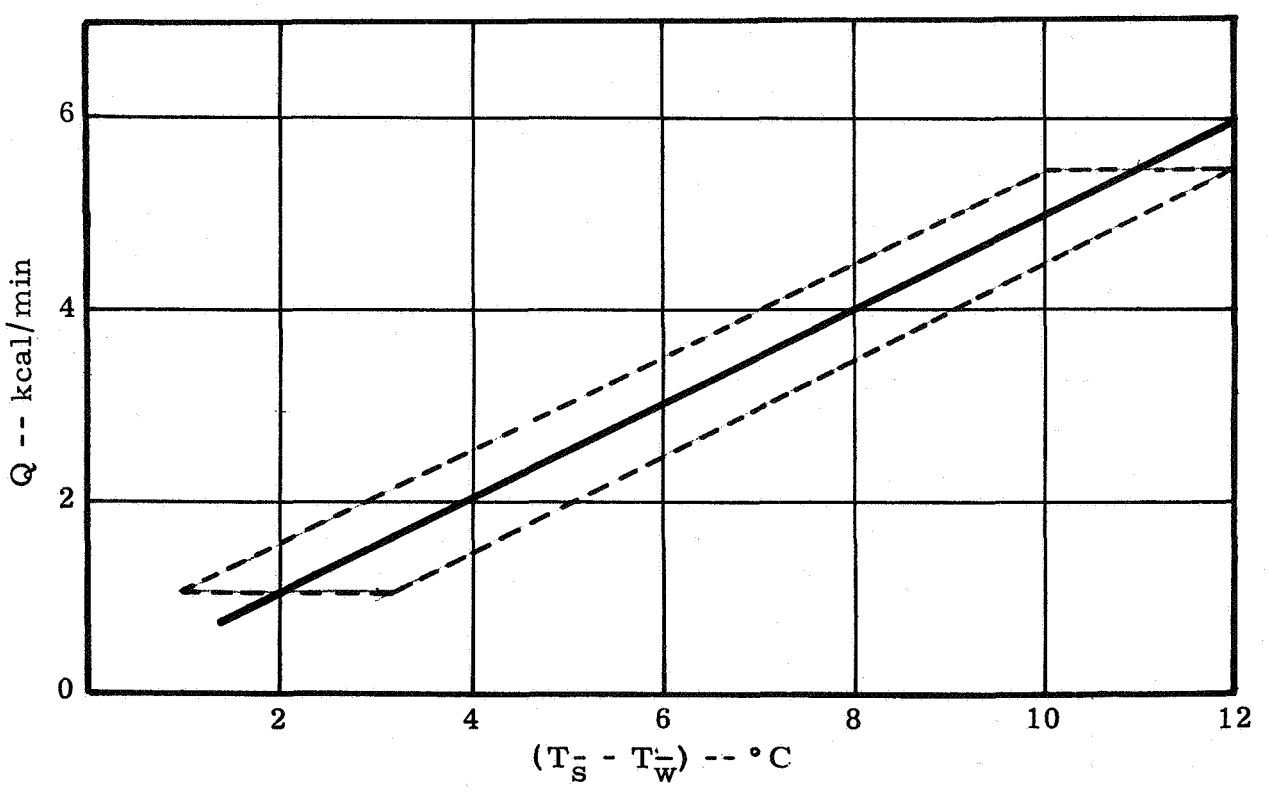

Figure 33. Q as a function of $(T_{\bar{s}} - T_{\overline{w}})$. The slope of the line is K_{sw}. The dotted envelope includes most of the data points.

B_4 and MR_0. -- These two values in Equation (31), the basic Q controller equation, were derived from the experimental data by plotting T_{wi} as a function of MR, figure 34.

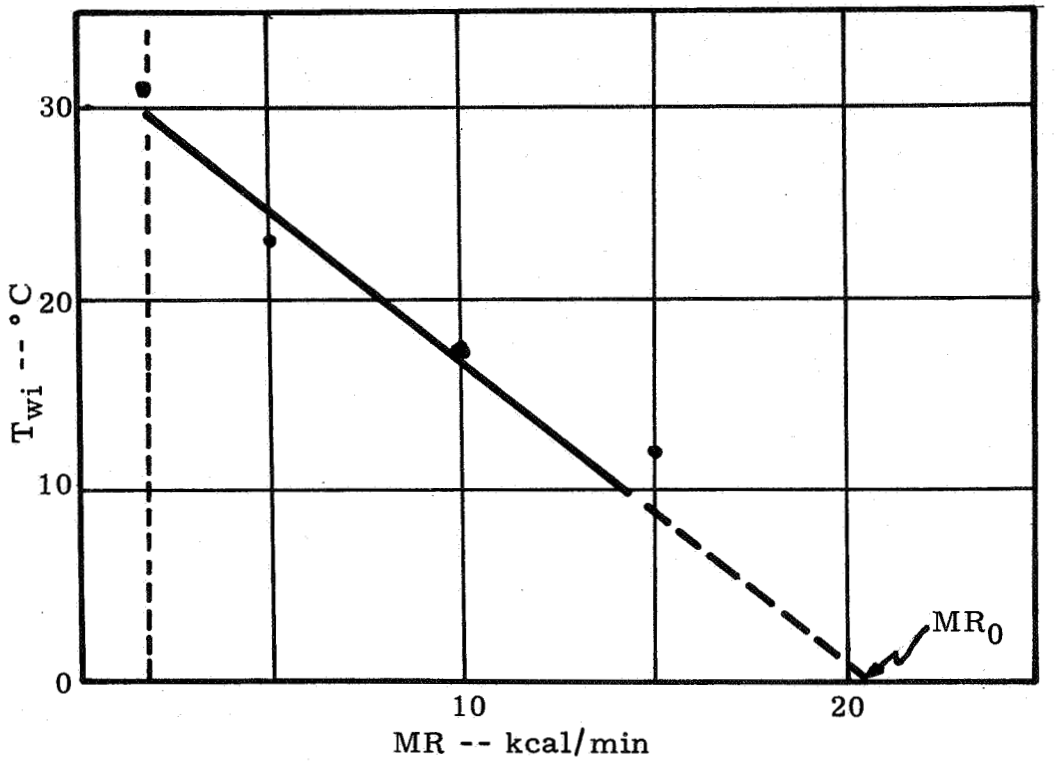

Figure 34. T_{wi} as a function of MR. The slope of the line is B_4.

The reference metabolic rate, MR_0, was taken as the MR value where T_{wi}, by extrapolation, would be 0°C. The 1966 data show this to be approximately 20 kcal/min. The slope of the line, 1.6°C/kcal/min, is the constant B_4. Again linearity was assumed, although in this case we feel that this is not correct and that B_4 varies as a function of MR.

COMPUTER SIMULATIONS

Equations (22), (23), (24), and (31) were mechanized on an analog computer (TR-20, Electronic Associates, Inc.). The analog computer diagram is shown in Figure 35. Scaling is shown on the diagram.

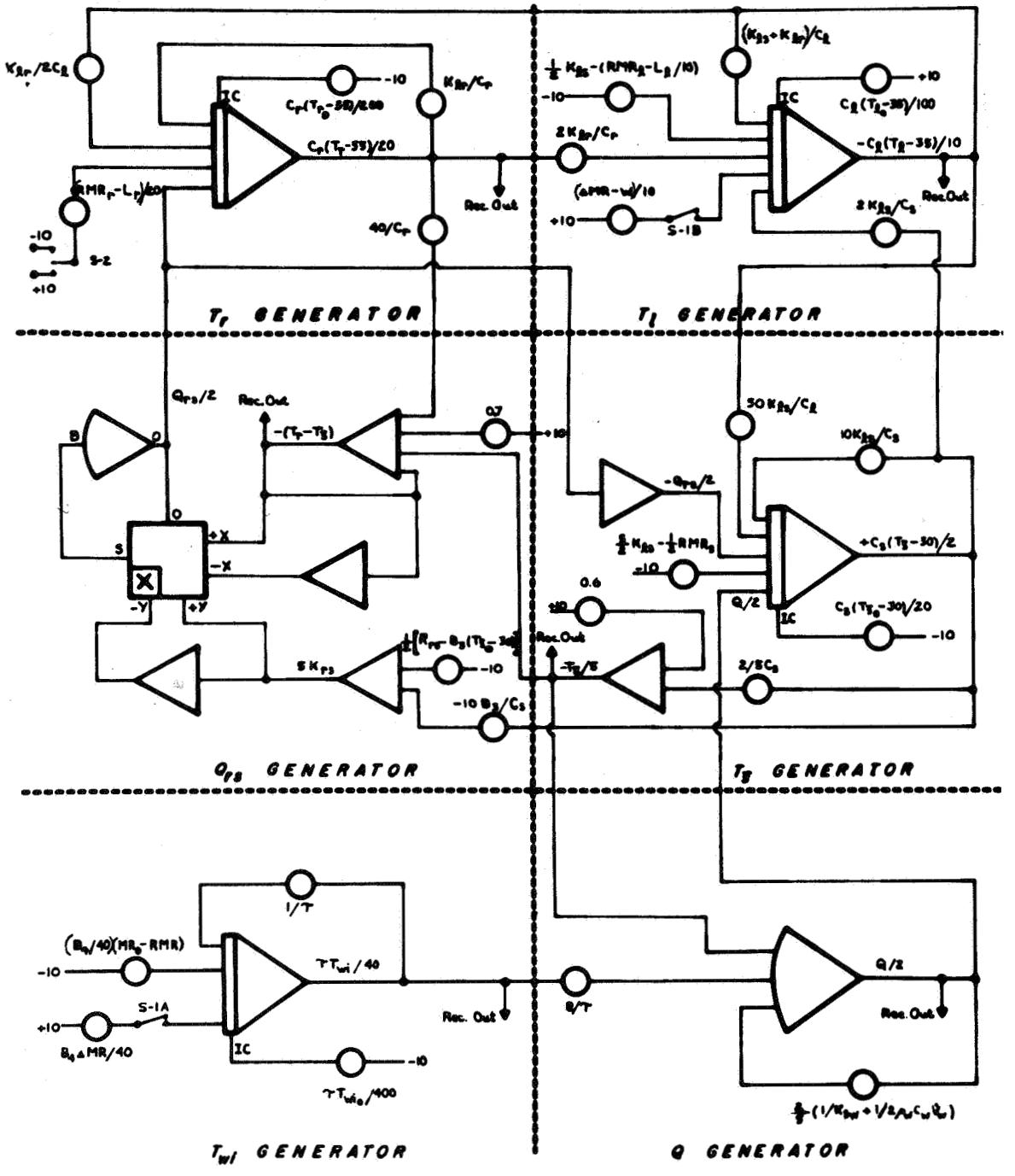

Figure 35. Analog computer diagram of the biothermal model.

Early runs were for adjusting and trimming coefficients and loss terms. When these adjustments were finished, we got equilibrium values at rest and in work which were close to those from the 1966 data, as shown in Figure 36.

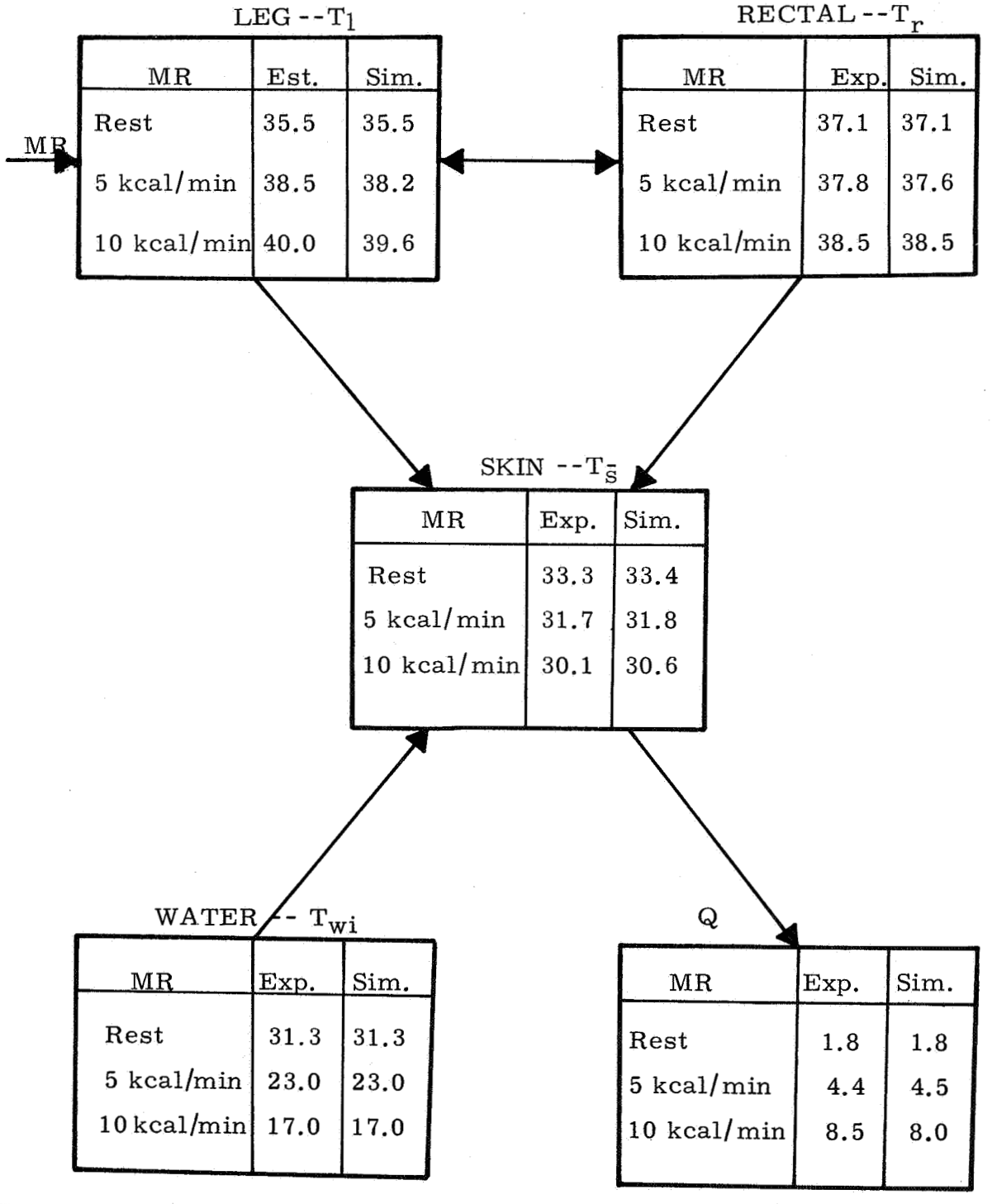

MR	Est.	Sim.
Rest	35.5	35.5
5 kcal/min	38.5	38.2
10 kcal/min	40.0	39.6

MR	Exp.	Sim.
Rest	37.1	37.1
5 kcal/min	37.8	37.6
10 kcal/min	38.5	38.5

MR	Exp.	Sim.
Rest	33.3	33.4
5 kcal/min	31.7	31.8
10 kcal/min	30.1	30.6

MR	Exp.	Sim.
Rest	31.3	31.3
5 kcal/min	23.0	23.0
10 kcal/min	17.0	17.0

MR	Exp.	Sim.
Rest	1.8	1.8
5 kcal/min	4.4	4.5
10 kcal/min	8.5	8.0

Figure 36. Comparison of experimental and simulation values for equilibria at rest and at two levels of work.

Dynamic behavior of the model was studied in simulations of going from rest to two levels of work, 5 kcal/min and 10 kcal/min. We recorded changing compartment temperatures, T_{wi}, and Q, to compare against experimental data. Computer and experiment curves are shown superimposed in Figures 37 - 41.

This performance of the model was quite satisfactory, although more trimming of the values and greater model complexity would have given even closer agreement with laboratory experiments.

DISCUSSION

The model building effort had limited objectives: to achieve a quantitative understanding of the simplest biothermal system which would behave like the data, to permit calculations of system performance, and to permit specification of the Q controller imbedded in the biothermal system. It was not intended to give comprehensive and precise detail about human thermoregulatory response, especially when driven by environmental stress.

In building the model we kept working toward the least feasible amount of complexity, which was the reason for linearizing a lot of relationships which looked to be far from linear in the data. At one stage the model was too simple. The man was considered to have only a skin and a core compartment. This model behaved sloppily, did not produce realistic T_r curves, and seemed to require second and third order differential equations. Adding the leg compartment solved these problems, allowing us to stick to ordinary differential equations and to get away with linearizing.

The great thing is that the simple model did the job. Not only were simulation runs reasonable approximations of the 1966 data, but also the model served its purpose when it came to designing an automatic Q controller.

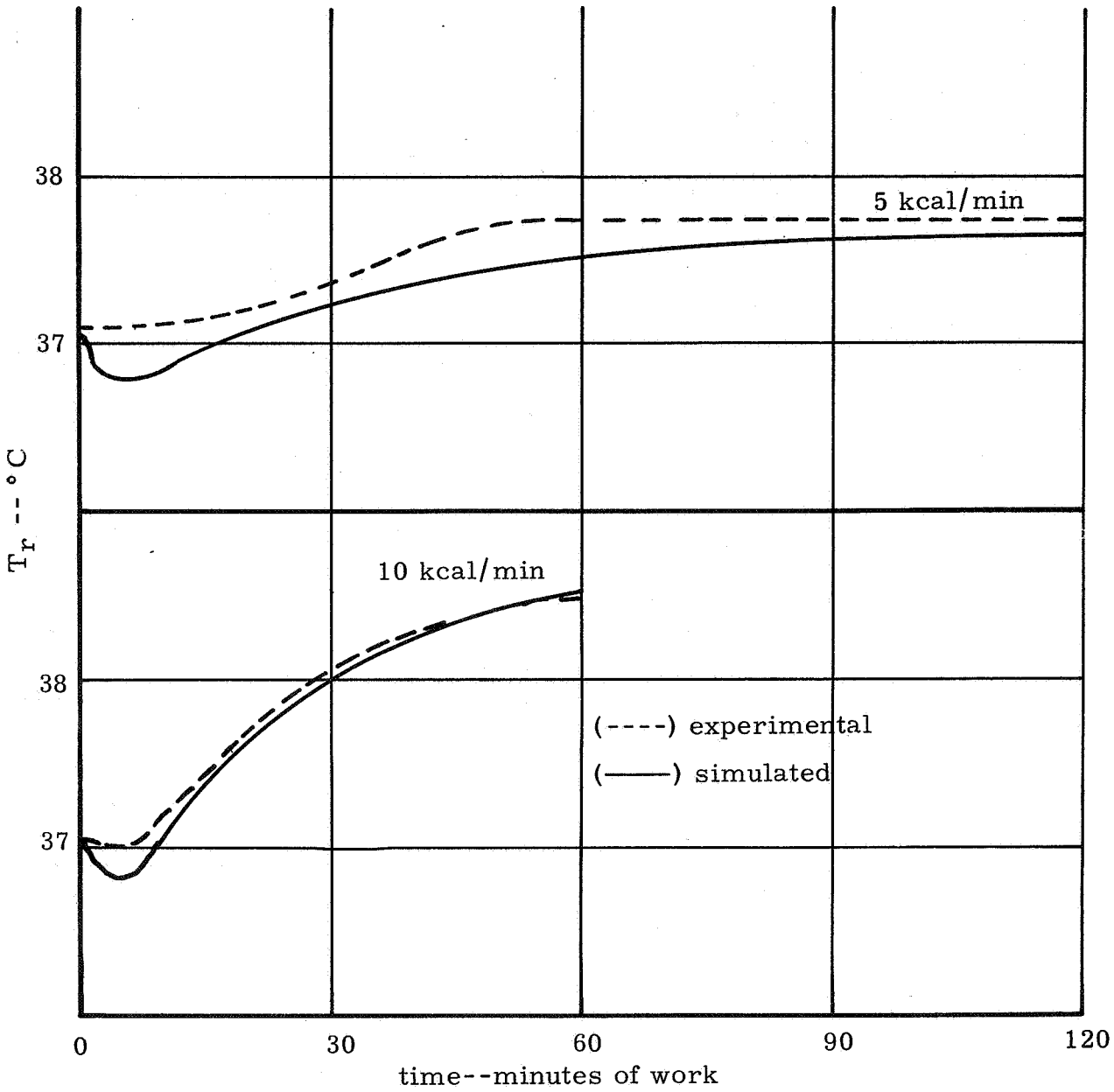

Figure 37. Simulated versus experimental rectal temperatures.

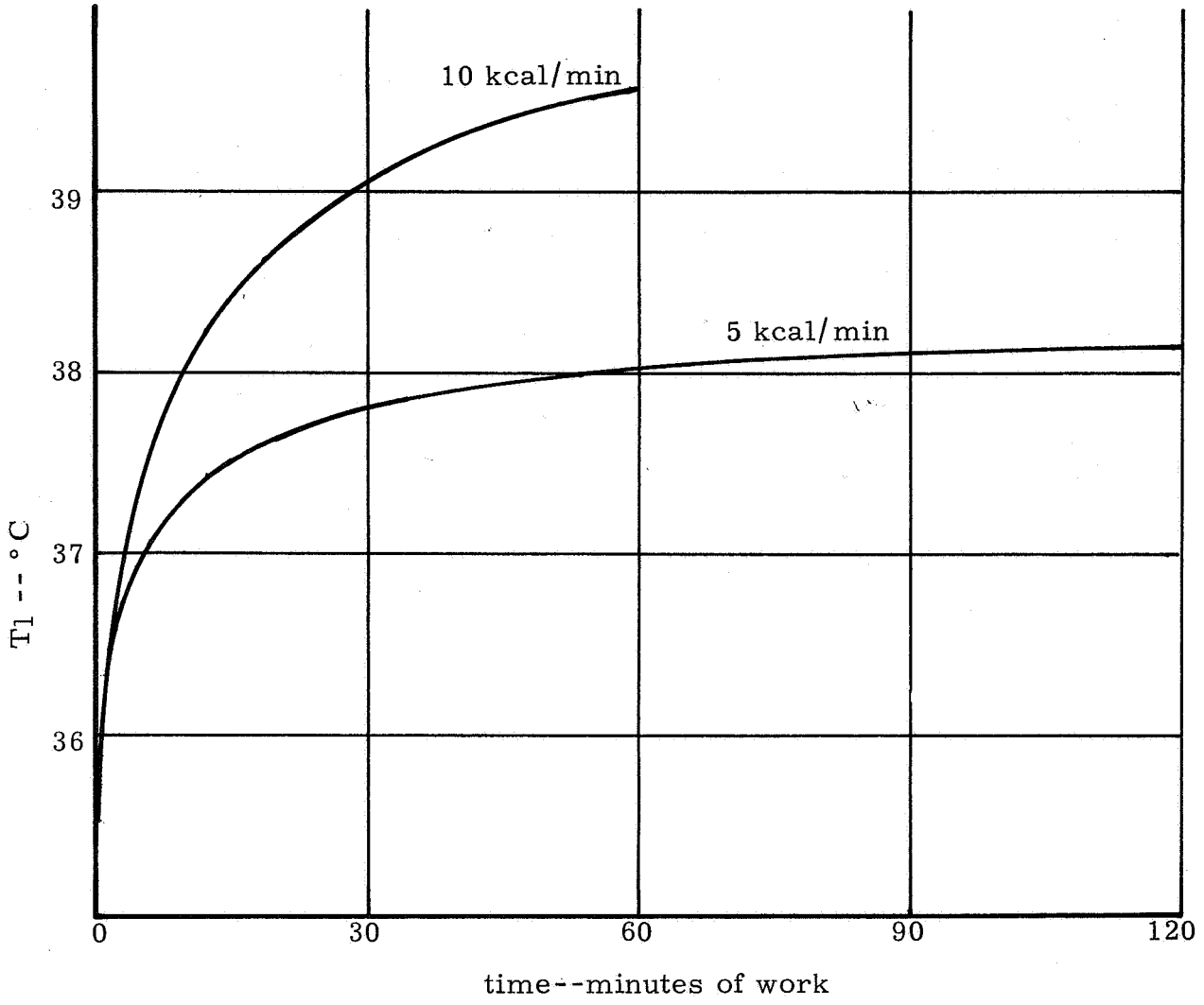

Figure 38. Simulated leg compartment temperatures at two work levels.

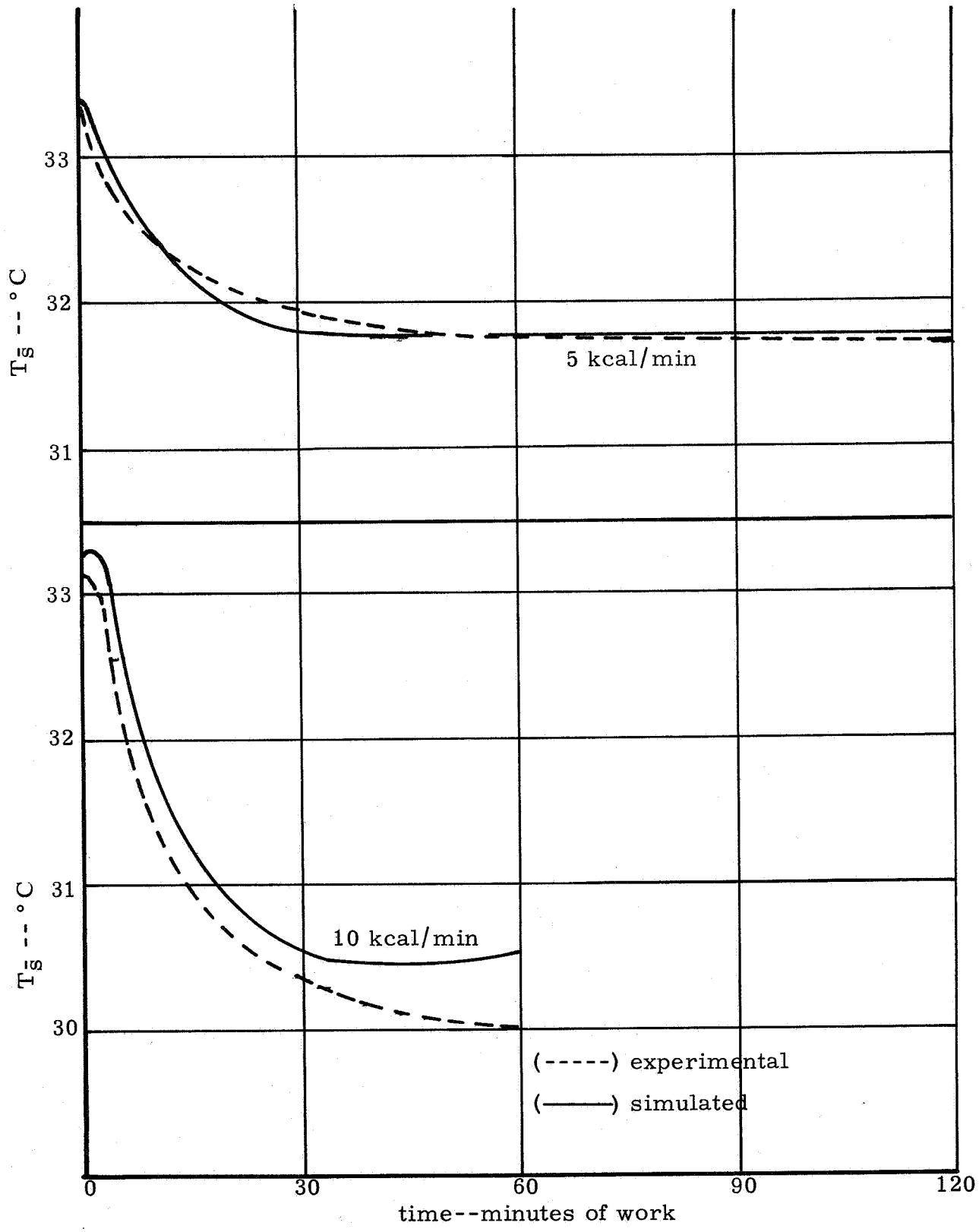

Figure 39. Simulated versus experimental mean skin temperatures.

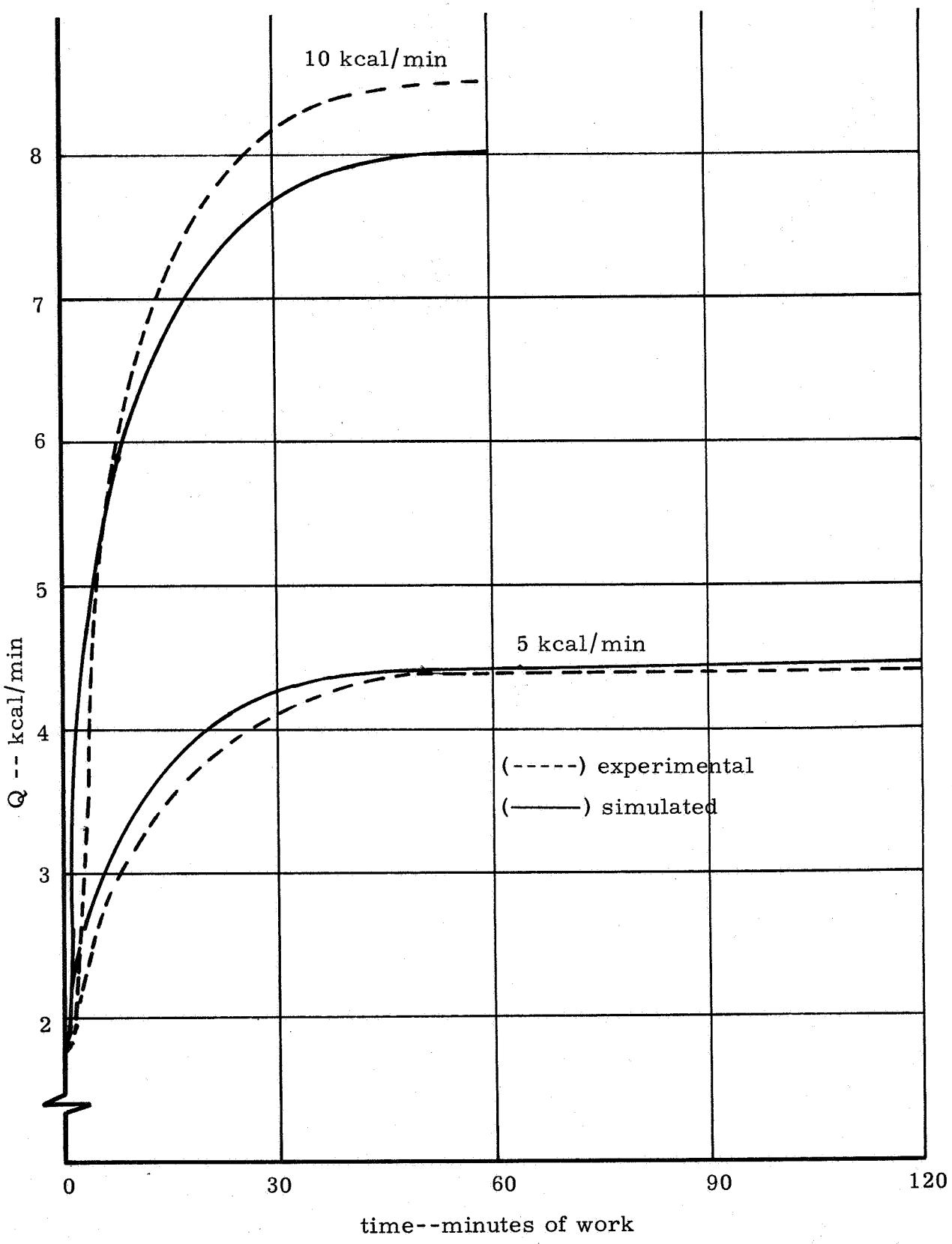

Figure 40. Simulated versus experimental heat extraction rate.

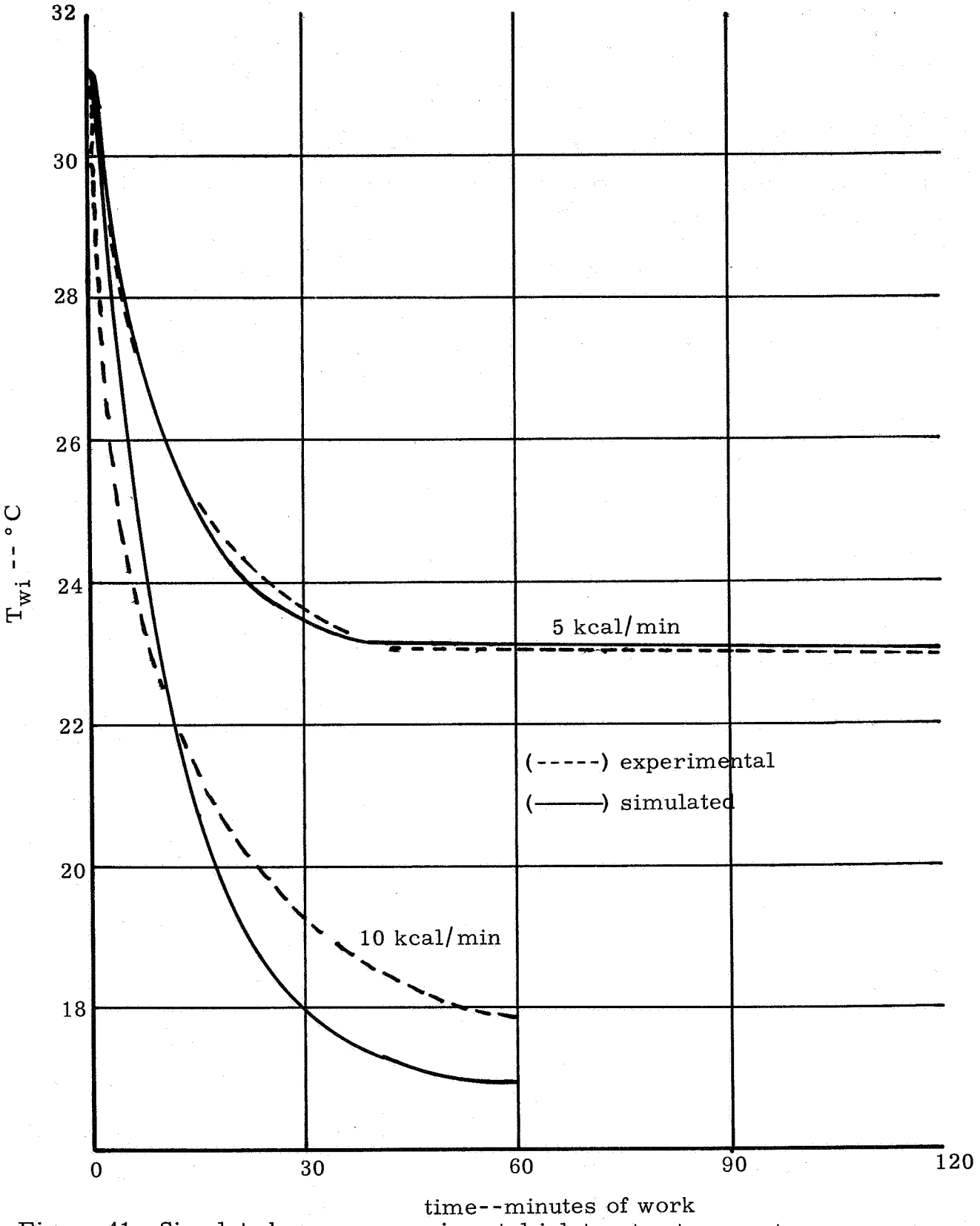

Figure 41. Simulated versus experimental inlet water temperature.

APPENDIX C

WATER COOLING GARMENT

A new water cooling garment was designed and constructed for the experiments. Cooling tubes and skin temperature sensors were incorporated into a single garment which provided the properties of insulation and water impermeability needed to thermally isolate our subjects. The basic garment was a 0.25 in. thick unicellular foam neoprene "wet suit" and helmet (Parkway Fabricators, South Amboy, N. J.) of the type used by SCUBA divers.

The cooling tubes of 7/32 in. o. d. × 5/32 in. i. d. neoprene rubber were cemented in place on the inner surface of the suit. The total length of the tubes was 150 feet. The Reynolds number for the small tubing was calculated to be about 1900; however, turbulent flow must have been minimal, since the total garment pressure drop (including approximately 4 ft each of pump inlet and outlet lines) was less than 2 psig.

The spaces between the tubes were filled with 1/8 in. thick nylon fabric lined foam neoprene. These inserts increased the total insulation, prevented collapse of the cooling tubes due to pressure applied by the garment against the subject's skin, and minimized crimping across joints during movement. The tubing bulged above this inner layer by 3/32" to make contact with the skin. The total thickness of the garment for the most part was 3/8 in. Since the clo value for a 1/4 in. thick foam neoprene wet suit has been given at 1.48 clo by Reeves et al (ref. 27), it is estimated that the total insulation was greater than 2.0 clo. The cross-sectional appearance of the garment structure is shown in Figure 42.

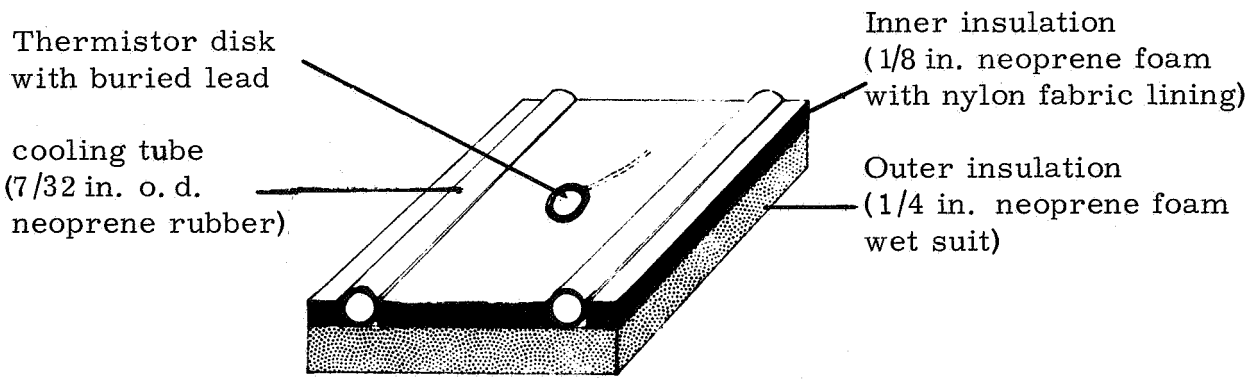

Figure 42. Cross-sectional appearance of the water cooling garment.

The WCG (including the water cooled helmet) covered approximately 86.4% of the total body surface. The uncooled areas were: the hands, which were covered by rubber surgeon's gloves, and the feet, which were covered by two pairs of wool socks and walking boots. The face also was not cooled; it was exposed to the air flow through the MRM mask attached to the helmet. Care was taken to avoid openings that would cause thermal or moisture leaks.

Since the flow pattern was from the inlet manifold to the most distal portion of the suit, the coldest water entered the cooling tubes at the wrists and ankles and the warmed water exited at the waist. The helmet inlet manifold was around the face and the outflow manifold was at the neck, which overlapped the trunk portion of the garment. The flow pattern with the number of cooling tubes for each of the major suit compartments is shown in Figure 43.

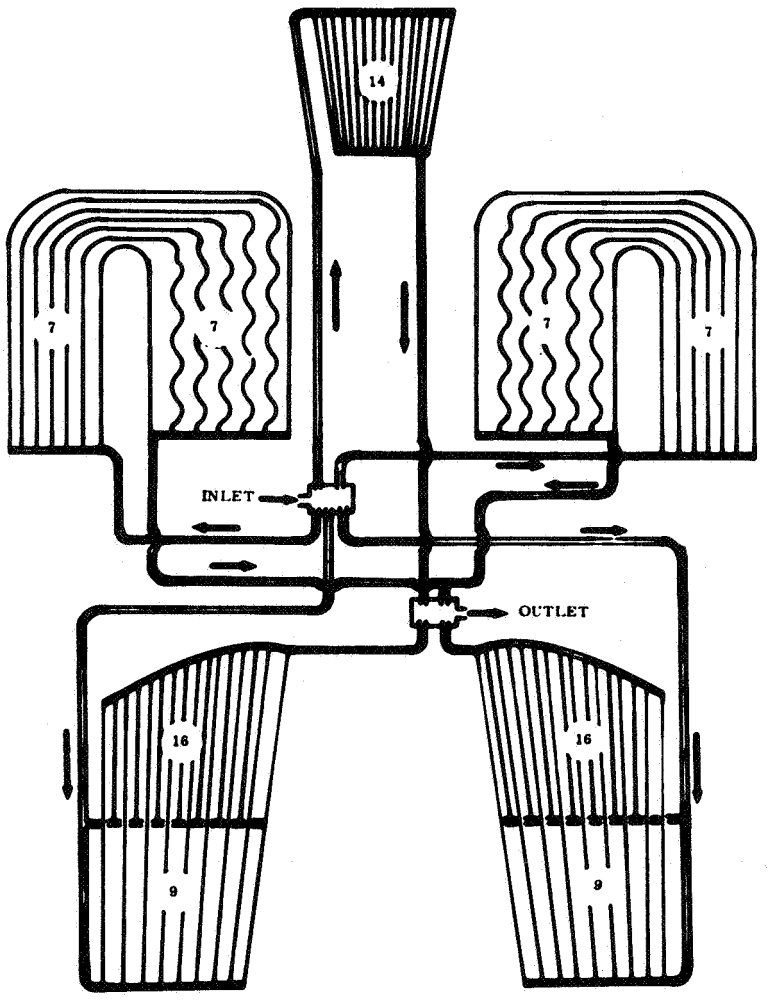

Figure 43. The flow pattern and tubing distribution of the water cooling garment.

Manifolding and delivery tubing (0.25 in. i.d. Tygon) was run on the exterior surface of the garment and insulated from the environment with 1/8 in. thick neoprene foam. The cooling water was distributed from and returned to manifolds containing the dual T_{wi} and T_{wo} sensing thermistors. The distributing and collecting points were located in the lateral waist area. To avoid countercurrent heat exchange, close lying inlet-outlet lines were insulated from one another.

Design goals for this WCG evolved primarily from our previous experiences with water cooling garments and from information gained via the mathematical model studies with regard to body thermodynamics. In the design and construction of the WCG the following objectives were considered:

1. The WCG should be a single garment which thermally isolates the subject, is quick and easy to donn and doff, is readily adjustable so that the cooling tubes have good contact with the skin for more than one subject, and is flexible enough to permit treadmill walking with reasonable effort and comfort. It should contain positioned skin temperature sensors which are attached to the garment.

2. The total water volume, the distribution pathways, the thermal isolation properties, and the cooling potential at a water flow rate of 1500 cc/min should be similar to that found with the diamond-pattern WCG used in the 1966 experiments.

3. Heat removing capacity (tubing density) should be proportioned so as to equal or exceed the predicted heat production of the compartmental areas to be cooled.

4. Since a major portion of the heat produced in a given area of the body can apparently be removed at the surface directly over the site of production without overcooling or vasoconstriction, and since the greatest amount of heat produced in work is in the active muscles, the heaviest concentration of cooling tubes should be over the thighs and back for leg work.

5. Body surface area and mass with a weighting factor for active muscle mass should be the final arbiter of the relative proportioning of tubes to each garment area.

6. The WCG should supply cooling to at least 80% of the body surface.

7. The garment should have three major compartments: head-neck, arms-trunk, and legs. The leg compartment should include the lower back and have greater cooling potential over the thighs and lower back than over the lower leg.

8. The head-neck compartmental cooling potential should be higher than its relative mass would indicate. The reverse is true for the arm-trunk compartment.

9. The compartmental flow should furnish correct cooling both at rest and work, since only inlet water temperature is to be changed, not total flow. No adjustments of flow distribution through the use of valves, clamps, etc., should be needed.

The design goals listed above were on the whole met very well by the neoprene wet suit garment. However, the garment was not as flexible or comfortable as it should have been. Other difficulties encountered were water leaks around manifolds, and the fact that the opaque tubing prevented visual flow checks on individual cooling tubes. The advantages of this WCG lay in its ease and quickness of donning and doffing, the exact placement of thermistors in relation to cooling tubes, the fact that the thermistors were donned with the garment, and the ease with which the neoprene suit could be patched or custom tailored.

The pertinent anatomical data used in design, and the resulting compartmental cooling tube lengths and volumes, are given in Table VI.

Table VI. Cooling Tube Design Data

Portion of body	% not cooled	Est. % heat production		% length of cooling tubes	Volume of cooling tubes
		rest	work		
Head & neck surface area 11% mass 7%	3.0	5	5	9.2	52 cc
Arms & trunk surface area 36% mass 45%	3.9	60	25	29.7	167 cc
Legs & lower back surface area 53% mass 48%	6.7	35	70	61.1	345 cc
Totals	13.6	100	100	100	564 cc

APPENDIX D

THE COOLING LOOP

The entire water cooling system, shown in Figure 6, page 10, was located inside an environmental chamber near the subject. It contained a total volume of approximately 1400 cc, including the interconnecting piping (1/4 in. i. d. Tygon) and the WCG. Since the flow rate was 1500 cc/min, the circulation time was somewhat less than 1 minute. The system pressure at this flow rate was 3 - 4 psig. The components of the loop were selected for low thermal inertia.

The pump selected for use (Model P-403-A, Weldon Tool Co., Cleveland, Ohio) was a directly driven, positive displacement, slung vane unit capable of delivering up to 2.5 lpm flow at 15 psig and 12,600 rpm when driven at full power (28 VAC, 7 amps) by its 0.25 horsepower motor. The pump was constructed of a non-corrosive metal, had a single inlet and outlet, and measured 2 in. in diameter by 1-1/8 in. in depth. At the flow rate and observed pressure the pump was operated far below its rated capacity. The pump motor also drove a tach generator (Electro-Craft Corp., Hopkins, Minn.), the output of which (3 v/1000 rpm) was meter calibrated to set the correct flow rate at various pressures. The pump power supply was variable and regulated to ±0.1%. This provided for smooth pump performance at the pre-set level without further circuitry.

An in-line immersion heater served to offset the static cooling of the water flowing in the heat sink of the thermoelectric cooler. When a suit inlet water temperature of 15°C or less was needed, the offset heater was turned off.

The other minor components of the loop, such as the pressure gage (0-15 psi, Bourdon type), the pressure relief valve set at 15 psi, the bubble trap, and water supply reservoir, were of standard design.

The environmental chamber in which the experiments were carried out is a 7 × 7 × 8-foot space having a low thermal mass. Temperature is automatically controllable to ±1°C with a lag-compensated proportional controller. The chamber was operated so that its air and wall temperatures always matched the measured garment temperature (T_g) to within 2°C.

Thermoelectric Cooler

The cooling system (Nova Thermotronics, Northfield, Ohio) consisted of three major components: power supply, thermoelectric modules, and controller.

The power supply, operated from a 220 VAC, 10 ampere source, provided an output of 38 VDC at 50 amperes with a maximum ripple of 3% at rated load, as diagrammed in Figure 44. The output was smoothed by a tuned series LR (inductive-resistive) network, where the resistive component was the thermoelectric modules. On/off control of the power to these modules was accomplished by silicon controlled rectifiers (SCR's) positioned back to back in the secondary circuit. The weight of the power supply was approximately 175 lbs, and it was housed in a metal enclosure 10 in. × 12 in. × 23 in.

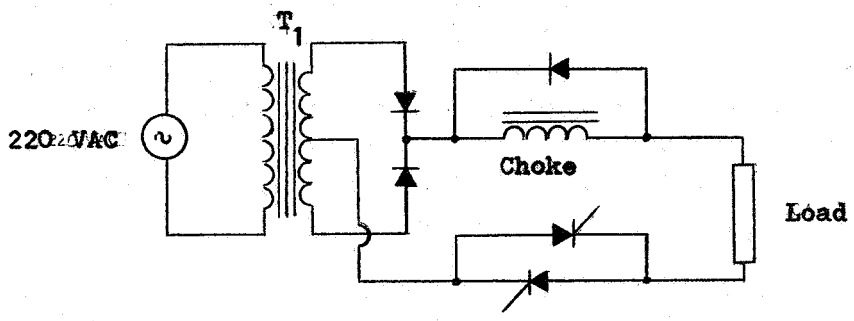

Figure 44. A simplified schematic of the cooler power supply.

Thermal cooling resulted from energizing 12 thermoelectric modules (Melcor, type CP-5-31-06) which provided a 3900 Btu/hr heat removal capability. The modules were connected in series and water jackets provided for the hot and cold junctions (Figure 45). Tap water was used as a heat sink at the hot junctions and its temperature varied between 15°C and 27°C, depending on the amount of heat removed. The cold junction water jacket provided the path through which the suit water passed to be cooled.

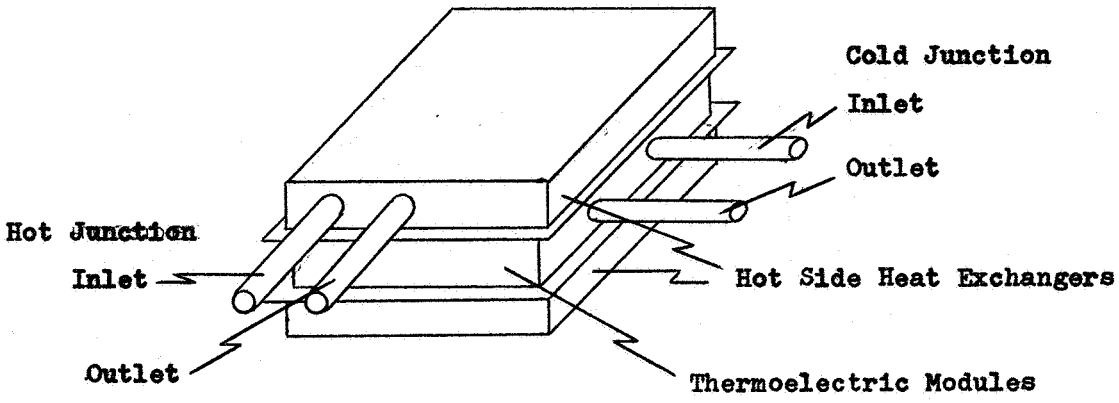

Figure 45. An illustration of the thermoelectric modules.

Precise control of the inlet water temperature was obtained using a monitor circuit (Control Data Corp., Model 70), Figure 46. Two types of control were incorporated: first, temperature sensing of the water leaving the cooler; and second, protection of the system with overload thermostats, one located at the cold junction set at 0°C and two at the hot junction set at +80°C. The controls, switches, and thermoelectric modules were housed in a metal enclosure 8 in. × 9 in. × 16 in.

The cooler outlet temperature was continuously monitored by a bead thermistor (Veco type 35A3) used as a dynamic element in a Wheatstone resistance bridge, the output of which was the input control signal to the monitor circuit. The control temperature was selected by means of a calibrated potentiometer in the resistance bridge. Temperature control was obtained by two modes: one, manual selection; the other, by computer (Q controller) output signal.

Manual control varied the bridge output by unbalancing the bridge, thus commanding the monitor circuit to fire the SCR's. Computer control did not unbalance the bridge but controlled the amplitude of the bridge driving voltage, thus decreasing its output below the hysteresis of the monitor circuit, thereby firing the SCR's. The SCR's remained on until the resistance change of the thermistor reset the bridge output to allow the firing command to be removed from the SCR's. The SCR's turned off automatically since the voltage and current in the secondary were in phase. As the bridge driving voltage was further reduced, cooling by the modules continued until a balance was established. The accuracy of this type of hysteresis control was found to be within ±0.2°C.

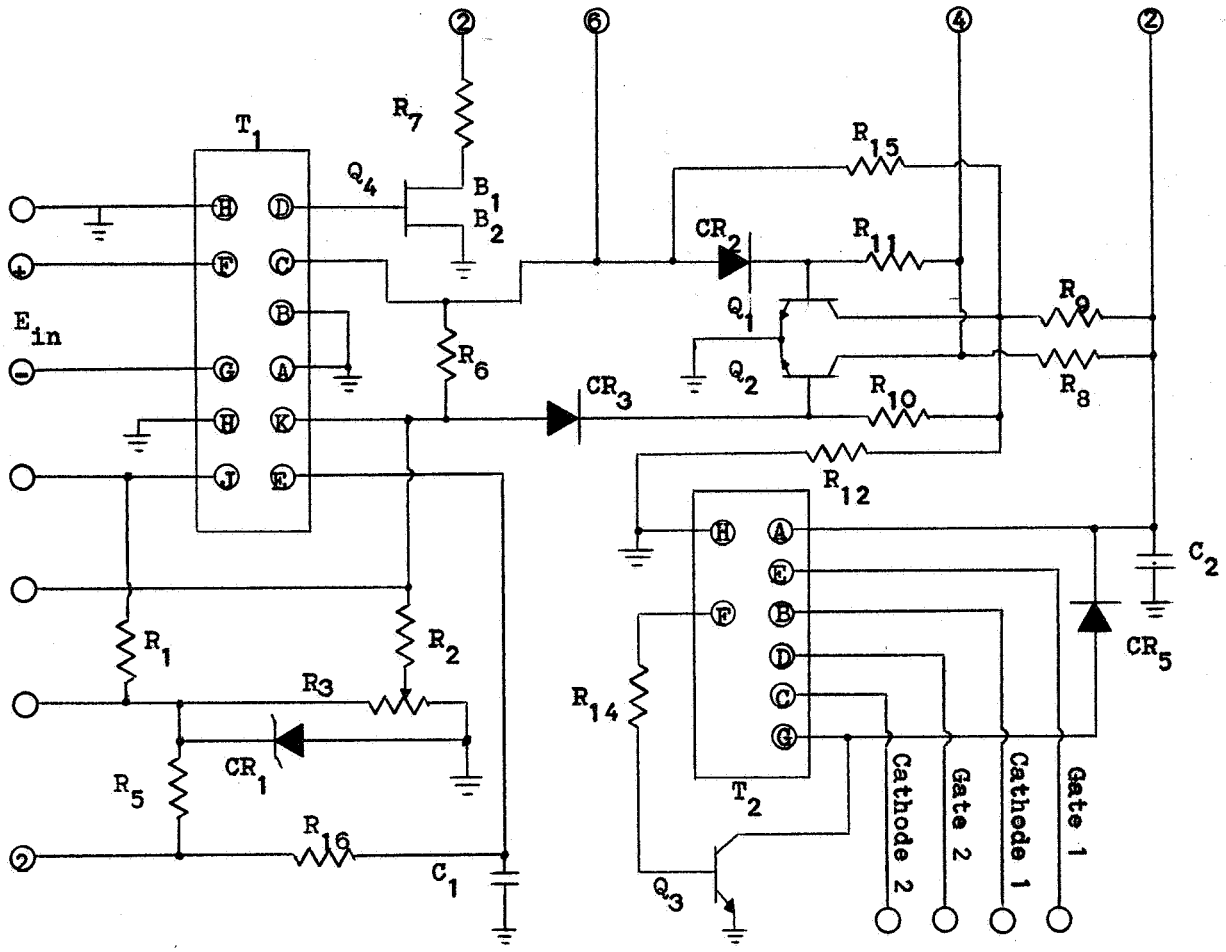

Figure 46. A simplified schematic of the monitor circuit.

APPENDIX E

PHYSIOLOGICAL MEASUREMENTS

Instruments and procedures used to collect physiological data are identified in the following paragraphs.

Skin temperatures were detected by 16 disc thermistors (Model 409, Yellow Springs Instrument Co.) which had been built into the WCG. The thermistors were proportioned over the body surface to make electrical weighting unnecessary in computing the $T_{\bar{s}}$. The placement and area weighting factors are given in Figure 47. Before installation the thermistors were calibrated in water and were required to be accurate to ±0.15°C against an N. B. S. certified mercury thermometer. Each thermistor disc was coated with a thin layer of neoprene rubber to isolate it electrically. The standard 0.2-second response time was affected little by this procedure. The closest any single probe came to a cooling tube was 1/4 in. (average distance 1/2 in.); therefore it is believed that the conductive cooling effect from cold water tubes was minimal. Mean skin temperature was recorded automatically every two minutes through the use of a parallel resistive network of the 16 probes. This permitted on-line plotting of $T_{\bar{s}}$, which was important in monitoring the performance of the Q controller.

Rectal temperature and ear canal temperature are indicative of the body core temperature. Stability during rest or prolonged work aided in determining thermal equilibrium in our subjects. Temperature levels at equilibrium and rates of change of temperature during transients assisted in assessment of the appropriateness of cooling. Rectal temperature was obtained by placing a thermistor probe (Model 401, Yellow Springs Instrument Co.) at a depth of 10 cm in the rectum. Ear canal temperature was detected by a small (0.1 in. diameter) epoxy coated bead thermistor (Yellow Springs Instrument Co. 400 series, interchangeable) which projected inwardly 1/8 in. from the tip of a custom molded foam-RTV silicone rubber plug (ref. 28). The insulating plug fitted snugly and filled nearly the entire length of the canal, and an outer cap covered the inner surface of the pinna. The thermistor bead was attached to 3-in. leads made from #49 gage copper wire, these short fine leads being buried in the insulating foam. Thus the bead was thermally isolated from the environment. Temperatures were read from a digital thermometer with an absolute accuracy of ±0.15°C.

Heart rate was obtained with either Ag-AgCl or bare wire electrodes. The active electrodes were placed at the top of the sternum (manubrium) and at the precordium, and the third electrode, which served as the indifferent or grounded electrode, was placed over the xiphoid process. Leads ran to a

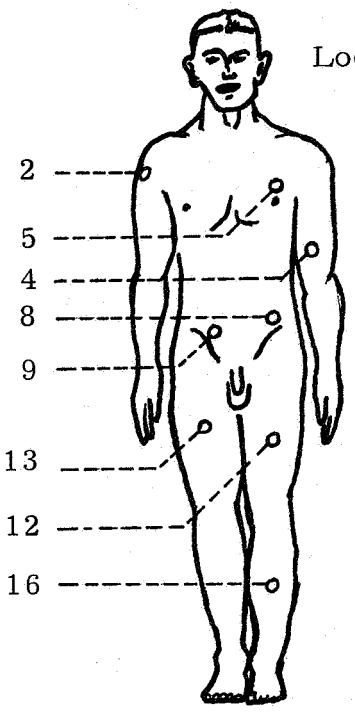

Location of Skin Temperature Sensors

1. Head-neck
2. R. deltoid
3. R. forearm
4. L. biceps
5. L. upper chest
6. L. Trapezius
7. R. scapular
8. L. upper abdomen
9. R. lower abdomen
10. R. kidney
11. L. gluteal
12. L. anterior thigh
13. R. anterior thigh
14. R. posterior thigh
15. R. calf
16. L. shin

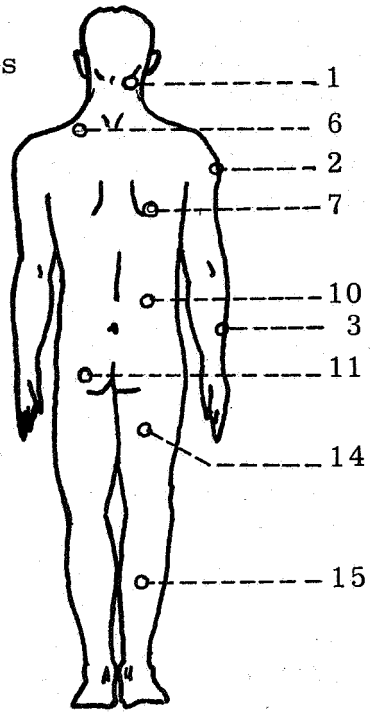

Schema for Surface Area Weighting of Thermistors

Body area represented	Thermistors no.	Thermistors % of total	% of total body area
head-neck	1	6.3	7
arms-hands	3	18.8	19
trunk	6	37.5	35
thighs	4	25.0	19
legs-feet	2	12.5	20

Figure 47 . Thermistor Locations and Schema for Surface Area Weighting.

small pre-amplifier carried by the subject, thence to a cardiotachometer (Model 122, Gilford Instruments Laboratories, Inc., Oberlin, Ohio) located outside the environmental chamber. Rates could be read from a meter or continuously recorded on one channel of a dual channel recorder (Model 322, Sanborn Co., Waltham, Mass.). Although heart rate did not represent an important control criterion, it was helpful in defining work levels, response times, and equilibria.

Change in body weight was measured on a platform scale (Model 5962, Fairbanks, Morse & Co., Yonkers, N. Y.) which has a sensitivity of 4.5 gms. Nude subject weights were obtained immediately before and after each experiment. Clothing accessories, e. g. athletic supporter, stockings, gloves, etc. were also weighed before and after each experiment. From these measurements we were able to calculate the evaporative heat loss from the mangarment complex. We separated respiratory water loss from cutaneous water loss by calculating respiratory water loss from the mean respiratory minute volumes ($\dot{V}_e$) and subtracting this amount from the total. In this way values for weight loss, adjusted for changes in $\dot{V}_e$ levels, could be converted to heat loss (1 gm H_2O evaporated = 0.58 kcal) and added to values for WCG heat extraction rate (Q). No sweat detectors were used and there was no air flow through the garment.

Heat production rate, or metabolic rate, was measured continuously with our MRM and periodically with a Douglas bag collection method (see Metabolism Measurement). The bag collection and analysis served as the reference standard for the MRM and was performed only during the more stable periods of the experiments. For conversion to heat terms, the calorific equivalent of O_2 was taken to be constant at 4.825 kcal/liter. MRM output was continuously recorded throughout each experiment on one channel of the two channel potentiometric recorder.

Metabolism Measurement

The metabolism measurement system was utilized primarily to obtain standardized values of oxygen consumption for comparison to the MRM output. Since it was necessary to remove the MRM mask from the subject's face for approximately two minutes during each collection of expired air, hence removing the input to the automatic controller, which had to be put in the "hold" condition, collections were limited (insofar as was feasible) to equilibrium periods. Equilibrium refers to the periods when T_{wi} was changing minimally, and these were not necessarily at physiological equilibrium of the subject.

Expired air samples were collected for timed periods of one or two minutes in a vinyl plastic Douglas bag located in the environmental chamber. Precise collection times were set by an electric timer which operated a solenoid valve in the collection line. An aliquot of the Douglas bag sample was pumped at a fixed flow rate via 0.25 in. i. d. polyethylene tubing through a drying chamber and the CO_2 and O_2 analyzers, which were located immediately outside the chamber. Oxygen partial pressure measurements were obtained with a paramagnetic analyzer (Model C-2, Beckman Instruments, Inc., Fullerton, Calif.) and CO_2 content with an infra-red analyzer (Model L/B 15A, Beckman Instruments Co.). Accuracy of measurement was established by calibration of these instruments with commercially obtained calibrating gases accurate to $\pm 0.2\%$. Oxygen consumption, RQ, and heat production in kcal/min were calculated in the usual manner. Respiratory minute volumes ($\dot{V}_e$) were determined by evacuation of the Douglas bag sample directly into a 120-liter Tissot gasometer (Warren E. Collins, Boston, Mass.). Ambient barometric pressures read daily from an aneroid barometer allowed conversion of all volumes to standard temperature and pressure dry (STPD). Since the analyzer aliquot was discarded, an equivalent volume was added to the gasometer reading before correction to STPD conditions.

REFERENCES

1. Roth, E. M.: Bioenergetics of Space Suits for Lunar Exploration. NASA SP-84, 1966.

2. Streimer, I.; Turner, D. P. W.; Tardiff, C. A.; and Stephens, T. L.: An Investigation of the Effects of Pressure Suit Wearing on Work Output Characteristics. Aerospace Med., vol. 35, pp. 747-751, 1964.

3. Wortz, E. C.; Edwards, D. K.; Diaz, R. A.; Prescott, E. J.; and Browne, L. E.: Study of Heat Balance in Full Pressure Suits. Aerospace Med., vol. 38, pp. 181-188, 1967.

4. Crocker, Jeremy F.; Webb, Paul; and Jennings, David C.: Metabolic Heat Balances in Working Men Wearing Liquid-Cooled Sealed Clothing. AIAA-NASA Third Manned Spaceflight Meeting (AIAA Publication CP-10) pp. 111-117, 1964.

5. Veghte, James H.: Efficacy of Pressure Suit Cooling Systems in Hot Environments. Aerospace Med., vol. 36, pp. 964-967, 1965.

6. Waligora, James M.; and Michel, Edward L.: Application of Conductive Cooling for Working Men in a Thermally Isolated Environment. (Abstract) Aerospace Med., vol. 37, pp. 306-307, 1966.

7. Webb, Paul; and Annis, James A.: Bio-Thermal Responses to Varied Work Programs in Men Kept Thermally Neutral by Water Cooled Clothing. NASA CR-739, 1967.

8. Annis, James F.; and Webb, Paul: Undercooling and Overcooling with Liquid Cooling Garments. Preprints, 1967 Annual Scientific Meeting, Aerospace Medical Association, Washington, D. C., April 1967, pp. 305-306.

9. Burton, D. R.: Performance of Water Conditioned Suits. Aerospace Med., vol. 37, pp. 500-504, 1966.

10. Stolwijk, J. A. J.; and Hardy, J. D.: Temperature Regulation in Man -- A Theoretical Study. Pflügers Archiv., vol. 291, pp. 129-162, 1966.

11. Crosbie, R. J.; Hardy, J. D.; and Fessenden, E.: Electrical analog simulation of temperature regulation in man. Chapter 55 in: Temperature, Its Measurement and Control in Science and Industry, edited by J. D. Hardy, Vol. 3, Part 3, New York, Reinhold, 1963.

12. Wissler, Eugene H.: An Analysis of Factors Affecting Temperature Levels in the Nude Human. Chapter 53 in: Temperature, Its Measurement and Control in Science and Industry, edited by J. D. Hardy, vol. 3, part 3, New York, Reinhold, 1963.

13. Brown, Arthur C.: Analog Computer Simulation of Temperature Regulation in Man. AMRL-TDR-63-116, Biomedical Laboratory, 6570th Aerospace Medical Research Laboratories, Wright-Patterson Air Force Base, Ohio, December 1963.

14. Brown, Arthur C.: Further Development of the Biothermal Analog Computer. AMRL-TR-66-197, Aerospace Medical Research Laboratories, Wright-Patterson Air Force Base, Ohio, December 1966.

15. Woodcock, A. H.; Thwaites, H. L.; and Breckenridge, J. R.: An Electrical Analogue for Studying Heat Transfer in Dynamic Situations. Technical Report EP-86, Environmental Protection Research Division, Hq., Quartermaster Research & Engineering Command, U. S. Army, Natick, Massachusetts, April 1958.

16. Smith, Paul E.; and James, Edward W., II.: Human Responses to Heat Stress--Simulation by Analog Computer. Arch. of Environmental Health, vol. 9, pp. 332-342, 1964.

17. Robinson, S.; Meyer, F. R.; Newton, J. L.; Ts'ao, C. H.; and Holgersen, L. O.: Relations between sweating, cutaneous blood flow, and body temperature in work. J. Appl. Physiol., vol. 20, pp. 575-582, 1965.

18. Carlson, L. D.; Burns, H. L.; Holmes, T. H.; and Webb, P. P.: Adaptive Changes During Exposure to Cold. J. Appl. Physiol., vol. 5, pp. 672-676, 1953.

19. Saltin, Bengt; and Hermansen, Lars: Esophageal, rectal, and muscle temperature during exercise. J. Appl. Physiol. 21, pp. 1757-1762, 1966.

20. Äikäs, E.; Karvonen, M. J.; Piironen, P.; and Ruosteenoja, R.: Intramuscular, Rectal and Oesophageal Temperature During Exercise. Acta physiol. scand., vol. 54, pp. 366-370, 1962.

21. Altman, Philip L.; and Dittmer, Dorothy S.: Blood and Other Body Fluids. ASD Technical Report 61-199. Biomedical Laboratory, Aerospace Medical Laboratory, Wright-Patterson Air Force Base, Ohio, June 1961.

22. Diem, Konrad, ed.: Documenta Geigy--Scientific Tables. 6th edition. Geigy Pharmaceuticals, Division of Geigy (Canada) Limited, Montreal, 1962.

23. Barcroft, H. Circulatory changes accompanying the contraction of voluntary muscle. Austral. J. Exptl. Biol. & Med. Sci., vol. 42, pp. 1-16, 1964.

24. Barcroft, H.; and Millen, J. L. E.: The blood flow through muscle through sustained contraction. J. Physiol., vol. 97, pp. 17-31, 1939.

25. Elsner, Robert W. and Carlson, Loren D.: Postexercise hyperemia in trained and untrained subjects. J. Appl. Physiol., vol. 17, pp. 436-440, 1962.

26. Cooper, Theodore; Randall, Walter C.; and Hertzman, Alrick B. The vascular convection of heat from active muscle to overlying skin. J. Appl. Physiol., vol. 14, pp. 207-211, 1959.

27. Reeves, E.; Stephens, M. P.; and Beckman, E. L.: An Evaluation of the Foamed Neoprene "Diver's Wet Suit" as a Survival Garment for Helicopter Aircrews. Aerospace Med., vol. 38, pp. 599-606, 1967.

28. Gibbons, Larry V.: Body Temperature Monitoring in the External Auditory Meatus. Aerospace Med., vol. 28, pp. 671-675, 1967.

NASA-Langley, 1968 —— 5 CR-1085

NATIONAL AERONAUTICS AND SPACE ADMINISTRATION
WASHINGTON, D.C. 20546

OFFICIAL BUSINESS

FIRST CLASS MAIL

POSTAGE AND FEES PAID
NATIONAL AERONAUTICS AND
SPACE ADMINISTRATION

POSTMASTER: If Undeliverable (Section 158 Postal Manual) Do Not Return

"The aeronautical and space activities of the United States shall be conducted so as to contribute . . . to the expansion of human knowledge of phenomena in the atmosphere and space. The Administration shall provide for the widest practicable and appropriate dissemination of information concerning its activities and the results thereof."

—NATIONAL AERONAUTICS AND SPACE ACT OF 1958

NASA SCIENTIFIC AND TECHNICAL PUBLICATIONS

TECHNICAL REPORTS: Scientific and technical information considered important, complete, and a lasting contribution to existing knowledge.

TECHNICAL NOTES: Information less broad in scope but nevertheless of importance as a contribution to existing knowledge.

TECHNICAL MEMORANDUMS: Information receiving limited distribution because of preliminary data, security classification, or other reasons.

CONTRACTOR REPORTS: Scientific and technical information generated under a NASA contract or grant and considered an important contribution to existing knowledge.

TECHNICAL TRANSLATIONS: Information published in a foreign language considered to merit NASA distribution in English.

SPECIAL PUBLICATIONS: Information derived from or of value to NASA activities. Publications include conference proceedings, monographs, data compilations, handbooks, sourcebooks, and special bibliographies.

TECHNOLOGY UTILIZATION PUBLICATIONS: Information on technology used by NASA that may be of particular interest in commercial and other non-aerospace applications. Publications include Tech Briefs, Technology Utilization Reports and Notes, and Technology Surveys.

Details on the availability of these publications may be obtained from:

SCIENTIFIC AND TECHNICAL INFORMATION DIVISION

NATIONAL AERONAUTICS AND SPACE ADMINISTRATION

Washington, D.C. 20546